NASA Technical Memorandum 4074

Effects of Independent Variation of Mach and Reynolds Numbers on the Low-Speed Aerodynamic Characteristics of the NACA 0012 Airfoil Section

Charles L. Ladson

OCTOBER 1988

NASA

NASA Technical Memorandum 4074

Effects of Independent Variation of Mach and Reynolds Numbers on the Low-Speed Aerodynamic Characteristics of the NACA 0012 Airfoil Section

Charles L. Ladson
Langley Research Center
Hampton, Virginia

National Aeronautics
and Space Administration

**Scientific and Technical
Information Division**

1988

Summary

Presented in this report is a description of a test program conducted in the Langley Low-Turbulence Pressure Tunnel to produce the low-speed aerodynamic characteristics of the NACA 0012 airfoil section. During the program, Mach number independently varied from 0.05 to 0.36 and the Reynolds number independently varied from about 2 to 12 $\times$ 10^6. The angle of attack variation covered the range from zero lift coefficient to maximum lift coefficient.

An analysis of the data shows that changes in Mach number affect lift-curve slope and maximum lift coefficient. These changes have little effect on either minimum drag or maximum lift-drag ratio. Changes in Reynolds number affect all parameters to some extent. Theoretical predictions of lift-curve slope generally show the trends of the experimental data with varying Mach number but do not accurately give the trends with Reynolds number. The magnitude of the predictions is generally higher than that of the experiment. Predictions of minimum drag are as much as 0.001 lower than experiment at the higher Mach and Reynolds numbers for the free-transition case. With transition fixed at the 5-percent-chord model station, the agreement between theory and experiment is excellent.

Introduction

Aeronautical researchers have been and are still using the NACA 0012 airfoil section as a reference model for the assessment of wall interference and correction procedures. This airfoil section is also an AGARD standard used in the testing of numerical solutions (ref. 1) and is in the AGARD two-dimensional experimental data base (ref. 2). Although a large experimental data base exists for this airfoil throughout the subsonic and transonic speed range, there are some areas in which additional data are desirable. One such area is the low-speed regime. In this regime, the independent effects of Mach number and Reynolds number on the aerodynamic characteristics of the airfoil are lacking. To supplement the data available in this area, researchers at Langley Research Center conducted an investigation of this airfoil in the Langley Low-Turbulence Pressure Tunnel in late 1975.

The purpose of this paper is to present a comprehensive data base of the low-speed aerodynamic characteristics of the NACA 0012 airfoil section. Included are the effects of varying Mach number and Reynolds number independently and the effects of fixing transition location. Comparisons of some of the results with previously published data and with theoretical estimates are also discussed. The Langley Low-Turbulence Pressure Tunnel is the facility used for these tests. The Mach number varied from 0.05 to 0.36. The Reynolds number, based on model chord, generally varied from about 2 to 12 $\times$ 10^6. One additional run at a Reynolds number of about 19 $\times$ 10^6 and a Mach number of 0.15 with free transition is in the tabulated data base but is not in the summary figures.

Symbols

All measurements and calculations are in U.S. Customary Units. The International System of Units (SI) values are in parentheses.

b	airfoil model span, 36.00 in. (91.44 cm)
c	airfoil model chord, 23.66 in. (60.10 cm)
c_d	section drag coefficient from integration of wake survey (CD in computer-generated figures)
$c_{d,o}$	section drag coefficient at zero lift
c_ℓ	section lift coefficient from integration of model surface pressure coefficients (CL in computer-generated figures)
$c_{\ell,\alpha}$	section lift-curve slope, per deg
c_m	section pitching-moment coefficient about 0.25c point from integration of model surface pressure coefficients (CM in computer-generated figures)
ℓ/d	lift-drag ratio (L/D in computer-generated figures)
M	average free-stream Mach number
R	Reynolds number based on model chord
α	angle of attack, deg ("Alpha" in computer-generated figures)

Subscript:

max	maximum

Apparatus

Wind Tunnel

The Langley Low-Turbulence Pressure Tunnel, used to conduct the tests on this model, is a closed-throat, single-return facility. The tunnel operates

at stagnation pressures from 1.0 to 10.0 atm. The Mach number is variable from about 0.05 to 0.46. An air-to-water heat exchanger maintains the stagnation temperature at or near ambient conditions. The maximum Reynolds number is about 15×10^6 per foot (4.92×10^7 per meter) at a Mach number of 0.22. The test section is 36.0 in. (91.4 cm) wide and 90.0 in. (228.6 cm) high. Descriptions of the operational characteristics and calibration results for this tunnel are in the appendix of reference 3. At the time of this test program the turbulence level of the tunnel was unknown, but there were many indications that it had increased from the original low level measured in the early 1940's. This increase was the result of successive damage to the heat exchanger because of freezing as well as deterioration of the screens. After these tests, the tunnel was refurbished and the turbulence level reduced. A description of the refurbishment and results of calibration are in reference 4.

The tunnel sidewalls contain circular end plates 40.0 in. (101.6 cm) in diameter. These plates are for positioning and attachment of the two-dimensional airfoil models. These hydraulically actuated plates rotate with the model and are flush with the test section sidewall. The airfoil ends attach to rectangular model attachment blocks in these plates. The airfoil mounting blocks locate the $0.25c$ model station on the center of rotation. Air gaps between the rectangular blocks and the circular plates are sealed with flexible sliding metal seals. For a sketch of these seals, see figure 1.

Wake Survey Rake

A fixed wake survey rake is cantilevered from the test section sidewall. This rake, located at the model midspan, is about $1c$ downstream of the model trailing edge. The rake consists of 91 total-pressure tubes 0.060 in. (0.152 cm) in diameter and 5 static-pressure tubes 0.125 in. (0.318 cm) in diameter. The total-pressure tubes are oval in cross section for the last 0.24 in. (0.61 cm) of the tube. A minimum opening of 0.040 in. (0.102 cm) remains at the tube end. The static-pressure tubes each have four flush orifices drilled 90° apart. These orifices, located eight tube diameters from the end of the tube, are in the plane of measurement of the total-pressure tubes. Also located on the test section sidewall in the plane of the total-pressure tubes is an array of flush static-pressure orifices. Shown in figure 2 is a sketch of the wake survey rake.

Instrumentation

To make measurements of both the airfoil surface static pressures and the wake total pressures, we use an automatic pressure scanning system and variable-capacitance-type pressure transducers. Precision quartz pressure transducers measure the tunnel stagnation pressure and the reference static pressure. The angle-of-attack measurement device is a calibrated digital shaft encoder operated by a pinion gear. A rack attached to the circular plates drives the pinion gear. A high-speed computer-controlled digital data-acquisition system records the analog output of all measurement devices on magnetic tape. This magnetic tape is the input for post-run data reduction and analysis of the aerodynamic data.

Accuracy

The differential pressure gauges used to measure the model pressures have a maximum range of 50 psi. The gauges for measurement of wake total-pressure loss have a maximum range of 7.5 psi. These precision transducers have an accuracy of 0.25 percent of reading from 25 percent of negative full scale to 100 percent of positive full scale. The precision quartz gauges used to measure stagnation pressure and the difference between reference static pressure and stagnation pressure have full-scale ranges of 150 psi and 15 psi, respectively. These gauges have an accuracy of about 0.01 percent of full scale at low pressures to about 0.02 percent of full scale at the high end of their range.

The repeatability of data is also an indication of the overall data accuracy. On many of the runs shown in the tabulated data, two points at $\alpha = 0°$ are listed. An analysis of these repeat points shows that when the two points are within 0.01° of each other, drag coefficient varies by 0.0002 or less, normal-force coefficient varies by 0.004 or less, and pitching-moment coefficient varies by 0.0002 or less.

Model

The model, machined from a solid aluminum billet, had a chord of 23.66 in. (60.10 cm) and a span of 36.00 in. (91.44 cm), which is the span of the tunnel. Instrumentation consisted of a total of 81 orifices. There were 24 orifices located in each chordwise row on both the upper and the lower surface. These chordwise rows were 4.20 in. (10.67 cm) to the left of the model center line. There were also 33 additional orifices arranged in 3 spanwise rows on the upper surface. Grooves, machined in the surface of the model, accommodated the pressure tubing for each orifice location. After the tube installation, the grooves were covered with a plastic resin. The orifices, drilled through the plastic and into the tubing,

had a diameter of 0.060 in. (0.152 cm). After completion of this potting process and the drilling of the orifice, the airfoil surface was machined to provide a surface finish of about 32 rms microinches. The surface was then hand polished in a chordwise direction with No. 400 carborundum paper to provide the final aerodynamic surface. The ordinates of the finished model were within $0.0002c$ of the design ordinates.

Tests and Procedures

The airfoil test program covered Mach numbers from 0.05 to 0.36 over angles of attack from about $-4°$ to $18°$. The Reynolds number based on model chord varied from about 2 to 12 $\times$ 10^6. Both the Reynolds number and the Mach number varied independently for this test program.

Included in the program were tests with both fixed and free boundary-layer transition. For the fixed-transition runs, carborundum strips were applied to both the model upper and lower surfaces at the $0.05c$ station. The strips were about $0.01c$ in width. The carborundum grit size varied with test Reynolds number to provide enough height to trip the boundary layer but not add incremental drag. The method of reference 5 was used to determine the appropriate grit size. Also included in the test program were tests made with an NACA-type wraparound transition strip. This strip extended from the $0.05c$ location on the upper surface, around the leading edge, to the $0.05c$ location on the lower surface. The grit size was No. 60 for these tests. The label "#60-W" indicates these runs on the data plots. This series of tests is for comparison with previously published data on this airfoil.

All data presented include corrections for the standard low-speed wind tunnel boundary effects described in reference 6. This correction amounts to about 2 percent of the measured coefficients.

Presentation of Results

Computer-generated plots of lift coefficient, drag coefficient, pitching-moment coefficient, and lift-drag ratio as a function of angle of attack present the basic results of this investigation. For a few of the polars presented, data at the angle of attack for maximum lift were not available. On the plots of these data, the lift coefficient was extrapolated to obtain the maximum value. A dashed line indicates these extrapolations. Also included in this report are tabulations of these integrated force and moment coefficients. These basic data plots and tabulations are presented as follows:

Mach number	Transition	Figure	Table
0.15	Free	3	I
.20		4	II
.25		5	III
.30		6	IV
.36		7	V
0.05	Fixed (No. 60-W grit)	8	VI
.15		9	VII
.30		10	VIII
0.15	Fixed (No. 80 grit)	11	IX
.30		12	X
0.15	Fixed (No. 120 grit)	13	XI
.30		14	XII
0.15	Fixed (No. 180 grit)	15	XIII
.30		16	XIV

Discussion

To summarize the results of these basic data plots, we present some of the important parameters as separate figures. These summary figures show some of the effects of variations of Mach number, Reynolds number, and transition fixing. The discussion which follows is the result of an analysis of these summary figures.

Lift-Curve Slope

Figures 17 to 23 illustrate the experimental lift-curve slope obtained by a least-squares curve-fit program. This program used data only from the linear angle-of-attack range. Figure 17 illustrates the effects of Mach number and Reynolds number on the lift-curve slope for the free-transition case. There is a gradual increase in the slope with increasing Mach number and Reynolds number. This increase in slope amounts to about 5 percent for increases in Mach number from 0.15 to 0.36. A similar percentage increase results from increases in Reynolds number from 4 to 12 $\times$ 10^6. It is thus clear that the effects of Mach number and Reynolds number are equally important in these ranges. Ignoring either of these effects in a comparison of data can be misleading.

Illustrated in figure 18 is a comparison of the lift-curve slopes for both free- and fixed-transition cases at a Mach number of 0.15. Fixing the transition at $0.05c$ has little effect on the data presented compared with the free-transition case. The effects of grit size are small and not consistent. For the case of wraparound transition (No. 60 grit), however, the

lift-curve slope decreases about 3 percent. This loss is about the same for all Reynolds numbers. Data at a Mach number of 0.30 (fig. 19) show essentially the same trends.

Presented in figures 20 and 21 are comparisons of the experimental and theoretical lift-curve slopes for the free-transition case. The theoretical values labeled Stevens are from the analysis program presented in reference 7, and the values labeled Eppler are from the program presented in reference 8. Figure 20 shows that both theories predict higher values than the experimental data throughout the Mach number range. The trends of the theories with Mach number, however, are very similar to the experimental data. Figure 21 shows that the overprediction of the magnitude of the experimental data reduces from about 7 percent at $R = 4 \times 10^6$ to about 3 percent at $R = 12 \times 10^6$. The results are about the same for both Mach numbers shown. This figure also shows that neither theory accurately predicts the trends of the data with increasing Reynolds number. The Eppler theory shows no effect of Reynolds number, and the increase in slope of the Stevens theory is only about half the experimental value.

Figure 22 presents the comparison of theoretical and experimental lift-curve slopes for the fixed-transition case. Like the free-transition results, the theory gives higher slopes and does not give the proper trends with Reynolds number. The Eppler code is in better agreement with experiment than the Stevens code, but it shows essentially no variation with Reynolds number.

Figure 23 shows a comparison of data from reference 9 with results from the present investigation. Both sets of data are from the same facility. The agreement is good for the free-transition case except at the low Reynolds numbers. With the transition fixed with wraparound grit, the lift-curve slopes from the present investigation are higher for Reynolds numbers below 6×10^6. The variation with Reynolds number is much greater for the data of reference 9. The agreement at $R = 6 \times 10^6$ is a crossover point and is probably not typical of the results. The suspected higher turbulence level of the facility during the present tests may account for some of these differences. The density of the grit may also be a contributing factor.

Maximum Lift Coefficient

The maximum lift coefficient attained before stall is an important parameter for low-speed airfoil tests. Figures 24 to 26 present this parameter for the present tests. For the free-transition case (fig. 24), the maximum lift coefficient decreases about 25 percent as the Mach number increases from 0.15 to 0.36. This percentage decrease is about the same for all Reynolds numbers. The maximum lift coefficient increases with increasing Reynolds number for all test Mach numbers. For $M = 0.15$, this increase amounts to 20 percent for $R = 2$ to 12×10^6.

As shown in figure 25 for $M = 0.15$ and in figure 26 for $M = 0.30$, fixing transition at the $0.05c$ location has very little effect on the maximum lift coefficient. Using the wraparound transition method (No. 60 grit) produces a large loss in maximum lift. This loss is about 25 percent at $M = 0.15$ and about half this value at $M = 0.30$. Again, these data show that Mach number and Reynolds number effects are appreciable at low speeds. Ignoring these effects in data comparisons can lead to erroneous conclusions.

Minimum Drag

Figures 27 to 29 summarize the minimum drag characteristics of this airfoil. For the free-transition data (fig. 27) there are no consistent trends in the data. Drag levels remain essentially constant with increasing Mach and Reynolds number. Fixed transition (figs. 28 and 29) increases the drag over that for free transition for both Mach numbers. There is little effect of grit size on drag for transition fixed at the $0.05c$ location. With the wraparound grit, however, drag increases by about 0.01 for both Mach numbers throughout the Reynolds number range. This increment is greater than expected from the increase in length of turbulent flow. Drag from the grit particles is the probable source of most of this drag increment.

Shown in figure 30 is a comparison of the experimental and theoretical values of minimum drag. Once again, results of both the Stevens code (ref. 7) and the Eppler code (ref. 8) are shown. For both Mach numbers, the experimental drag values with free transition are higher than theoretical values. At the lower Mach number, the experimental values are as much as 0.0006 higher than those from the Stevens theory. The results from the Eppler code show only about half this difference. At the higher Mach number, the data are as much as 0.0010 higher than the Stevens code results. The Eppler code results again show only about half this difference. As stated in the discussion of lift-curve slope, the higher experimental values are probably the result of the tunnel turbulence level. Turbulence will move the transition point forward on the model compared with the theoretical location, thus increasing drag. At $M = 0.30$, the experimental drag with free transition approaches that for fixed transition at the higher Reynolds numbers. This shows that the transition location is approaching the $0.05c$ station on the model. The orifice locations on this model are about 23 percent of the model semispan to the left of the tunnel center line.

This offset reduces the possibility of orifice-induced turbulence on the measurement of wake drag, which is measured on the tunnel center line.

With the transition location fixed, figure 30 shows that the agreement between theory and experiment is excellent. Both theoretical programs give nearly identical results.

Figure 31 presents a comparison of the present test results with those from reference 9. With free transition, the present test results are about 0.0005 higher at most Reynolds numbers. This again is likely the result of differences in tunnel turbulence levels. With fixed transition, the present test results are lower by about 0.001 for all but the lowest Reynolds number. This difference may be the result of differences in density of grit application.

Maximum Lift-Drag Ratio

Plotted in figures 32 to 34 are the variations with Mach and Reynolds number of the maximum lift-drag ratio. For free transition, figure 32 shows little variation in this parameter with Mach number. Maximum lift-drag ratio increases with increasing Reynolds number up to about 6×10^6. Above this value little variation occurs.

With fixed transition (figs. 33 and 34), the values of this maximum ratio are slightly less than for free transition. The data also show a continual increase with increasing Reynolds number. The use of wraparound grit produces a 20- to 30-percent decrease in maximum lift-drag ratio when compared with that produced for the $0.05c$ transition location.

Conclusions

An investigation conducted in the Langley Low-Turbulence Pressure Tunnel has produced the low-speed aerodynamic characteristics of the NACA 0012 airfoil. This investigation covered a Mach number range of 0.05 to 0.36. The corresponding Reynolds number range was about 2 to 12×10^6. The angle-of-attack variation covered the range from zero lift coefficient to maximum lift coefficient. An analysis of the data yields the following conclusions:

1. Increasing Mach number at constant Reynolds number increases the lift-curve slope and decreases maximum lift coefficient, but it has little effect on minimum drag and maximum lift-drag ratio.
2. Increasing Reynolds number at constant Mach number increases the lift-curve slope, maximum lift coefficient, and, to some extent, maximum lift-drag ratio. Minimum drag decreases with increasing Reynolds number only for the fixed-transition case.
3. Fixing transition at the 5-percent-chord location on the model has little effect on either lift-curve slope or maximum lift coefficient. Minimum drag increases with fixed transition and the maximum lift-drag ratio thus decreases.
4. The theoretical values of lift-curve slope are higher than the experimental values by as much as 7 percent at the lower Reynolds number with free transition. Both theories presented generally predict the experimental trends with variation of Mach number but do not adequately predict the trends with Reynolds number. With fixed transition, the Stevens theory predicts values as much as 10 percent higher than experimental values.
5. With free transition, both theories underestimate the minimum drag level. The Stevens theory is as much as 0.0010 low at the higher Mach numbers and Reynolds numbers. The Eppler code is within 0.0005 for most cases. Theoretical values of minimum drag with fixed transition are in excellent agreement with the data.

NASA Langley Research Center
Hampton, Virginia 23665-5225
August 23, 1988

References

1. *Experimental Data Base for Computer Program Assessment.* AGARD-AR-138, May 1979.
2. Lock, R. C.: *Test Cases for Numerical Methods in Two-Dimensional Transonic Flows.* AGARD Rep. No. 575, Nov. 1970.
3. Beasley, William D.; and McGhee, Robert J.: *Experimental and Theoretical Low-Speed Aerodynamic Characteristics of the NACA 65_1-213, $a = 0.50$, Airfoil.* NASA TM X-3160, 1975.
4. McGhee, Robert J.; Beasley, William D.; and Foster, Jean M.: *Recent Modifications and Calibration of the Langley Low-Turbulence Pressure Tunnel.* NASA TP-2328, 1984.
5. Braslow, Albert L.; and Knox, Eugene C.: *Simplified Method for Determination of Critical Height of Distributed Roughness Particles for Boundary-Layer Transition at Mach Numbers From 0 to 5.* NACA TN 4363, 1958.
6. Allen, H. Julian; and Vincenti, Walter G.: *Wall Interference in a Two-Dimensional-Flow Wind Tunnel, With Consideration of the Effect of Compressibility.* NACA Rep. 782, 1944. (Supersedes NACA WR A-63.)
7. Stevens, W. A.; Goradia, S. H.; and Braden, J. A.: *Mathematical Model for Two-Dimensional Multicomponent Airfoils in Viscous Flow.* NASA CR-1843, 1971.
8. Eppler, Richard; and Somers, Dan M.: *A Computer Program for the Design and Analysis of Low-Speed Airfoils.* NASA TM-80210, 1980.
9. Loftin, Laurence K., Jr.; and Smith, Hamilton A.: *Aerodynamic Characteristics of 15 NACA Airfoil Sections at Seven Reynolds Numbers From 0.7×10^6 to 9.0×10^6.* NACA TN 1945, 1949.

Table I. Force Coefficients at $M = 0.15$ for Free Transition

$R = 2.00 \times 10^6$

α, deg.	c_d	c_ℓ	c_m	ℓ/d
-4.25	.00730	-.4300	-.0040	-58.90
-2.10	.00620	-.2150	-.0020	-34.68
.00	.00620	.0000	.0000	.00
1.85	.00620	.1940	.0030	31.29
4.25	.00670	.4450	.0040	66.42
6.05	.00870	.6250	.0070	71.84
8.15	.01270	.8550	.0080	67.32
10.15	.01350	1.0450	.0120	77.41
11.15	.01490	1.1350	.0140	76.17
12.10	.01640	1.2180	.0180	74.27
13.08	.01880	1.2900	.0190	68.62
14.25	.02280	1.3620	.0220	59.74
15.25	.02910	1.4080	.0250	48.38
16.25		.7530	-.1060	

$R = 3.94 \times 10^6$

α, deg.	c_d	c_ℓ	c_m	ℓ/d
-4.06	.00701	-.4019	.0022	-57.33
-.04	.00659	-.0033	-.0002	-.50
3.96	.00631	.4203	.0015	66.61
6.00	.00712	.636	.0019	89.33
8.17	.00985	.8657	.0077	87.89
10.02	.00934	1.0629	.0071	113.79
11.07	.01069	1.1622	.0080	108.72
12.08	.01289	1.2489	.0095	96.93
13.37	.01523	1.3587	.0116	89.22
14.10	.01725	1.4215	.0145	82.41
15.14	.02045	1.4844	.0196	72.60
18.09	.22773	1.0946	-.0800	4.81

$R = 5.97 \times 10^6$

α, deg.	c_d	c_ℓ	c_m	ℓ/d
-4.05	.00700	-.4280	.0000	-61.14
-2.00	.00650	-.2150	.0000	-33.08
.05	.00650	.0040	.0000	.62
1.98	.00680	.2080	.0020	30.59
4.18	.00760	.4520	.0030	59.47
6.20	.00680	.6630	.0040	97.50
8.22	.00800	.8800	.0050	110.00
10.18	.01050	1.0880	.0070	103.62
11.08	.01140	1.1800	.0080	103.51
12.25	.01250	1.2920	.0090	103.36
13.10	.01300	1.3680	.0110	105.23
14.28	.01620	1.4580	.0150	90.00
15.20	.01870	1.5280	.0180	81.71
16.18	.02180	1.5900	.0210	72.94
16.90	.02440	1.6180	.0230	66.31
17.35	.02750	1.6600	.0250	60.36
17.65		1.6450	.0270	
18.65		1.0050	-.1080	

Table I. Concluded

$R = 8.86 \times 10^6$

α, deg.	c_d	c_ℓ	c_m	ℓ/d
-4.00	.00680	-.4300	.0030	-63.24
-1.98	.00630	-.2150	.0010	-34.13
-.10	.00630	-.0050	.0000	-.79
2.13	.00650	.2300	.0020	35.38
4.13	.00700	.4500	.0030	64.29
6.08	.00720	.6650	.0050	92.36
8.02	.00850	.8750	.0060	102.94
10.30	.00980	1.1150	.0080	113.78
11.18	.01050	1.2050	.0080	114.76
12.22	.01150	1.3050	.0090	113.48
13.42	.01280	1.4120	.0130	110.31
14.13	.01480	1.4700	.0150	99.32
15.12	.01680	1.5430	.0180	91.85
16.48	.02250	1.6300	.0240	72.44
17.38	.02470	1.6730	.0280	67.73
18.42	.02950	1.6930	.0320	57.39

$R = 11.90 \times 10^6$

α, deg.	c_d	c_ℓ	c_m	ℓ/d
-4.20	.00684	-.4665	.0006	-68.23
-2.01	.00611	-.2286	.0006	-37.45
-.05	.00637	-.0111	.0001	-1.74
-.03	.00634	-.0090	.0003	-1.42
2.00	.00692	.2159	-.0001	31.20
4.17	.00687	.4575	.0002	66.60
6.10	.00713	.6693	.0007	93.84
8.11	.00826	.8885	.0016	107.53
10.40	.00975	1.1289	.0040	115.84
11.43	.01058	1.2308	.0057	116.28
12.52	.01166	1.3331	.0078	114.31
13.25	.01293	1.3963	.0096	107.95
16.05	.02156	1.6004	.0198	74.25
18.04	.05429	1.6174	.0225	29.79
18.25	.25587	1.2188	-.1341	4.76
19.46	.29135	1.1064	-.1823	3.80

$R = 18.90 \times 10^6$

α, deg.	c_d	c_ℓ	c_m	ℓ/d
-2.07	.00617	-.2369	.0009	-38.36
-.03	.00655	-.0091	.0006	-1.39
.03	.00664	-.0019	.0005	-.28
1.99	.00716	.2177	-.0001	30.40
4.20	.00716	.4644	-.0001	64.90
6.05	.00737	.6694	.0000	90.82
8.37	.00916	.9290	.0016	101.44
10.02	.01075	1.1007	.0036	102.40
11.57	.01203	1.2557	.0060	104.42
12.40	.01292	1.3339	.0079	103.25
13.12	.01345	1.3968	.0094	103.86
14.16	.01514	1.4833	.0127	97.96
15.14	.01900	1.5541	.0167	81.79
16.17	.02175	1.6169	.0215	74.35
17.84	.03728	1.6593	.0288	44.51
18.69	.26619	1.0867	-.1108	4.08
20.17	.32534	1.1321	-.1148	3.48

Table II. Force Coefficients at $M = 0.20$ for Free Transition

$R = 2.66 \times 10^6$

α, deg.	c_d	c_ℓ	c_m	ℓ/d
-4.11	.00729	-.4265	-.0034	-58.53
-2.00	.00655	-.2138	-.0012	-32.63
.00	.00599	-.0058	.0006	-.97
.00	.00607	-.0062	.0004	-1.02
2.07	.00612	.2138	.0016	34.96
4.27	.00663	.4457	.0033	67.25
6.03	.00771	.6304	.0051	81.80
8.21		.8590	.0052	
10.19	.01318	1.0593	.0099	80.39
11.15	.01410	1.1497	.0116	81.55
12.25	.01549	1.2444	.0139	80.36
13.27	.01784	1.3246	.0165	74.25
14.29	.02140	1.3937	.0198	65.13
15.18	.02592	1.4420	.0233	55.63
16.28	.03599	1.4604	.0266	40.58
17.25	.25283	1.1140	-.0827	4.41
18.16	.26666	1.1328	-.0830	4.25
19.24	.28507	1.1597	-.0846	4.07

$R = 3.99 \times 10^6$

α, deg.	c_d	c_ℓ	c_m	ℓ/d
-4.09	.00695	-.4416	-.0002	-63.54
-2.04	.00638	-.2219	-.0009	-34.78
-.04	.00648	-.0097	.0000	-1.49
.03	.00670	-.0016	-.0001	-.25
2.04	.00687	.2119	.0016	30.84
4.02	.00654	.4220	.0023	64.53
6.08	.00717	.6446	.0034	89.91
8.07	.00963	.8553	.0060	88.80
10.18	.01178	1.0789	.0070	91.61
11.19	.01242	1.1749	.0094	94.58
12.45	.01412	1.2902	.0122	91.40
13.08	.01532	1.3430	.0140	87.65
14.24	.01817	1.4299	.0177	78.68
15.27	.02136	1.4976	.0220	70.12
16.34	.02660	1.5489	.0263	58.23
17.34	.07842	1.5745	.0146	20.08
18.08	.29925	1.0123	-.1022	3.38
19.00	.28959	1.1632	-.0839	4.02

$R = 5.95 \times 10^6$

α, deg.	c_d	c_ℓ	c_m	ℓ/d
-4.08	.00688	-.4313	-.0007	-62.65
-2.11	.00631	-.2210	.0002	-35.01
-.12	.00637	-.0080	.0003	-1.25
-.11	.00638	-.0042	.0002	-.65
1.95	.00680	.2152	.0001	31.66
3.97	.00731	.4375	.0008	59.82
6.03	.00686	.6623	.0018	96.51
7.91	.00796	.8674	.0033	108.93
9.99	.01044	1.0843	.0053	103.85
11.15	.01156	1.1994	.0073	103.78
12.12	.01244	1.2902	.0093	103.72
13.13	.01422	1.3792	.0121	96.99
14.04	.01591	1.4539	.0153	91.37
15.03	.01918	1.5238	.0189	79.43
16.29	.02339	1.5966	.0244	68.26
17.08	.02723	1.6258	.0279	59.70
18.00	.26026	1.1169	-.1062	4.29
19.04	.28442	.9393	-.1086	3.30

Table II. Concluded

$R = 8.93 \times 10^6$

α, deg.	c_d	c_ℓ	c_m	ℓ/d
-4.05	.00696	-.4490	.0002	-64.53
-2.17	.00638	-.2464	.0002	-38.62
-.03	.00619	-.0101	-.0001	-1.63
.02	.00625	-.0025	-.0004	-.40
2.07	.00685	.2245	-.0003	32.78
4.03	.00721	.4431	.0002	61.47
6.05	.00719	.6683	.0009	92.94
8.21	.00864	.9046	.0023	104.67
10.22	.00995	1.1147	.0047	112.04
11.09	.01117	1.2070	.0061	108.01
12.13	.01189	1.3089	.0084	110.12
13.33	.01359	1.4162	.0116	104.22
14.17	.01553	1.4845	.0145	95.60
15.16	.01835	1.5586	.0181	84.93
16.24	.02220	1.6231	.0230	73.10
17.53	.02784	1.6681	.0283	59.92
18.23	.26063	1.2387	-.1230	4.75
19.08	.28015	1.1290	-.1032	4.03

$R = 11.95 \times 10^6$

α, deg.	c_d	c_ℓ	c_m	ℓ/d
-4.08	.00679	-.4602	.0007	-67.76
-2.12	.00626	-.2422	-.0004	-38.69
-.05	.00633	-.0101	.0001	-1.60
2.00	.00694	.2190	-.0001	31.54
4.12	.00705	.4576	.0002	64.93
6.05	.00711	.6719	.0007	94.49
8.12	.00830	.9056	.0020	109.08
10.47	.00978	1.1547	.0052	118.06
11.32	.01082	1.2400	.0066	114.60
13.13	.01309	1.4101	.0109	107.69
14.73	.01738	1.5376	.0164	88.47
15.21	.01886	1.5713	.0185	83.33
16.18	.02249	1.6279	.0237	72.39
17.46	.03427	1.6669	.0295	48.64
18.35	.25142	1.2593	-.0980	5.01
19.10	.30417	1.0541	-.1288	3.47

Table III. Force Coefficients at $M = 0.25$ for Free Transition

$R = 3.29 \times 10^6$

α, deg.	c_d	c_ℓ	c_m	ℓ/d
-4.00	.00736	-.4258	-.0028	-57.88
-2.00	.00656	-.2178	-.0011	-33.21
.00	.00662	-.0045	.0003	-.68
.05	.00661	.0005	.0004	.07
2.06	.00614	.2169	.0015	35.34
4.25	.00662	.4509	.0030	68.12
6.09	.00738	.6491	.0044	87.91
8.33	.01189	.8916	.0068	74.99
10.13	.01263	1.0752	.0096	85.16
11.39	.01403	1.1982	.0134	85.43
12.28	.01529	1.2713	.0146	83.17
13.10	.01759	1.3397	.0170	76.18
14.32	.02165	1.4185	.0222	65.52
15.20	.02708	1.4576	.0262	53.83
16.16	.23673	1.1493	-.0883	4.85
17.66	.25620	1.1435	-.0869	4.46
18.61	.27777	1.1636	-.0868	4.19

$R = 3.98 \times 10^6$

α, deg.	c_d	c_ℓ	c_m	ℓ/d
-4.00	.00717	-.4284	-.0024	-59.76
-2.08	.00648	-.2274	-.0010	-35.11
.01	.00653	-.0019	.0000	-.29
1.99	.00688	.2104	.0010	30.57
4.04	.00655	.4326	.0023	66.01
6.24	.00723	.6542	.0154	90.49
8.19	.01047	.8794	.0067	83.98
10.36	.01229	1.1089	.0091	90.22
12.51	.01490	1.3071	.0147	87.76
13.24	.01677	1.3658	.0172	81.45
14.11	.01953	1.4269	.0209	73.05
15.17	.02487	1.4860	.0258	59.75
16.34	.05556	1.4104	.0183	25.39
17.11	.25278	1.1775	-.0904	4.66
18.19	.26552	1.1703	-.0897	4.41
19.12	.28717	1.1760	-.0881	4.10

$R = 5.95 \times 10^6$

α, deg.	c_d	c_ℓ	c_m	ℓ/d
-4.22	.00715	-.4512	.0010	-63.12
-2.13	.00630	-.2329	-.0040	-36.97
-.03	.00623	-.0119	-.0002	-1.92
-.01	.00634	-.0078	-.0002	-1.23
2.09	.00672	.2245	.0005	33.41
3.99	.00725	.4325	.0012	59.66
6.00	.00694	.6557	.0026	94.45
8.06	.00803	.8740	.0046	108.84
10.13	.01173	1.1034	.0074	94.10
11.17	.01189	1.2096	.0092	101.73
12.09	.01262	1.2960	.0116	102.69
13.14	.01465	1.3929	.0152	95.07
14.34	.01784	1.4835	.0204	83.16
15.15	.02157	1.5364	.0248	71.22
16.21	.02903	1.5616	.0310	53.80
17.32	.23316	1.1335	-.0924	4.86
18.41	.25539	1.1233	-.1069	4.40

Table III. Concluded

$R = 8.92 \times 10^6$

α, deg.	c_d	c_ℓ	c_m	ℓ/d
-4.01	.00696	-.4493	.0001	-64.58
-2.02	.00638	-.2327	.0001	-36.49
.00	.00673	-.0043	-.0004	-.63
1.93	.00728	.2116	-.0002	29.07
4.13	.00744	.4625	.0002	62.17
6.07	.00778	.6801	.0014	87.39
8.09	.00874	.9081	.0031	103.86
10.12	.01006	1.1258	.0060	111.94
11.20	.01165	1.2352	.0080	106.05
12.15	.01218	1.3285	.0109	109.03
13.14	.01412	1.4188	.0141	100.46
14.14	.01646	1.5002	.0183	91.14
15.28	.02061	1.5724	.0241	76.28
16.13	.02642	1.5948	.0297	60.37
17.29	.23437	1.2748	-.1173	5.44
18.21	.26412	1.1905	-.0907	4.51

$R = 11.95 \times 10^6$

α, deg.	c_d	c_ℓ	c_m	ℓ/d
-4.04	.00680	-.4630	.0004	-68.13
-2.10	.00629	-.2443	.0006	-38.86
-.03	.00653	-.0078	.0000	-1.20
-.03	.00633	-.0085	.0001	-1.34
1.99	.00705	.2211	-.0003	31.37
3.97	.00719	.4464	.0001	62.08
6.23	.00742	.7028	.0011	94.73
8.13	.00879	.9203	.0029	104.64
10.10	.01076	1.1327	.0056	105.31
11.08	.01085	1.2321	.0078	113.61
12.09	.01225	1.3329	.0103	108.77
13.23	.01406	1.4385	.0141	102.29
14.29	.01683	1.5240	.0184	90.56
15.26	.02065	1.5807	.0234	76.54
16.19	.02770	1.6007	.0284	57.79
17.43	.24160	1.2119	-.0942	5.02
18.19	.26570	1.1466	-.1001	4.32

Table IV. Force Coefficients at $M = 0.30$ for Free Transition

$R = 3.90 \times 10^6$

α, deg.	c_d	c_ℓ	c_m	ℓ/d
-4.11	.00727	-.4479	-.0026	-61.60
-1.96	.00651	-.2191	-.0011	-33.66
.04	.00657	.0001	.0000	.02
.05	.00657	.0013	.0001	.19
2.05	.00698	.2216	.0011	31.73
4.19	.00672	.4561	.0028	67.93
6.20	.00743	.6781	.0048	91.27
8.06	.01030	.8821	.0074	85.62
10.15	.01270	1.1089	.0112	87.32
11.11	.01374	1.2014	.0139	87.46
12.10	.01569	1.284	.0167	81.84
13.16	.02122	1.3468	.0221	63.48
14.13	.03118	1.3466	.0292	43.18
15.33	.17380	1.0964	-.0656	6.31
16.46	.24760	1.1197	-.0995	4.52
17.09	.25661	1.1578	-.0878	4.51
18.61	.27777	1.1636	-.0868	4.19

$R = 5.93 \times 10^6$

α, deg.	c_d	c_ℓ	c_m	ℓ/d
-4.37	.00648	-.4894	-.0015	-75.54
-2.02	.00630	-.2316	-.0005	-36.80
-.01	.00635	-.0079	-.0002	-1.25
.03	.00659	-.0026	-.0002	-.40
4.03	.00728	.4452	.0015	61.19
6.08	.00711	.6762	.0031	95.13
8.13	.00822	.9039	.0057	110.01
10.12	.01200	1.1251	.0094	93.78
11.13	.01232	1.2273	.0117	99.58
12.12	.01397	1.3172	.0155	94.26
13.32	.01994	1.3939	.0226	69.91
14.27	.03023	1.3917	.0294	46.04
15.14	.12487	1.2273	.0278	9.83
16.25	.20698	1.1132	.0124	5.38

$R = 8.96 \times 10^6$

α, deg.	c_d	c_ℓ	c_m	ℓ/d
-4.12	.00706	-.4587	-.0001	-64.96
-2.14	.00649	-.2367	.0001	-36.50
-.12	.00673	-.0065	-.0001	-.96
1.85	.00729	.2184	.0000	29.95
3.96	.00752	.4608	.0004	61.30
6.04	.00783	.6995	.0019	89.35
7.97	.00918	.9228	.0041	100.54
10.02	.01023	1.1454	.0079	111.99
11.09	.01215	1.2536	.0105	103.20
12.01	.01336	1.3442	.0147	100.58
13.13	.01829	1.4241	.0223	77.87
14.14	.02821	1.4274	.0298	50.59
15.20	.16128	1.3001	-.0772	8.06
15.99	.20284	1.2011	-.0818	5.92

Table IV. Concluded

$R = 11.90 \times 10^6$

α, deg.	c_d	c_ℓ	c_m	ℓ/d
-4.03	.00720	-.4620	.0010	-64.17
-2.01	.00680	-.2330	.0000	-34.26
.02	.00680	.0030	.0000	.44
2.02	.00780	.2350	.0010	30.13
3.92	.00770	.4550	.0020	59.09
6.05	.00800	.7030	.0050	87.88
8.08	.00890	.9350	.0060	105.06
10.05	.01120	1.1580	.0100	103.39
11.13	.01170	1.2700	.0130	108.55
12.10	.01300	1.3700	.0150	105.38
13.20	.01780	1.4500	.0240	81.46
14.28	.02910	1.4400	.0330	49.48
15.30		1.2950	-.0550	

Table V. Force Coefficients at $M = 0.36$ for Free Transition

$R = 3.93 \times 10^6$

α, deg.	c_d	c_ℓ	c_m	ℓ/d
-3.97	.00727	-.4467	-.0026	-61.48
-2.03	.00659	-.2335	-.0009	-35.41
-.03	.00668	-.0108	.0000	-1.61
.00	.00672	-.0075	.0001	-1.12
2.06	.00702	.2243	.0010	31.97
4.01	.00678	.4460	.0027	65.77
6.34	.00777	.7097	.0053	91.38
8.03	.01036	.8981	.0090	86.69
10.15	.01415	1.1260	.0163	79.60
11.27	.02119	1.1828	.0269	55.81
12.14	.03128	1.2044	.0322	38.51
13.36	.14591	1.1093	-.0394	7.60
14.12	.18655	1.0554	-.0774	5.65

$R = 5.88 \times 10^6$

α, deg.	c_d	c_ℓ	c_m	ℓ/d
-4.00	.00618	-.4722	-.0017	-76.41
-2.04	.00636	-.2387	-.0005	-37.54
-.02	.00646	-.0096	-.0003	-1.49
2.03	.00685	.2291	.0016	33.44
4.08	.00737	.4682	.0019	63.52
6.06	.00789	.6843	.0052	86.70
8.12	.00865	.9171	.0070	105.98
10.18	.01357	1.1439	.0112	84.27
11.23	.02008	1.2171	.0259	60.61
12.12	.02867	1.2274	.0322	42.81
13.30	.09164	1.1671	.0048	12.74
14.24	.15857	1.1641	-.0434	7.34
15.18	.19763	1.1281	-.0670	5.71

$R = 8.90 \times 10^6$

α, deg.	c_d	c_ℓ	c_m	ℓ/d
-4.27	.00718	-.4743	.0003	-66.06
-2.01	.00755	-.2377	-.0017	-31.48
1.95	.00780	.2229	.0021	28.58
3.92	.00800	.4604	.0009	57.55
5.94	.00798	.6971	.0027	87.36
8.03	.00975	.9135	.0007	93.69
10.81	.01785	1.2265	.0233	68.71
12.21	.03055	1.2398	.0294	40.58
13.26	.05821	1.2466	.0190	21.42
13.99	.72320	1.2193	.0228	1.69

Table VI. Force Coefficients at $M = 0.05$ for Transition Fixed With No. 60-W Grit

$R = 0.70 \times 10^6$

α, deg.	c_d	c_ℓ	c_m	ℓ/d
-4.03	.01121	-.3507	-.0055	-31.29
-1.98	.00857	-.1716	-.0050	-20.03
.00	.00872	-.0094	-.0003	-1.08
2.00	.00847	.1545	.0032	18.24
4.00	.01080	.3283	.0070	30.39
6.06	.01237	.5327	.0025	43.07
8.12	.01450	.6878	.0086	47.43
10.15	.01853	.8030	.0171	43.34
11.12	.02147	.8495	.0200	39.56
12.18	.02716	.8957	.0233	32.98
13.19	.08334	.8918	-.0089	10.70
14.10	.15345	.9391	-.0479	6.12
15.32	.16754	.8626	-.0580	5.15
16.03	.21721	.7506	-.0669	3.46
17.29	.23011	.9005	-.0762	3.91
18.15	.23479	.9382	-.0672	4.00

Table VII. Force Coefficients at $M = 0.15$ for Transition Fixed With No. 60-W Grit

$R = 2.00 \times 10^6$

α, deg.	c_d	c_ℓ	c_m	ℓ/d
-4.16	.01213	-.4300	-.0041	-35.44
-2.14	.01080	-.2271	-.0022	-21.03
-.03	.01091	-.0102	-.0005	-.93
.00	.01100	-.0060	-.0001	-.54
1.97	.01084	.1970	.0017	18.17
4.14	.01152	.4219	.0039	36.63
5.98	.01336	.6084	.0063	45.54
8.10	.01631	.8123	.0098	49.82
10.04	.02093	.9789	.0143	46.78
11.22	.02497	1.0644	.0170	42.63
12.25	.02921	1.1276	.0194	38.60
13.15	.03599	1.1647	.0221	32.36
14.15	.21056	.9020	-.0828	4.28
15.17	.23758	.9025	-.0939	3.80

$R = 4.00 \times 10^6$

-4.07	.01099	-.4332	-.0032	-39.42
-2.06	.00952	-.2243	-.0016	-23.55
.00	.00954	-.0075	-.0003	-.78
.02	.00952	-.0052	-.0003	-.54
2.08	.00991	.2130	.0011	21.48
3.93	.01015	.4102	.0024	40.42
5.99	.01119	.6256	.0044	55.90
8.06	.01448	.8262	.0088	57.04
10.04	.01939	1.0068	.0121	51.91
11.04	.02247	1.0844	.0152	48.26
12.06	.02668	1.1518	.0183	43.17
13.18	.03355	1.2003	.0222	35.78
14.26	.04445	1.2068	.0249	27.15
15.03	.22424	.9101	-.0845	4.06

$R = 6.00 \times 10^6$

-4.15	.01048	-.4455	-.0022	-42.53
-2.13	.00905	-.2321	-.0011	-25.64
.00	.00895	-.0043	-.0002	-.48
2.06	.00945	.2145	.0008	22.69
4.06	.00976	.4296	.0020	44.04
6.01	.01116	.6359	.0037	56.99
8.03	.01406	.8354	.0066	59.43
10.12	.01928	1.0209	.0112	52.96
11.17	.02188	1.1002	.0146	50.28
12.05	.02551	1.1585	.0177	45.42
13.24	.03200	1.2083	.0221	37.76
14.02	.03891	1.2169	.0246	31.27
15.06	.21816	.9470	-.0828	4.34
16.16	.25187	.8884	-.0940	3.53

Table VII. Concluded

$R = 8.95 \times 10^6$

α, deg.	c_d	c_ℓ	c_m	ℓ/d
-4.09	.01008	-.4498	-.0020	-44.62
-2.05	.00867	-.2331	-.0007	-26.88
-.01	.00862	-.0107	-.0002	-1.24
.01	.00847	-.0093	.0000	-1.10
2.03	.00905	.2100	.0005	23.21
4.03	.00926	.4262	.0015	46.04
6.12	.01048	.6467	.0042	61.71
8.05	.01340	.8438	.0059	62.97
10.09	.01840	1.0279	.0107	55.85
11.15	.02110	1.1102	.0141	52.61
12.26	.02538	1.1800	.0181	46.49
13.18	.03068	1.2209	.0214	39.79
14.17	.03814	1.2289	.0243	32.22
15.08	.21771	.7151	.0767	3.28
16.27	.25842	.9974	-.1008	3.86

$R = 12.10 \times 10^6$

-4.07	.01004	-.4506	-.0016	-44.86
-2.01	.00834	-.2310	-.0004	-27.70
.01	.00842	-.0088	.0001	-1.04
.08	.00827	-.0024	-.0001	-.29
2.01	.00882	.2074	.0006	23.51
4.01	.00917	.4262	.0013	46.46
6.13	.01036	.6514	.0034	62.85
8.07	.01286	.8474	.0060	65.90
10.26	.01845	1.0438	.0116	56.57
11.23	.02131	1.1209	.0139	52.61
12.37	.02305	.9704	.1128	42.10

Table VIII. Force Coefficients at $M = 0.30$ for Transition Fixed With No. 60-W Grit

α, deg.	c_d	c_ℓ	c_m	ℓ/d
		$R = 4.00 \times 10^6$		
-4.18	.01124	-.4607	-.0040	-40.99
-2.14	.00969	-.2421	-.0021	-24.98
-.04	.00964	-.0100	-.0004	-1.04
-.03	.00967	-.0112	-.0004	-1.16
2.03	.00986	.2171	.0013	22.02
4.03	.01049	.4365	.0033	41.59
6.03	.01203	.6515	.0061	54.18
8.09	.01534	.8647	.0106	56.36
10.09	.02138	1.0389	.0170	48.60
11.58	.02910	1.1333	.0232	38.94
12.26	.11061	.9854	-.0357	8.91
13.04	.18059	.9263	-.0596	5.13
		$R = 6.00 \times 10^6$		
-4.20	.01067	-.4719	-.0033	-44.21
-2.01	.00914	-.2313	-.0014	-25.31
-.04	.00921	-.0115	-.0003	-1.25
.01	.00925	-.0060	-.0003	-.65
1.92	.00947	.2075	.0010	21.92
4.05	.00999	.4456	.0028	44.58
6.00	.01144	.6588	.0053	57.61
8.02	.01458	.8673	.0096	59.50
10.11	.02073	1.0546	.0167	50.87
11.09	.02524	1.1243	.0210	44.54
12.17	.03259	1.1685	.0257	35.86
13.07	.17991	.9609	-.0638	5.34
14.03	.20761	.9278	-.0690	4.47
		$R = 8.95 \times 10^6$		
-4.26	.01040	-.4872	-.0028	-46.85
-2.19	.00880	-.2562	-.0012	-29.12
-.01	.00860	-.0084	-.0002	-.97
.00	.00863	-.0063	-.0001	-.73
2.08	.00927	.2285	.0008	24.66
3.94	.00956	.4379	.0023	45.81
6.18	.01117	.6859	.0053	61.41
8.21	.01450	.8984	.0100	61.98
10.08	.02016	1.0672	.0167	52.93
11.27	.02559	1.1490	.0217	44.90
12.12	.03171	1.1816	.0263	37.26
13.31	.18204	.9565	-.0710	5.25
14.21	.21204	.9134	-.0724	4.31
		$R = 12.00 \times 10^6$		
-4.07	.01004	-.4707	-.0022	-46.87
-1.96	.00851	-.2351	-.0009	-27.62
-.02	.00826	-.0112	-.0001	-1.35
.00	.00838	-.0088	.0000	-1.05
2.05	.00893	.2237	.0010	25.04
4.03	.00939	.4511	.0023	48.05
6.04	.01070	.6724	.0048	62.86
8.15	.01377	.8957	.0095	65.02
11.38	.02580	1.1595	.0228	44.94
12.23	.03140	1.1906	.0263	37.92
13.12	.16692	.9603	-.0588	5.75

Table IX. Force Coefficients at $M = 0.15$ for Transition Fixed With No. 80-W Grit

$R = 2.00 \times 10^6$

α, deg.	c_d	c_ℓ	c_m	ℓ/d
-4.03	.01006	-.4205	-.0018	-41.80
-2.03	.00973	-.2159	-.0007	-22.19
.00	.00992	-.0037	-.0002	-.38
.02	.00995	-.0025	.0002	-.25
1.99	.00979	.2060	.0010	21.04
4.01	.01033	.4187	.0019	40.54
6.11	.01068	.6374	.0040	59.70
8.08	.01286	.8214	.0067	63.85
10.24	.01552	1.0261	.0112	66.12
11.15	.01615	1.1118	.0135	68.86
12.25	.01807	1.2013	.0160	66.47
13.17	.01963	1.2654	.0176	64.47
14.18	.02360	1.3308	.0208	56.39
15.16	.02910	1.3748	.0238	47.24
16.02	.22889	1.0732	-.0815	4.69
16.99	.24907	1.0919	-.0838	4.38

$R = 3.99 \times 10^6$

-4.03	.00930	-.4319	-.0008	-46.47
-2.08	.00852	-.2279	-.0002	-26.74
-.05	.00874	-.0118	.0001	-1.36
.04	.00864	-.0037	-.0001	-.43
2.03	.00865	.2105	.0003	24.33
4.06	.00872	.4300	.0009	49.31
6.13	.00917	.6498	.0020	70.87
8.17	.01120	.8631	.0041	77.10
10.19	.01288	1.0643	.0069	82.66
11.15	.01372	1.1559	.0084	84.25
12.12	.01401	1.2413	.0103	88.59
13.23	.01597	1.3349	.0131	83.58
14.20	.01853	1.4103	.0159	76.10
15.27	.02115	1.4818	.0199	70.06
16.15	.02498	1.5287	.0229	61.20
17.26	.03039	1.5692	.0267	51.64
18.03	.25362	.9899	-.0868	3.90
19.08	.28752	.9033	-.1123	3.14

$R = 5.95 \times 10^6$

-4.04	.00871	-.4417	-.0003	-50.74
-2.14	.00800	-.2385	.0001	-29.79
-.05	.00809	-.0126	.0001	-1.55
2.05	.00816	.2125	.0003	26.05
4.04	.00823	.4316	.0005	52.46
6.09	.00885	.6546	.0012	74.00
8.30	.01050	.8872	.0031	84.47
10.12	.01201	1.0707	.0052	89.19
11.13	.01239	1.1685	.0069	94.33
12.12	.01332	1.2605	.0089	94.64
13.08	.01503	1.3455	.0111	89.51
14.22	.01625	1.4365	.0145	88.40
15.26	.01900	1.5129	.0178	79.64
16.30	.02218	1.5739	.0216	70.95
17.13	.02560	1.6116	.0253	62.95
18.02	.18785	.9967	-.0681	5.31
19.08	.27292	1.1358	-.0989	4.16

Table X. Force Coefficients at $M = 0.30$ for Transition Fixed With No. 80 Grit

$R = 4.00 \times 10^6$

α, deg.	c_d	c_ℓ	c_m	ℓ/d
-4.16	.00958	-.4637	-.0012	-48.40
-2.10	.00869	-.2379	-.0005	-27.38
.00	.00876	-.0043	.0000	-.49
.01	.00874	-.0045	.0001	-.52
2.13	.00879	.2338	.0007	26.61
4.10	.00888	.4546	.0015	51.17
6.02	.00947	.6661	.0032	70.37
8.22	.01156	.9038	.0069	78.20
10.20	.01424	1.1102	.0116	77.95
11.18	.01541	1.2050	.0144	78.19
12.22	.01775	1.2899	.0174	72.66
13.29	.02341	1.3474	.0239	57.56
14.21	.03608	1.3485	.0286	37.38
15.03	.19522	1.1712	-.0647	6.00
16.06	.24735	1.1447	-.0903	4.63
17.37	.26673	1.1407	-.0835	4.28

$R = 6.00 \times 10^6$

-4.17	.00881	-.4746	-.0007	-53.87
-2.04	.00810	-.2377	-.0002	-29.36
.00	.00824	-.0058	.0001	-.70
.04	.00826	-.0023	.0000	-.28
2.06	.00828	.2285	.0002	27.59
4.02	.00832	.4527	.0008	54.40
6.14	.00913	.6895	.0025	75.54
8.11	.01060	.9065	.0053	85.52
10.12	.01420	1.1231	.0096	79.10
11.13	.01598	1.2230	.0121	76.54
12.09	.01605	1.3117	.0161	81.75
13.40	.02360	1.3900	.0236	58.90
14.31	.03430	1.3824	.0296	40.30
15.08	.14073	1.2059	-.0485	8.57
16.12	.20900	1.1508	-.0893	5.51

Table XI. Force Coefficients at $M = 0.15$ for Transition Fixed With No. 120 Grit

$R = 3.95 \times 10^6$

α, deg.	c_d	c_ℓ	c_m	ℓ/d
-4.13	.00924	-.4508	-.0009	-48.80
-2.00	.00857	-.2251	-.0003	-26.26
.03	.00865	-.0080	-.0001	-.93
.05	.00874	-.0048	.0000	-.55
2.09	.00867	.2165	.0003	24.98
4.09	.00872	.4336	.0009	49.75
6.05	.00924	.6448	.0020	69.80
8.19	.01100	.8703	.0040	79.13
10.08	.01272	1.0623	.0067	83.54
11.25	.01334	1.1722	.0083	87.88
12.29	.01396	1.2659	.0106	90.67
13.37	.01592	1.3583	.0135	85.35
14.31	.01749	1.4309	.0163	81.82
15.14	.02078	1.4934	.0191	71.88
16.25	.02443	1.5528	.0232	63.55
17.29	.03095	1.5919	.0266	51.43
18.05	.25330	1.0423	-.1002	4.11
19.25	.28423	.9771	-.0838	3.44

$R = 6.00 \times 10^6$

-4.01	.00843	-.4466	-.0001	-52.98
-2.12	.00789	-.2425	.0002	-30.72
-.01	.00811	-.0120	.0001	-1.48
.01	.00804	-.0122	.0008	-1.52
2.15	.00823	.2236	.0004	27.18
4.11	.00879	.4397	.0004	50.03
6.01	.00842	.6487	.0011	77.00
8.08	.00995	.8701	.0026	87.47
10.10	.01175	1.0775	.0049	91.73
11.23	.01248	1.1849	.0069	94.97
12.13	.01282	1.2720	.0082	99.21
13.26	.01408	1.3699	.0109	97.29
14.30	.01628	1.4571	.0143	89.51
15.27	.01790	1.5280	.0175	85.39
16.16	.02093	1.5838	.0208	75.68
17.24	.02519	1.6347	.0251	64.90
18.18	.25194	1.1886	-.0910	4.72
19.25	.28015	1.1888	-.0931	4.24

$R = 8.90 \times 10^6$

-3.99	.00806	-.4503	.0007	-55.89
-2.01	.00745	-.2339	.0005	-31.40
-.01	.00761	-.0138	.0001	-1.81
1.97	.00776	.2050	.0001	26.40
4.01	.00765	.4329	-.0001	56.58
6.13	.00823	.6659	.0007	80.91
8.21	.00929	.8920	.0019	96.01
10.08	.01108	1.0852	.0038	97.92
11.11	.01169	1.1871	.0056	101.53
12.12	.01249	1.2839	.0073	102.80
13.16	.01350	1.3754	.0098	101.90
14.24	.01499	1.4664	.0120	97.80
15.54	.01814	1.5663	.0164	86.35
16.30	.02003	1.6172	.0190	80.72
17.21	.02266	1.6627	.0226	73.37
18.38	.02685	1.7026	.0270	63.41
19.53	.28685	1.3083	-.0900	4.56
20.35	.30408	1.3512	-.1132	4.44

Table XII. Force Coefficients at $M = 0.30$ for Transition Fixed With No. 120 Grit

$R = 3.90 \times 10^6$

α, deg.	c_d	c_ℓ	c_m	ℓ/d
-4.06	.00936	-.4610	-.0011	-49.23
-1.93	.00853	-.2252	-.0004	-26.41
.01	.00881	-.0073	.0000	-.83
.05	.00874	-.0044	.0001	-.50
2.05	.00876	.2205	.0007	25.18
4.13	.00889	.4565	.0015	51.37
6.09	.00952	.6745	.0033	70.89
8.19	.01160	.9025	.0067	77.79
10.17	.01397	1.1102	.0114	79.46
11.15	.01502	1.2047	.0141	80.20
12.15	.01702	1.2880	.0169	75.68
13.21	.02194	1.3482	.0231	61.45
14.11	.03255	1.3517	.0276	41.53
15.12	.16052	1.1447	-.0590	7.13
16.07	.25551	.8559	-.1171	3.35

$R = 5.95 \times 10^6$

-4.02	.00876	-.4646	-.0004	-53.02
-2.08	.00799	-.2472	.0000	-30.93
.02	.00823	-.0088	.0001	-1.07
.03	.00825	-.0064	.0001	-.78
1.99	.00824	.2168	.0003	26.32
4.06	.00835	.4544	.0009	54.42
6.21	.00903	.6975	.0024	77.27
8.29	.01069	.9270	.0054	86.70
10.21	.01290	1.1345	.0096	87.96
11.11	.01380	1.2247	.0119	88.77
12.22	.01591	1.3268	.0162	83.40
13.23	.02009	1.3908	.0220	69.23
14.32	.03175	1.3941	.0289	43.91
15.18	.14253	1.2873	-.0635	9.03
16.02	.20164	1.1514	-.0843	5.71

$R = 8.90 \times 10^6$

-4.07	.00834	-.4784	.0001	-57.40
-2.11	.00757	-.2557	.0005	-33.77
.01	.00766	-.0101	.0002	-1.32
.05	.00765	-.0052	.0003	-.69
2.22	.00785	.2459	.0001	31.33
4.15	.00778	.4691	.0004	60.29
6.29	.00843	.7238	-.0012	85.87
8.13	.00976	.9263	.0042	94.91
10.16	.01204	1.1468	.0081	95.22
11.10	.01290	1.2435	.0107	96.36
12.31	.01496	1.3570	.0159	90.70
13.47	.02043	1.4266	.0236	69.83
14.29	.03011	1.4195	.0303	47.15
15.29	.14155	1.2813	-.0358	9.05
16.20	.20968	1.2531	-.0894	5.98
17.08	.23815	1.1755	-.0853	4.94

Table XIII. Force Coefficients at $M = 0.15$ for Transition Fixed With No. 180 Grit

$R = 5.95 \times 10^6$

α, deg.	c_d	c_ℓ	c_m	ℓ/d
-3.99	.00871	-.4363	-.0004	-50.11
-1.98	.00792	-.2213	.0000	-27.93
-.03	.00803	-.0115	.0000	-1.44
.04	.00811	-.0013	.0002	-.15
2.00	.00814	.2113	.0001	25.97
4.06	.00814	.4365	.0003	53.59
6.09	.00851	.6558	.0011	77.10
8.09	.00985	.8689	.0027	88.24
10.18	.01165	1.0809	.0050	92.80
11.13	.01247	1.1731	.0064	94.07
12.10	.01299	1.2644	.0082	97.35
13.31	.01408	1.3676	.0111	97.16
14.08	.01533	1.4316	.0133	93.38
15.24	.01870	1.5169	.0173	81.14
16.33	.02186	1.5855	.0213	72.53
17.13	.02513	1.6219	.0247	64.54
18.21	.25899	1.0104	-.1070	3.90
19.27	.43446	1.0664	-.0693	2.45

$R = 8.95 \times 10^6$

-4.07	.00843	-.4550	.0004	-53.99
-2.11	.00753	-.2428	.0005	-32.26
.03	.00765	-.0052	.0001	-.68
2.04	.00793	.2150	-.0001	27.10
4.06	.00780	.4410	-.0001	56.52
6.12	.00808	.6655	.0004	82.41
8.15	.00929	.8868	.0014	95.48
10.16	.01147	1.0947	.0037	95.48
11.10	.01173	1.1852	.0051	101.03
12.11	.01218	1.2813	.0071	105.17
13.11	.01316	1.3716	.0091	104.21
14.36	.01511	1.4750	.0128	97.63
15.31	.01722	1.5487	.0163	89.93
16.46	.02025	1.6187	.0193	79.92
17.33	.02220	1.6611	.0238	74.83
18.59	.25066	1.1825	-.0461	4.72
19.22	.26933	1.2901	-.1036	4.79

$R = 11.95 \times 10^6$

-4.05	.00810	-.4594	.0008	-56.70
-1.98	.00719	-.2337	.0007	-32.50
.01	.00736	-.0121	.0003	-1.65
.03	.00726	-.0097	.0003	-1.34
2.07	.00763	.2183	.0001	28.60
4.09	.00746	.4437	-.0002	59.45
6.01	.00768	.6571	.0003	85.60
8.03	.00907	.8777	.0011	96.81
10.12	.01092	1.0983	.0032	100.60
11.27	.01126	1.2150	.0047	107.93
12.12	.01175	1.2954	.0062	110.26
13.24	.01376	1.3965	.0093	101.48
14.16	.01491	1.4736	.0117	98.83
15.15	.01683	1.5514	.0143	92.20
16.27	.01996	1.6212	.0190	81.23
17.28	.02378	1.6693	.0236	70.18
18.18	.23217	1.3948	-.1218	6.01

Table XIV. Force Coefficients at $M = 0.30$ for Transition Fixed With No. 180 Grit

$R = 5.95 \times 10^6$

α, deg.	c_d	c_ℓ	c_m	ℓ/d
-4.04	.00891	-.4610	-.0007	-51.74
-2.03	.00800	-.2363	-.0002	-29.53
.00	.00816	-.0045	-.0001	-.56
2.09	.00819	.2321	.0002	28.36
4.00	.00826	.4508	.0007	54.55
6.13	.00893	.6906	.0023	77.30
8.08	.01043	.9074	.0050	87.01
10.23	.01303	1.1359	.0095	87.16
11.10	.01382	1.2241	.0119	88.56
12.34	.01633	1.3354	.0170	81.79
13.23	.02069	1.3693	.0203	66.19
14.15	.03180	1.3815	.0287	43.44
15.06	.14715	1.2390	-.0308	8.42
16.09	.20338	1.2505	-.1093	6.15

$R = 8.85 \times 10^6$

-4.11	.00856	-.4753	-.0003	-55.52
-2.06	.00769	-.2430	.0002	-31.60
-.02	.00767	-.0094	.0001	-1.23
-.02	.00765	-.0090	.0001	-1.17
2.04	.00793	.2282	.0002	28.79
4.07	.00774	.4638	.0003	59.91
6.04	.00828	.6909	.0016	83.48
8.12	.00959	.9276	.0042	96.73
10.09	.01175	1.1582	.0125	98.54
11.17	.01294	1.2515	.0110	96.71
12.16	.01456	1.3433	.0151	92.26
13.17	.01886	1.4155	.0220	75.05
14.12	.02817	1.4173	.0295	50.31
15.35	.15957	1.2265	-.0315	7.69
16.30	.21003	1.2134	-.0704	5.78

$R = 11.90 \times 10^6$

-4.04	.00811	-.4714	-.0004	-58.14
-1.94	.00738	-.2358	.0006	-31.94
-.05	.00737	-.0144	.0001	-1.96
-.03	.00732	-.0126	.0004	-1.72
.00	.00737	-.0102	.0005	-1.38
2.03	.00774	.2290	.0001	29.59
4.08	.00755	.4714	.0002	62.47
6.01	.00798	.6956	.0014	87.19
8.06	.00910	.9285	.0036	102.05
10.24	.01148	1.1684	.0077	101.77
11.18	.01250	1.2678	.0106	101.46
12.28	.01417	1.3711	.0152	96.77
13.34	.01971	1.4250	.0250	72.31
14.35	.03165	1.4225	.0321	44.95
15.27	.16237	1.3117	-.0581	8.08

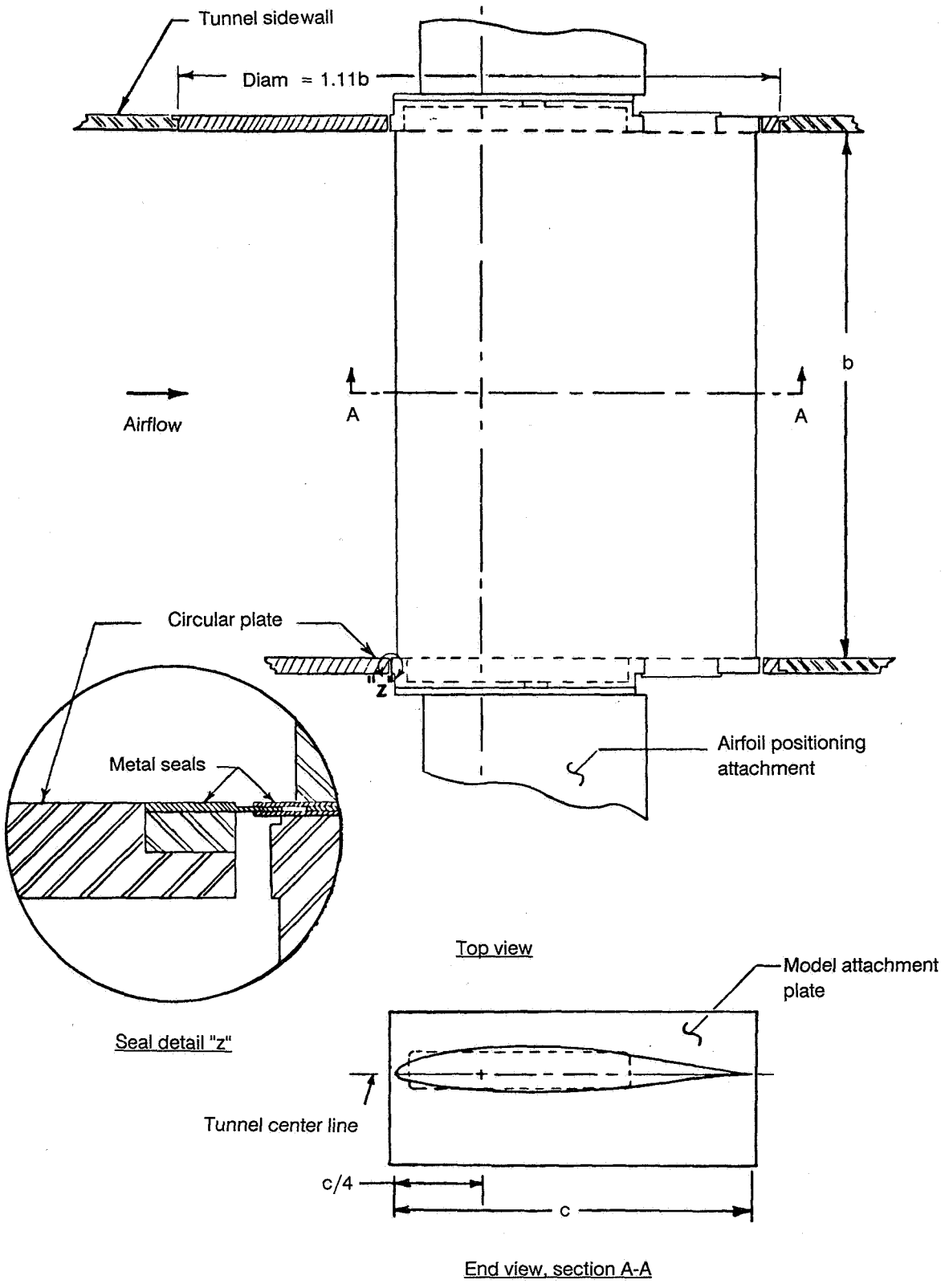

Figure 1. Airfoil mounted in wind tunnel. All dimensions are in terms of airfoil span. $b = 36.00$ in. (91.44 cm).

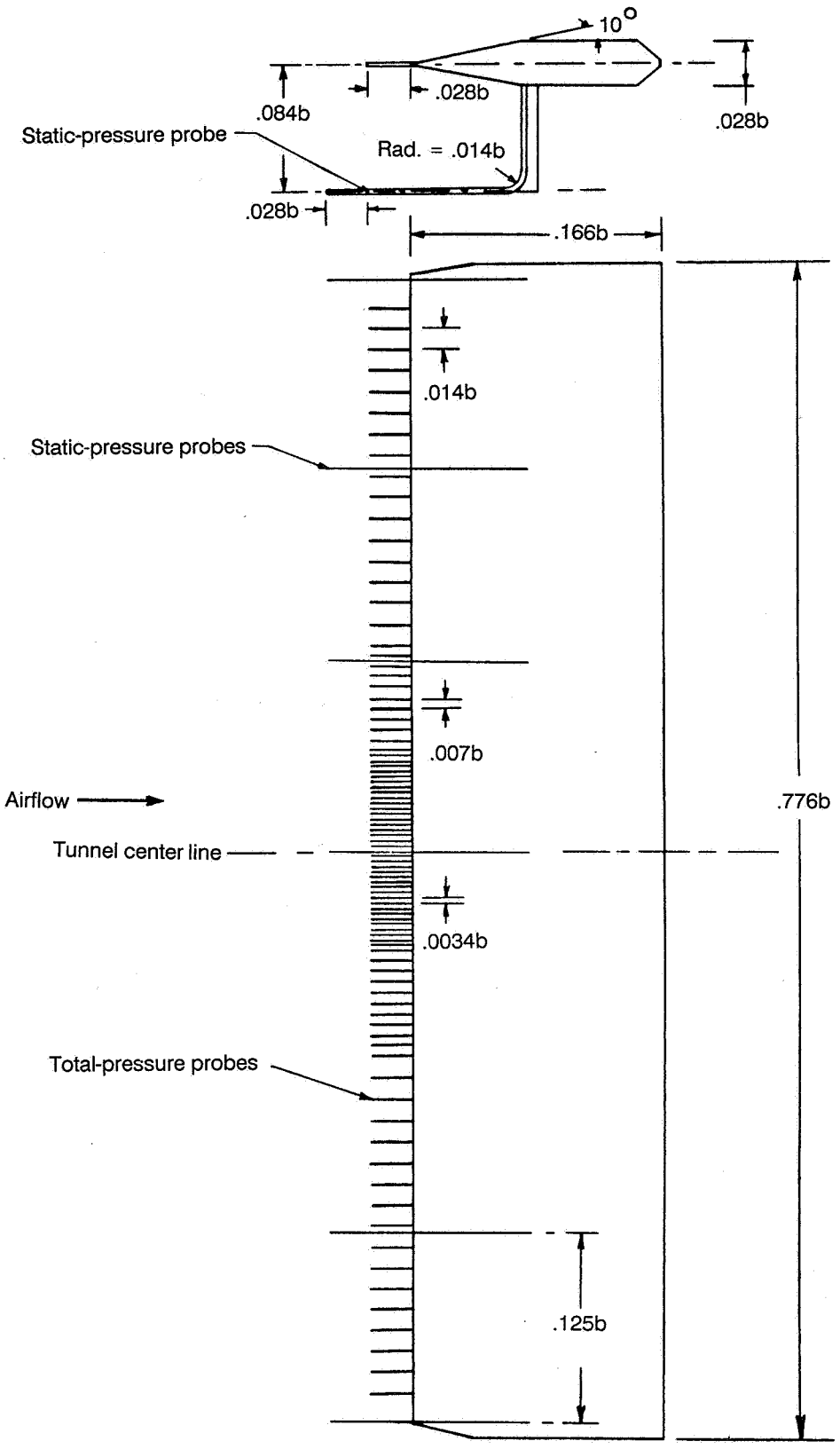

Figure 2. Wake survey rake. All dimensions are in terms of airfoil span. $b = 36.00$ in. (91.44 cm).

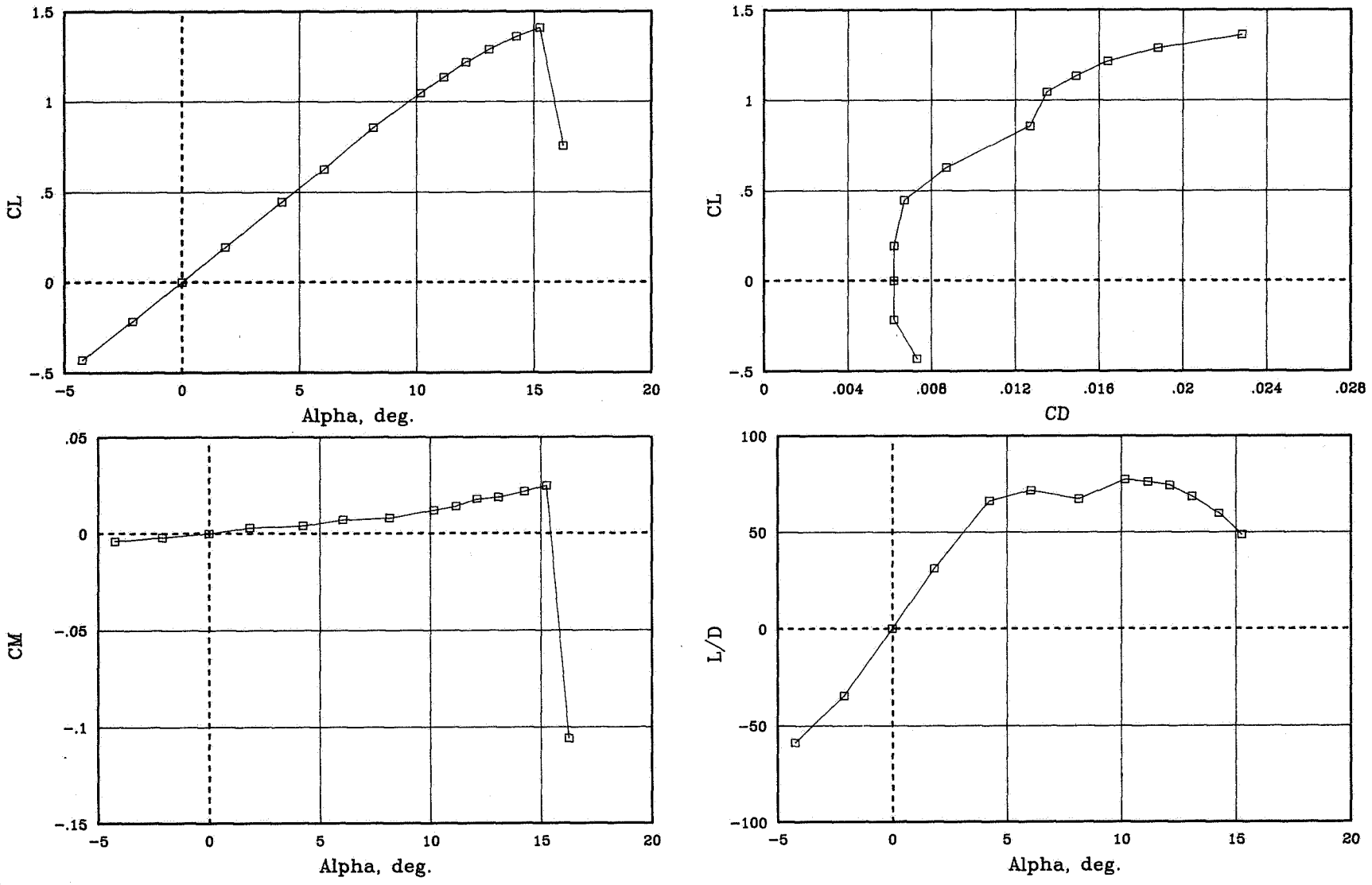

(a) $R = 2.0 \times 10^6$.

Figure 3. Variation of basic aerodynamic characteristics with angle of attack for various Reynolds numbers at $M = 0.15$ for free transition.

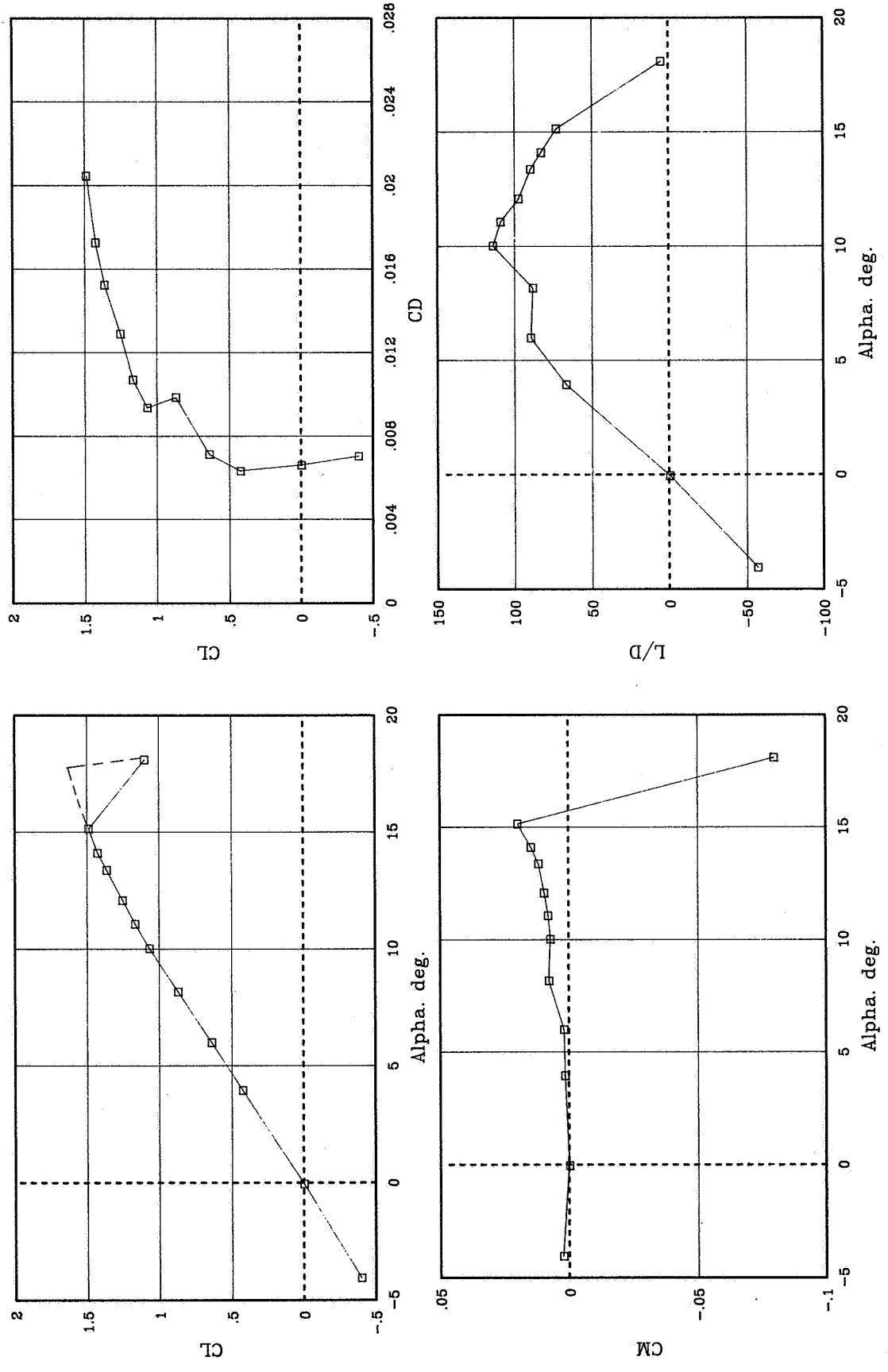

(b) $R = 3.9 \times 10^6$.

Figure 3. Continued.

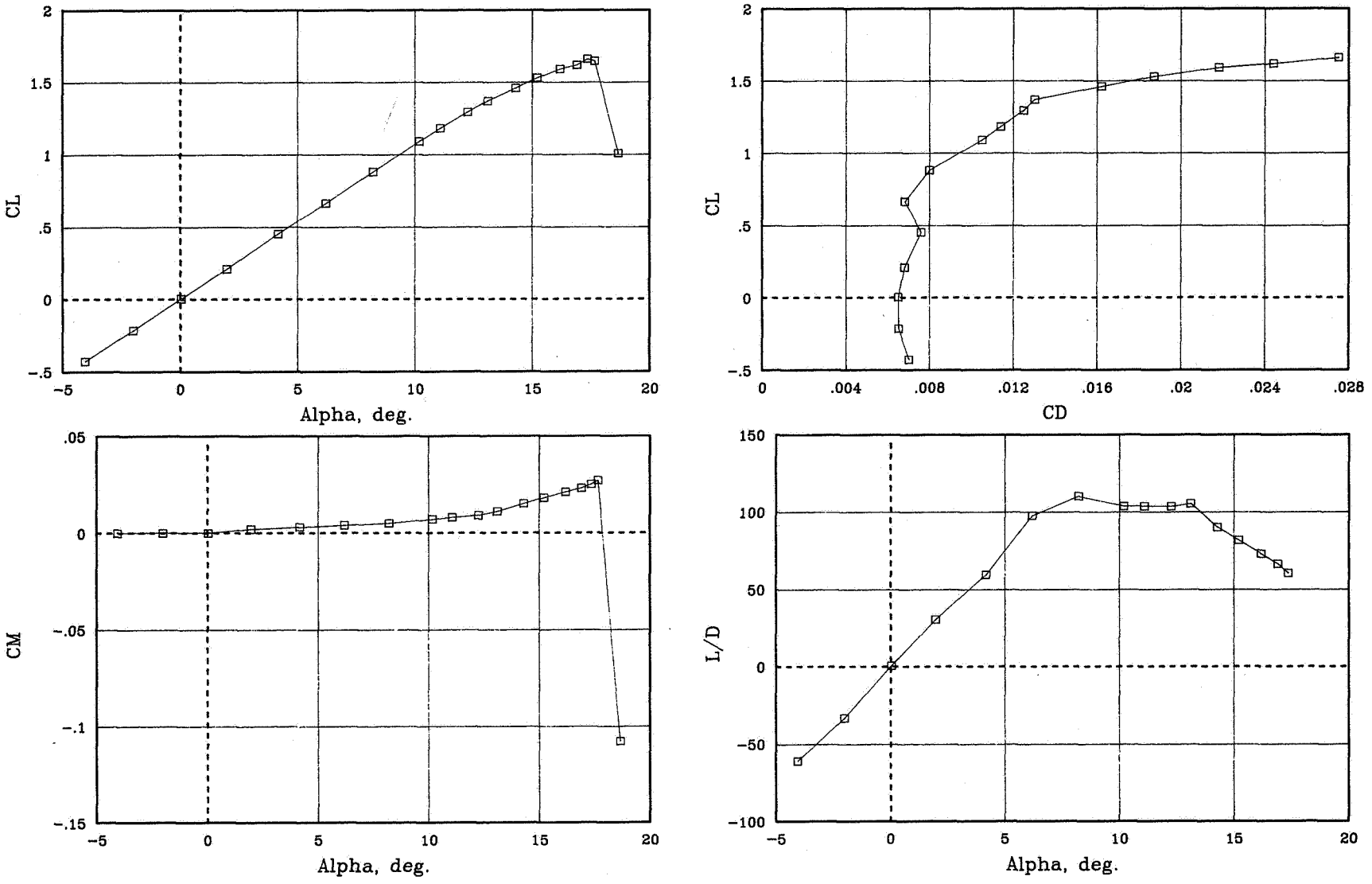

(c) $R = 6.0 \times 10^6$.

Figure 3. Continued.

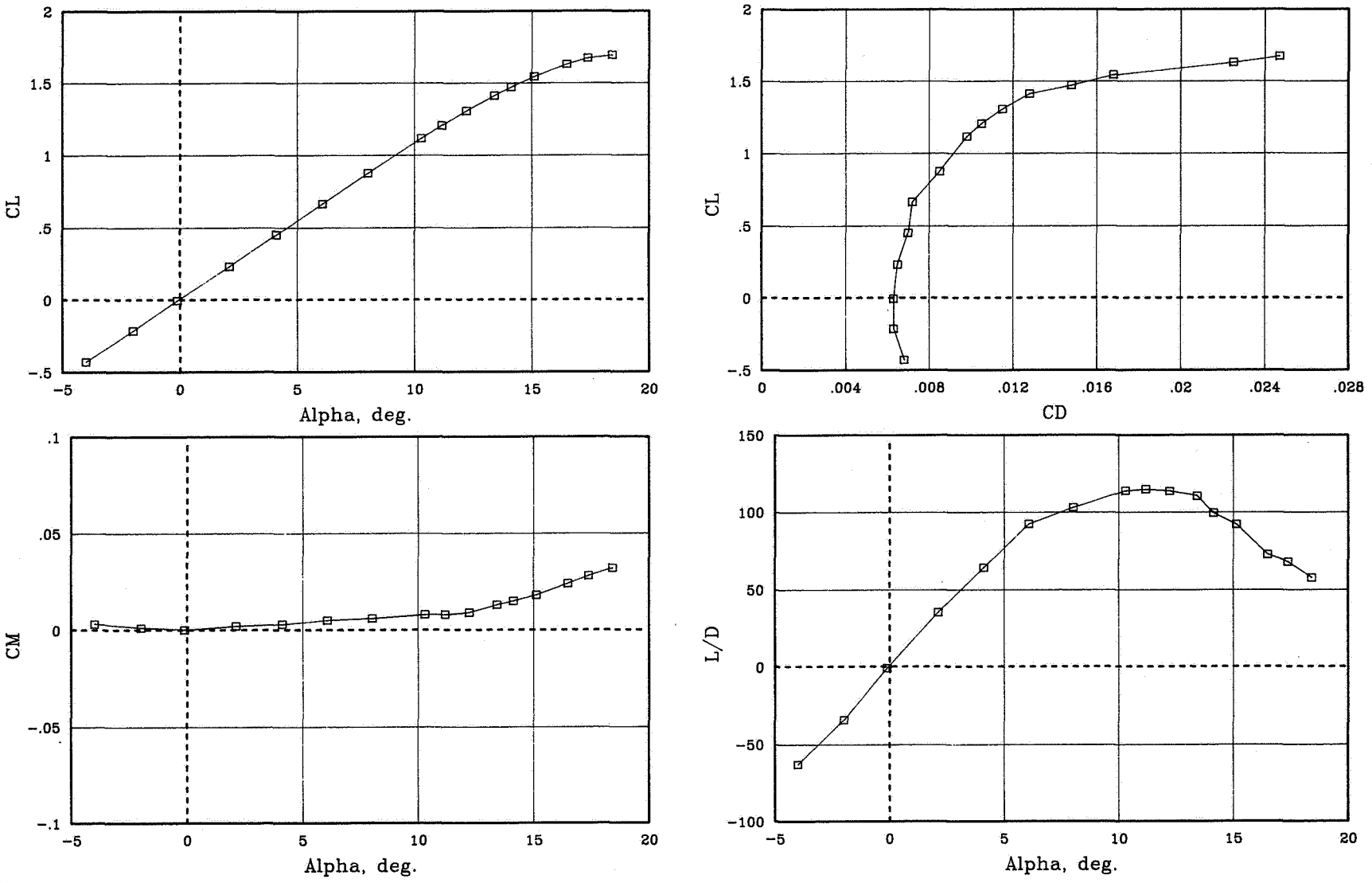

(d) $R = 8.9 \times 10^6$.

Figure 3. Continued.

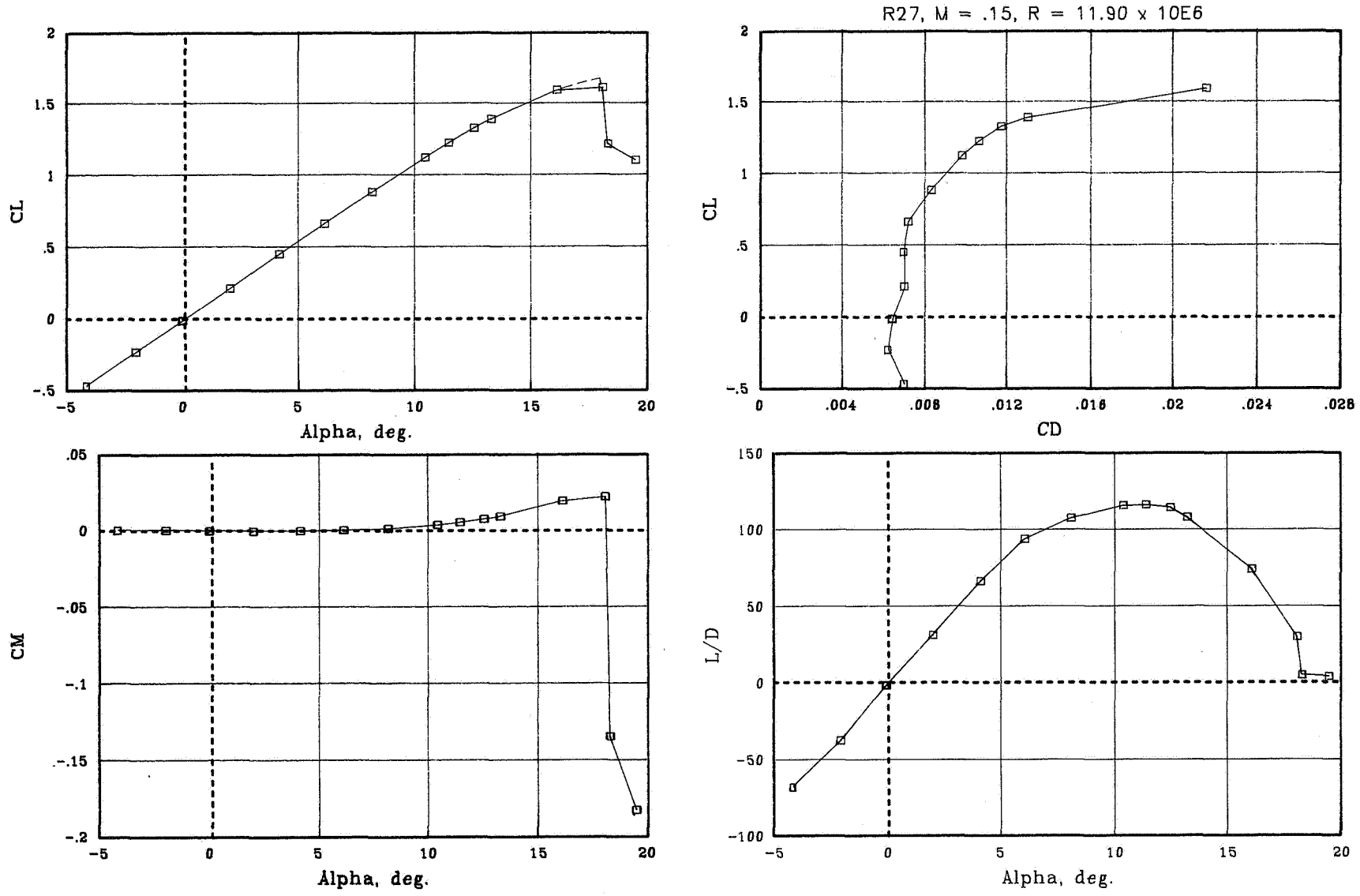

(e) $R = 11.9 \times 10^6$.

Figure 3. Continued.

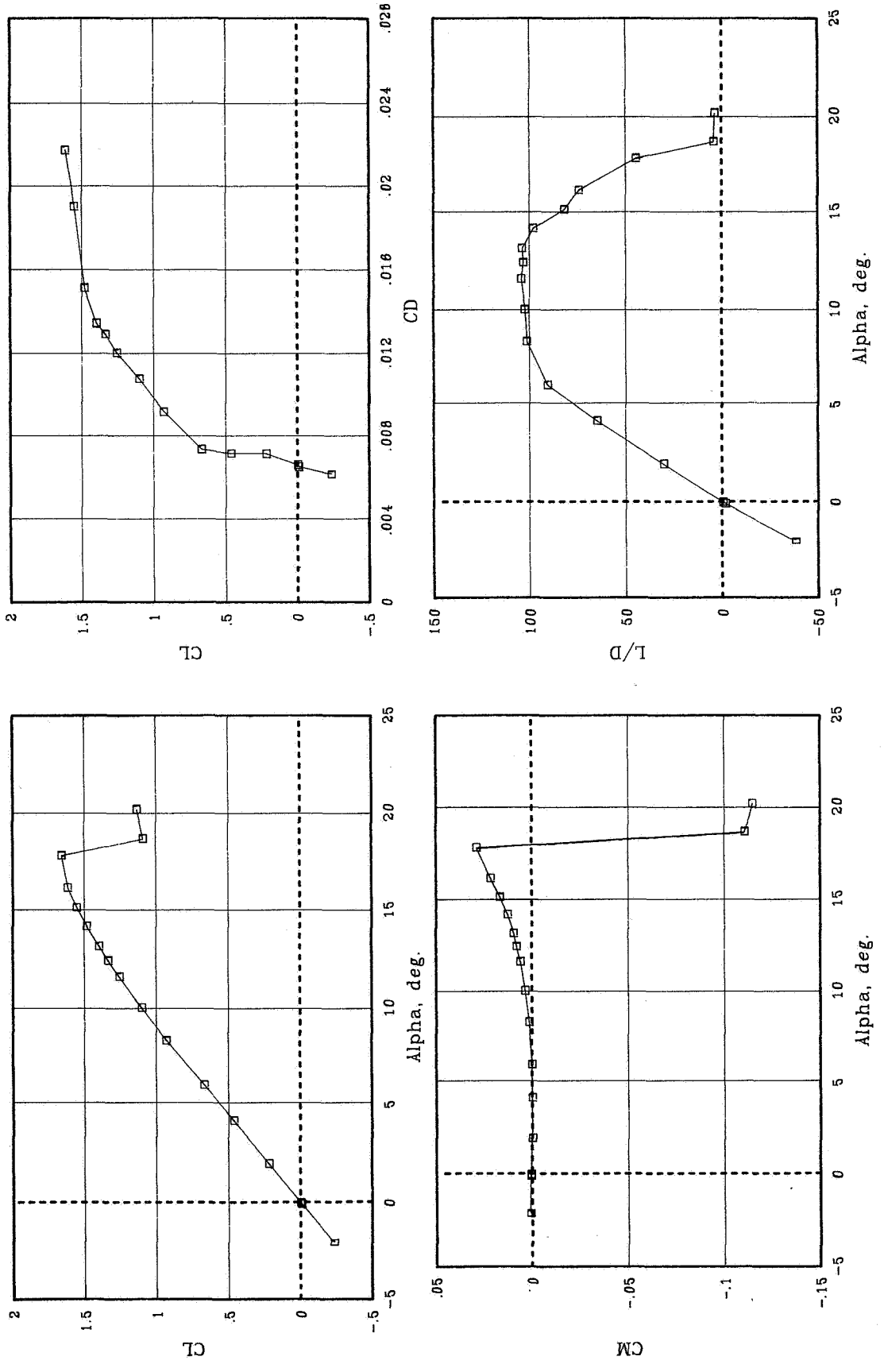

(f) $R = 18.9 \times 10^6$.

Figure 3. Concluded.

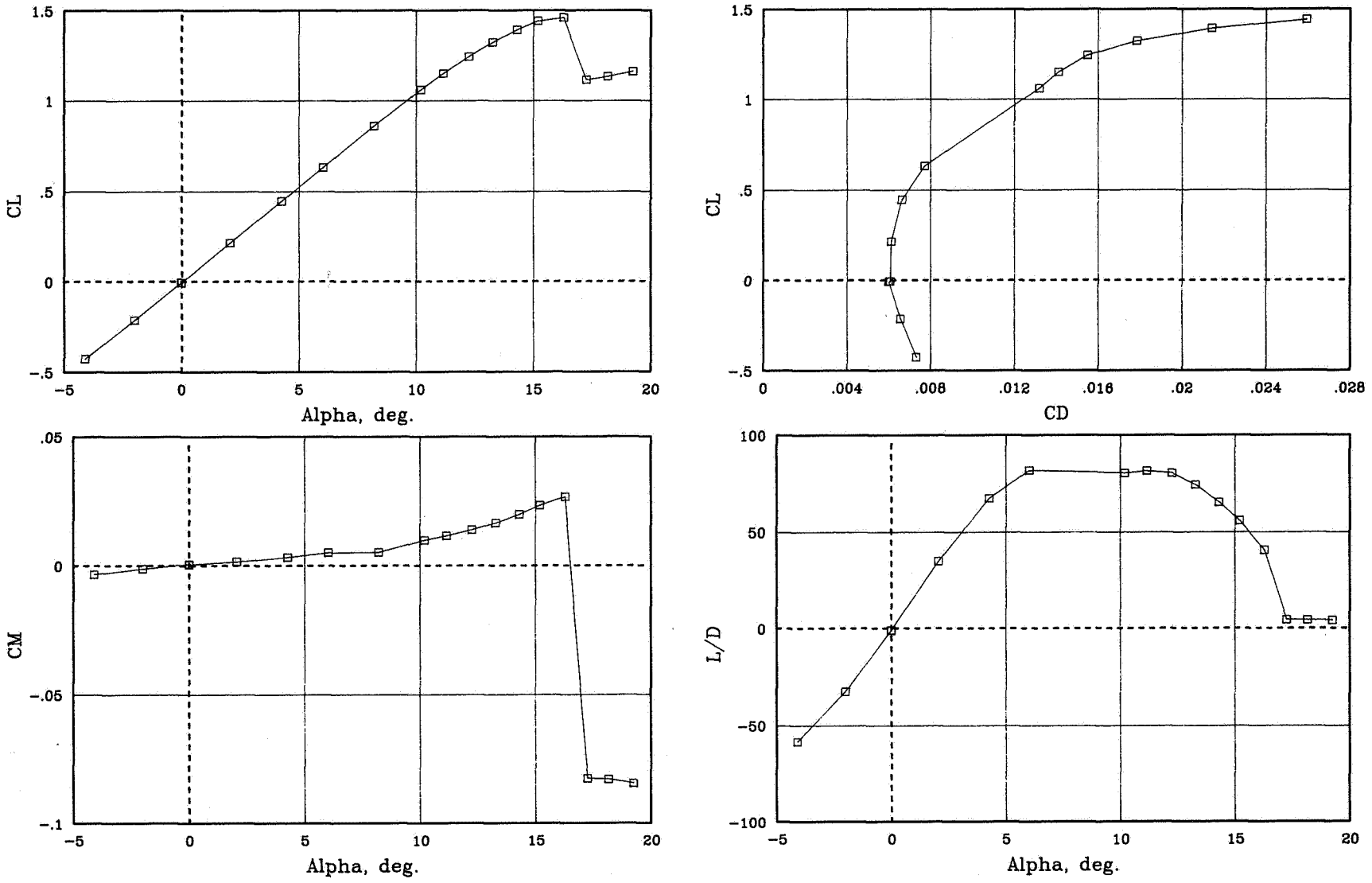

(a) $R = 2.7 \times 10^6$.

Figure 4. Variation of basic aerodynamic characteristics with angle of attack for various Reynolds numbers at $M = 0.20$ for free transition.

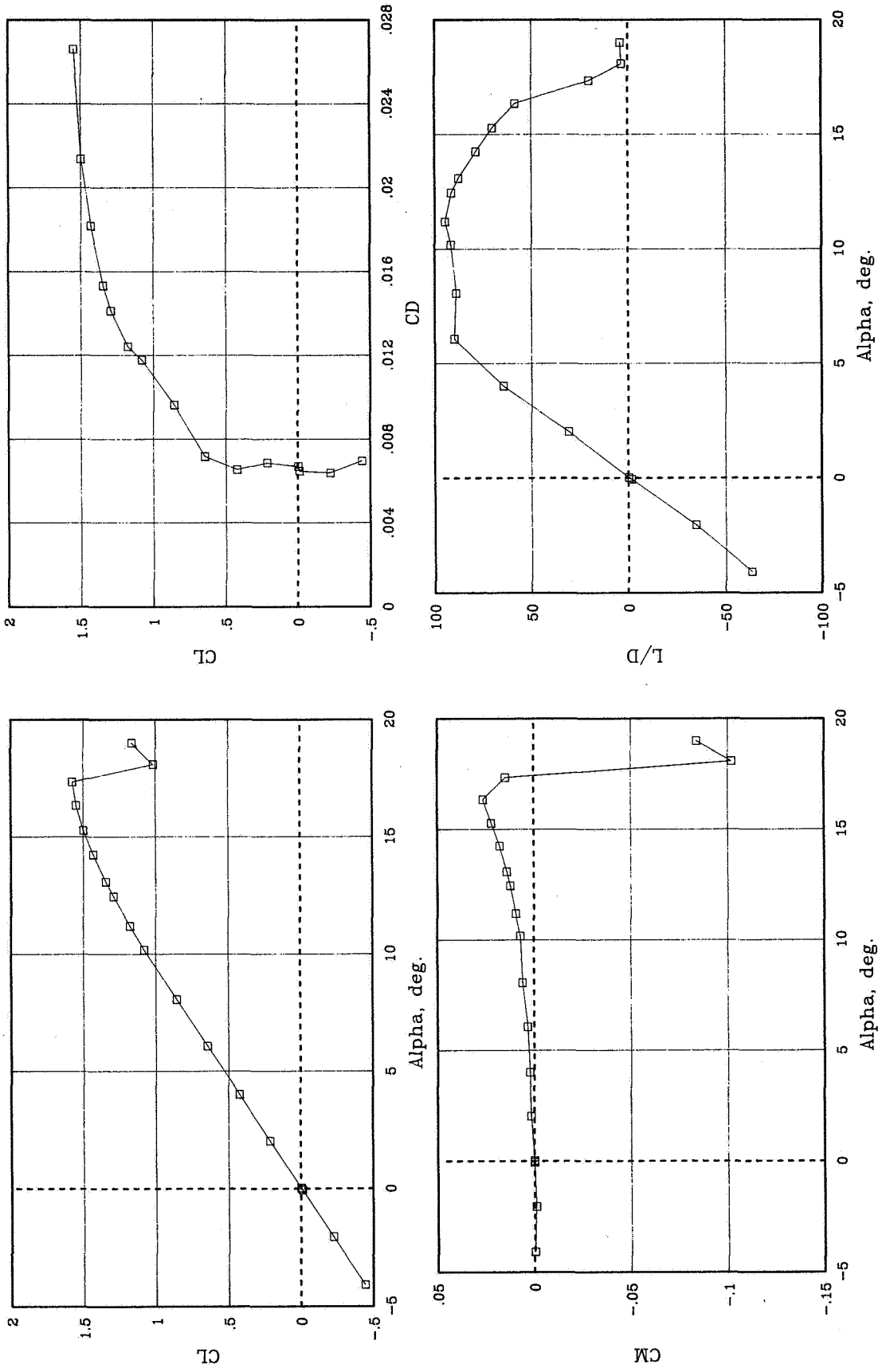

(b) $R = 4.0 \times 10^6$.

Figure 4. Continued.

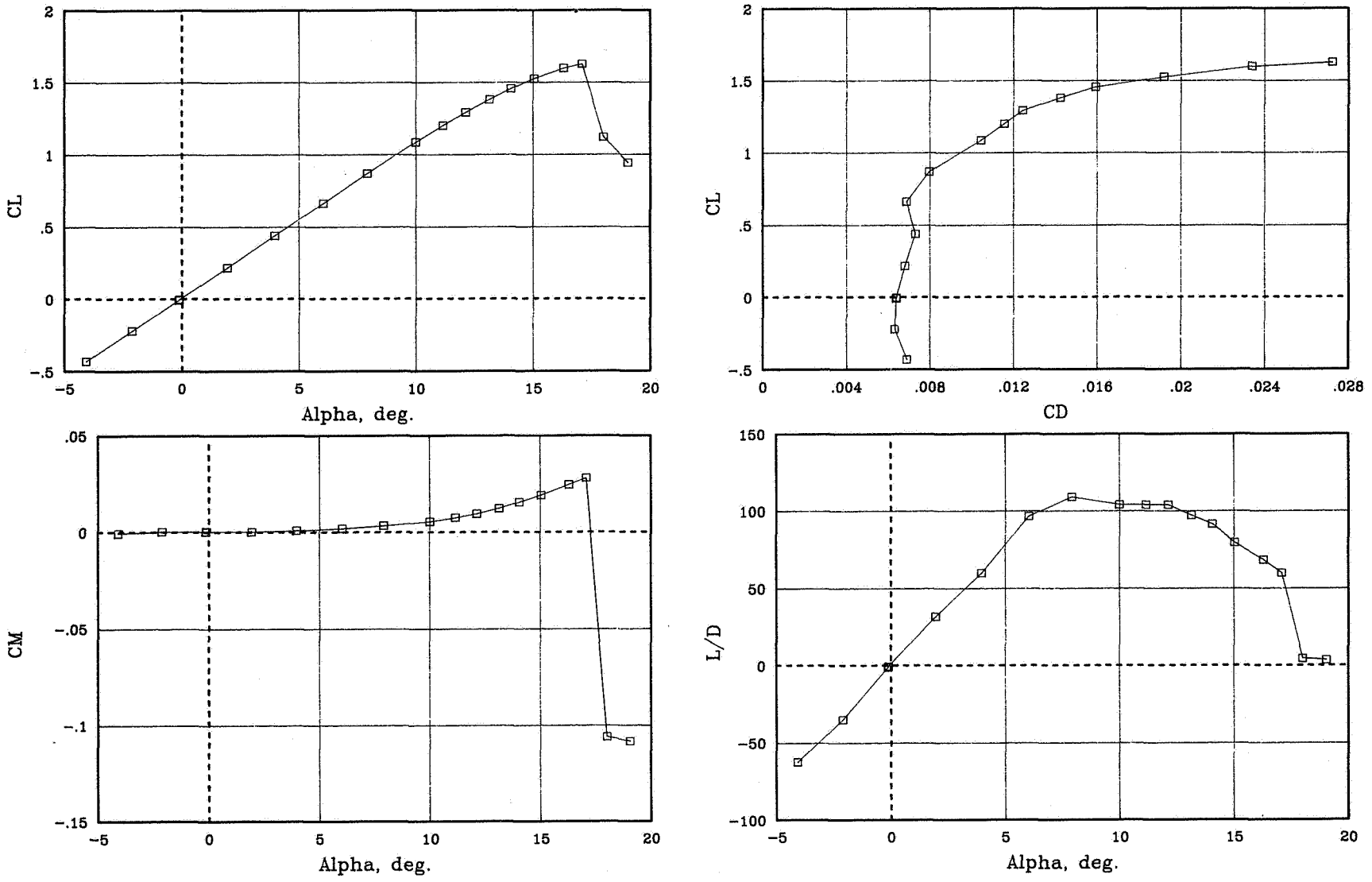

(c) $R = 6.0 \times 10^6$.

Figure 4. Continued.

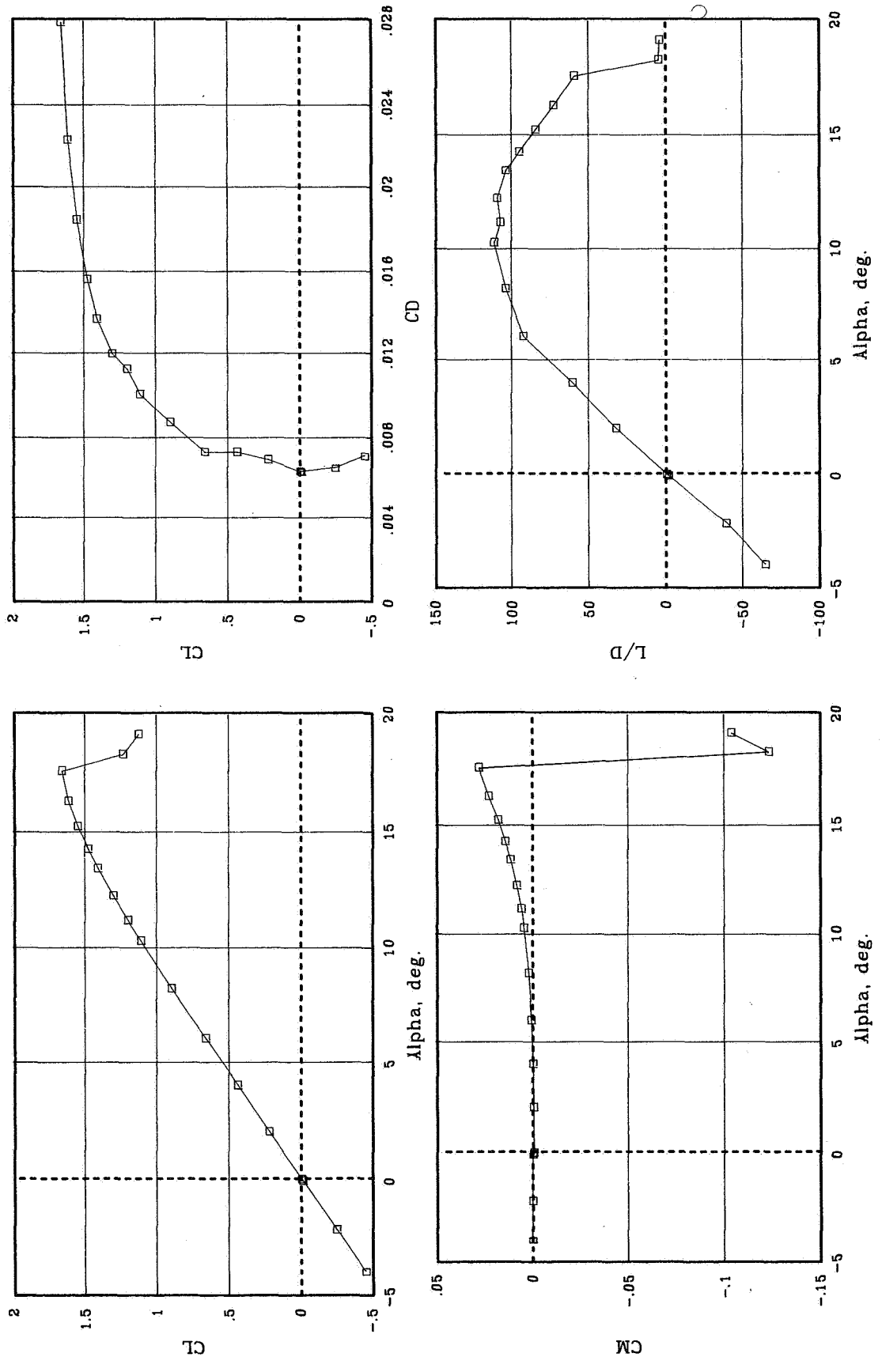

(d) $R = 8.9 \times 10^6$.

Figure 4. Continued.

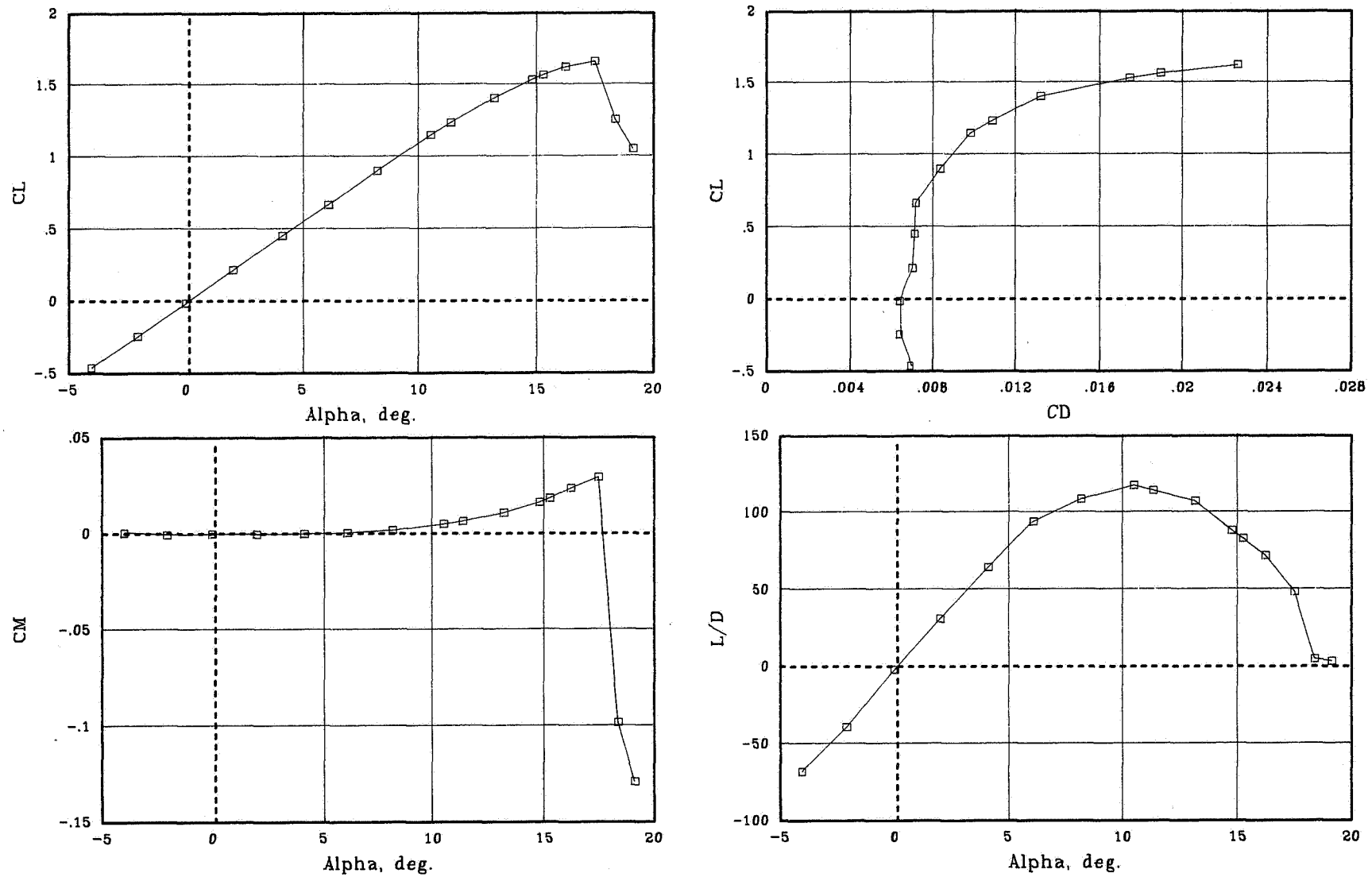

(e) $R = 12.0 \times 10^6$.

Figure 4. Concluded.

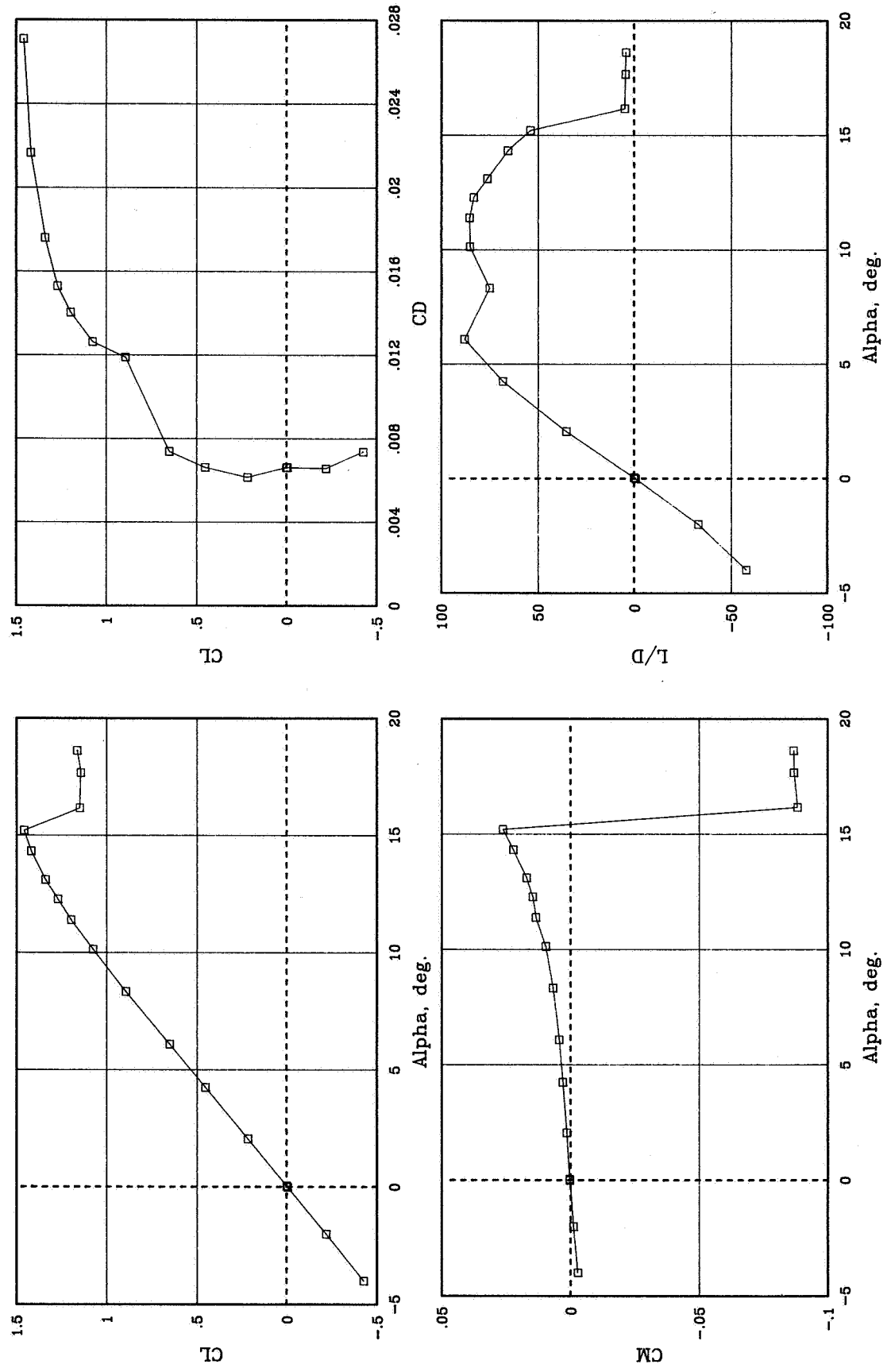

(a) $R = 3.3 \times 10^6$.

Figure 5. Variation of basic aerodynamic characteristics with angle of attack for various Reynolds numbers at $M = 0.25$ for free transition.

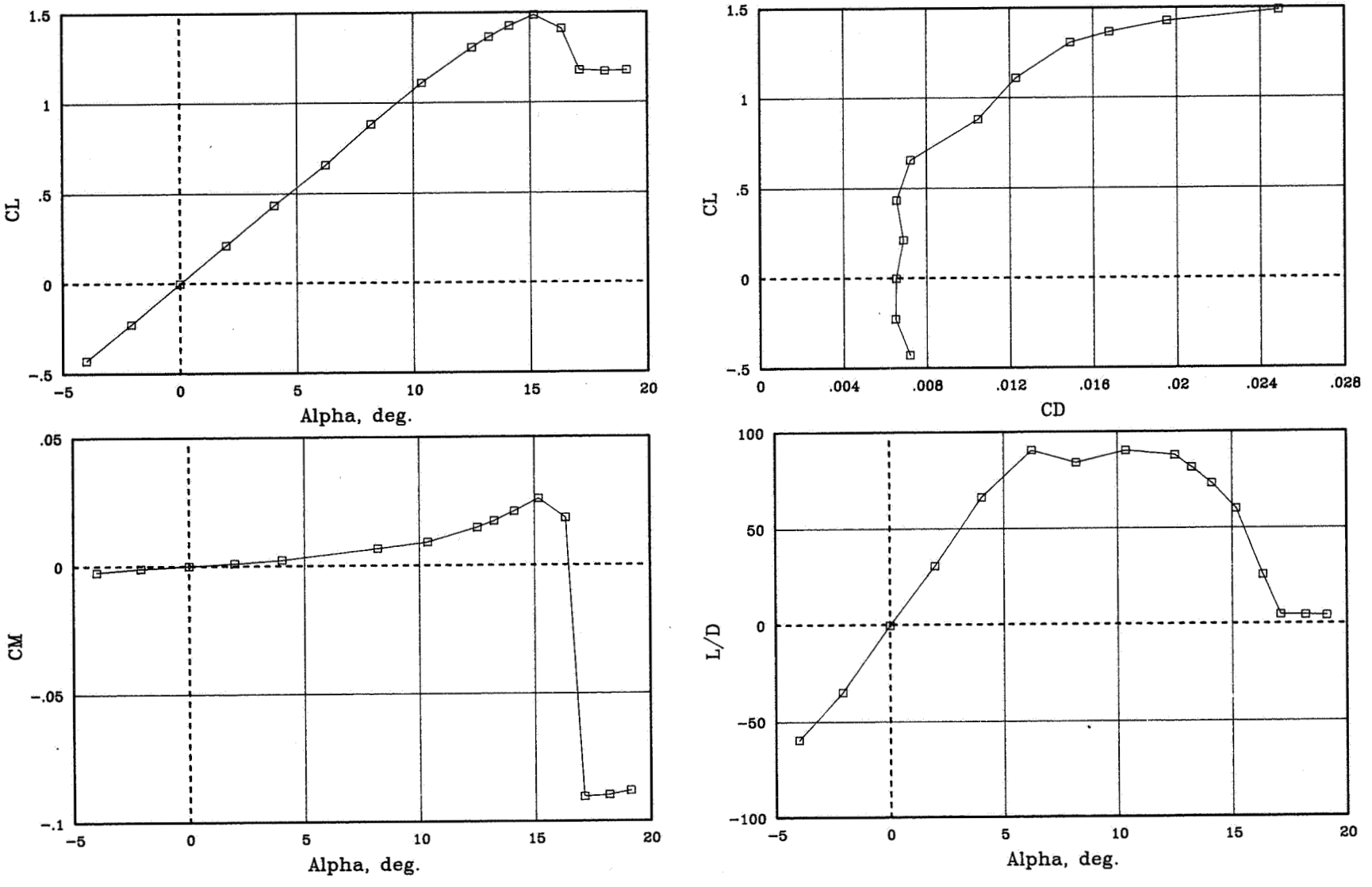

(b) $R = 4.0 \times 10^6$.

Figure 5. Continued.

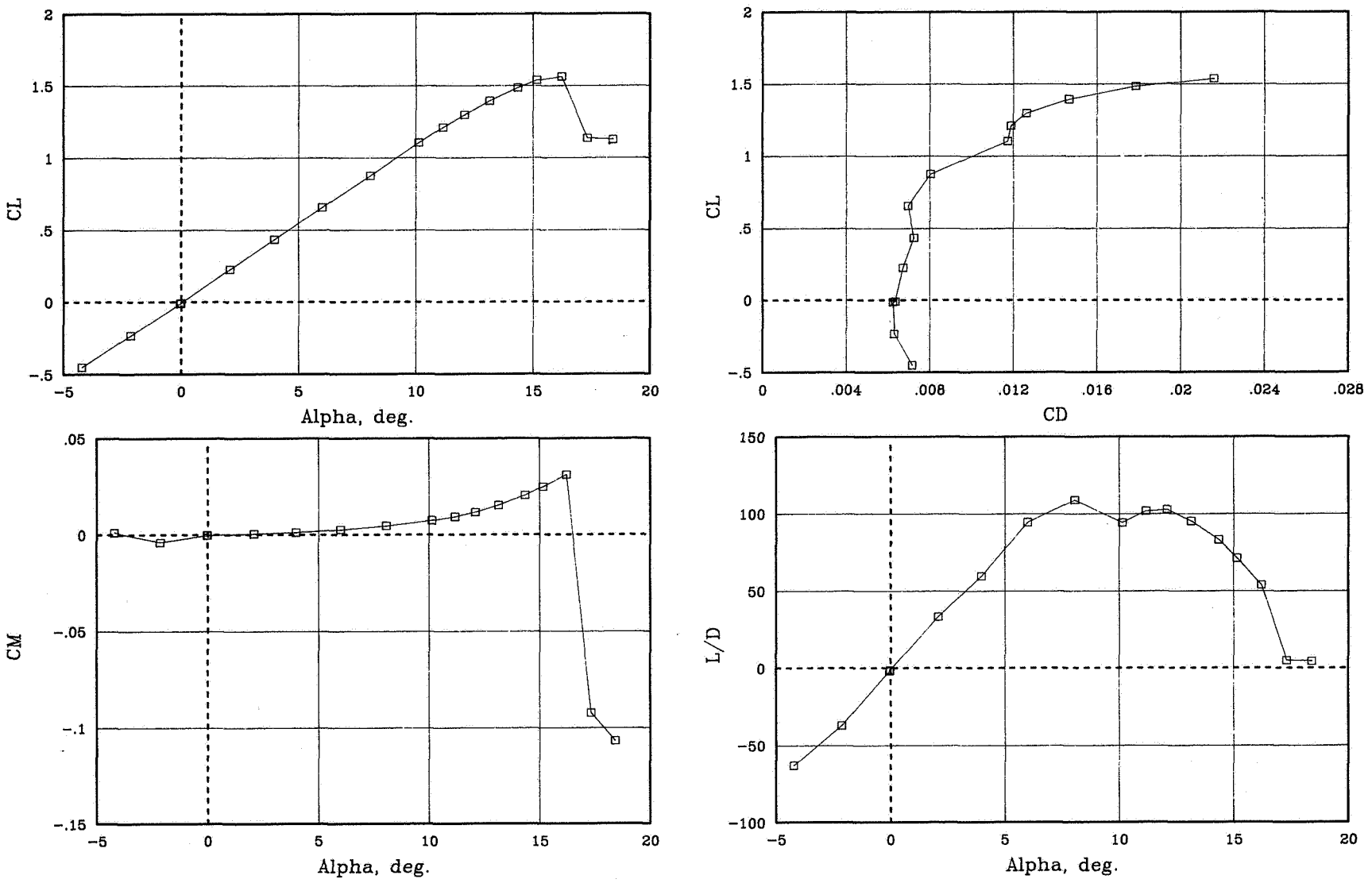

(c) $R = 6.0 \times 10^6$.

Figure 5. Continued.

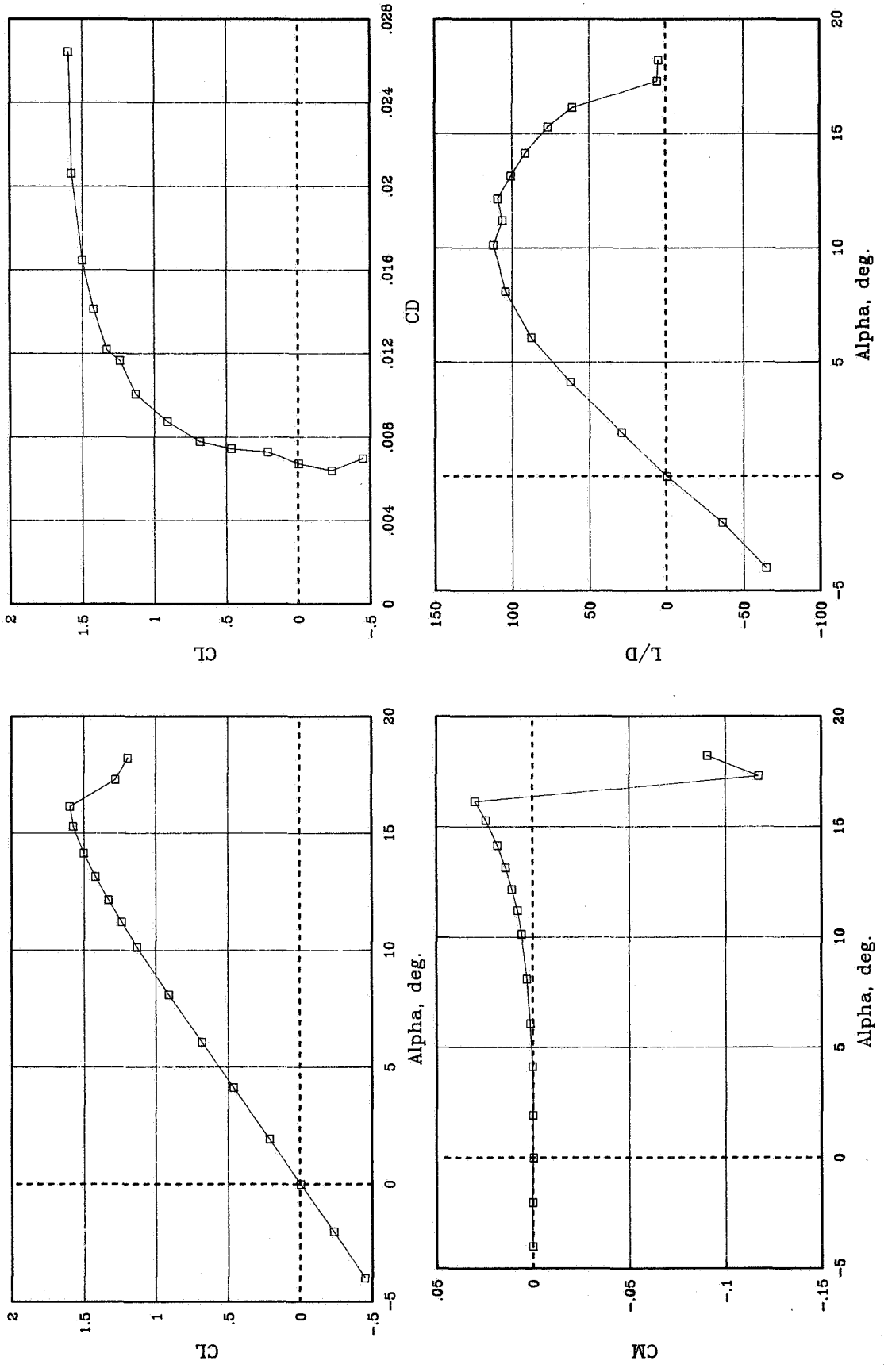

(d) $R = 8.9 \times 10^6$.

Figure 5. Continued.

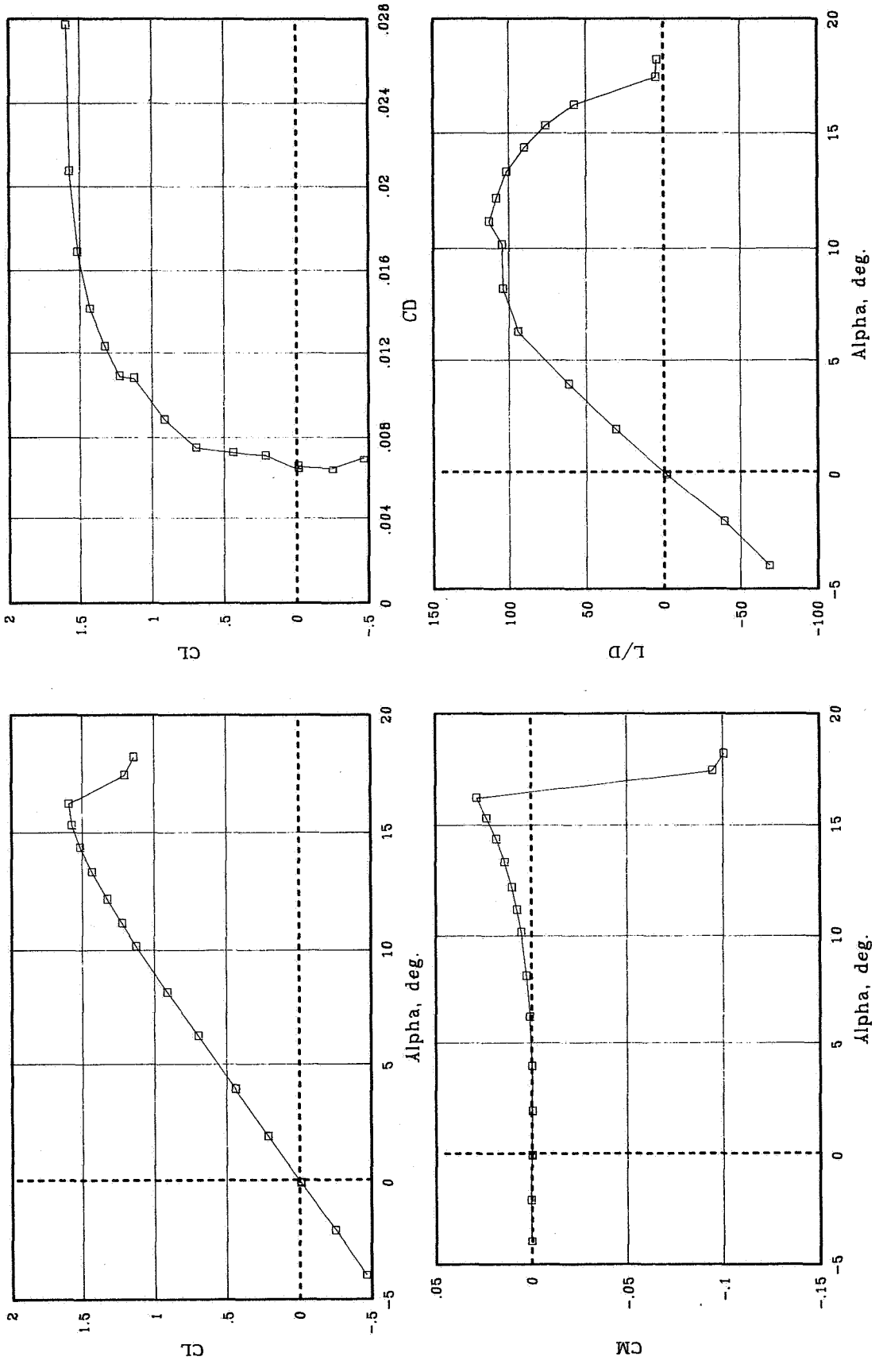

(e) $R = 12.0 \times 10^6$.

Figure 5. Concluded.

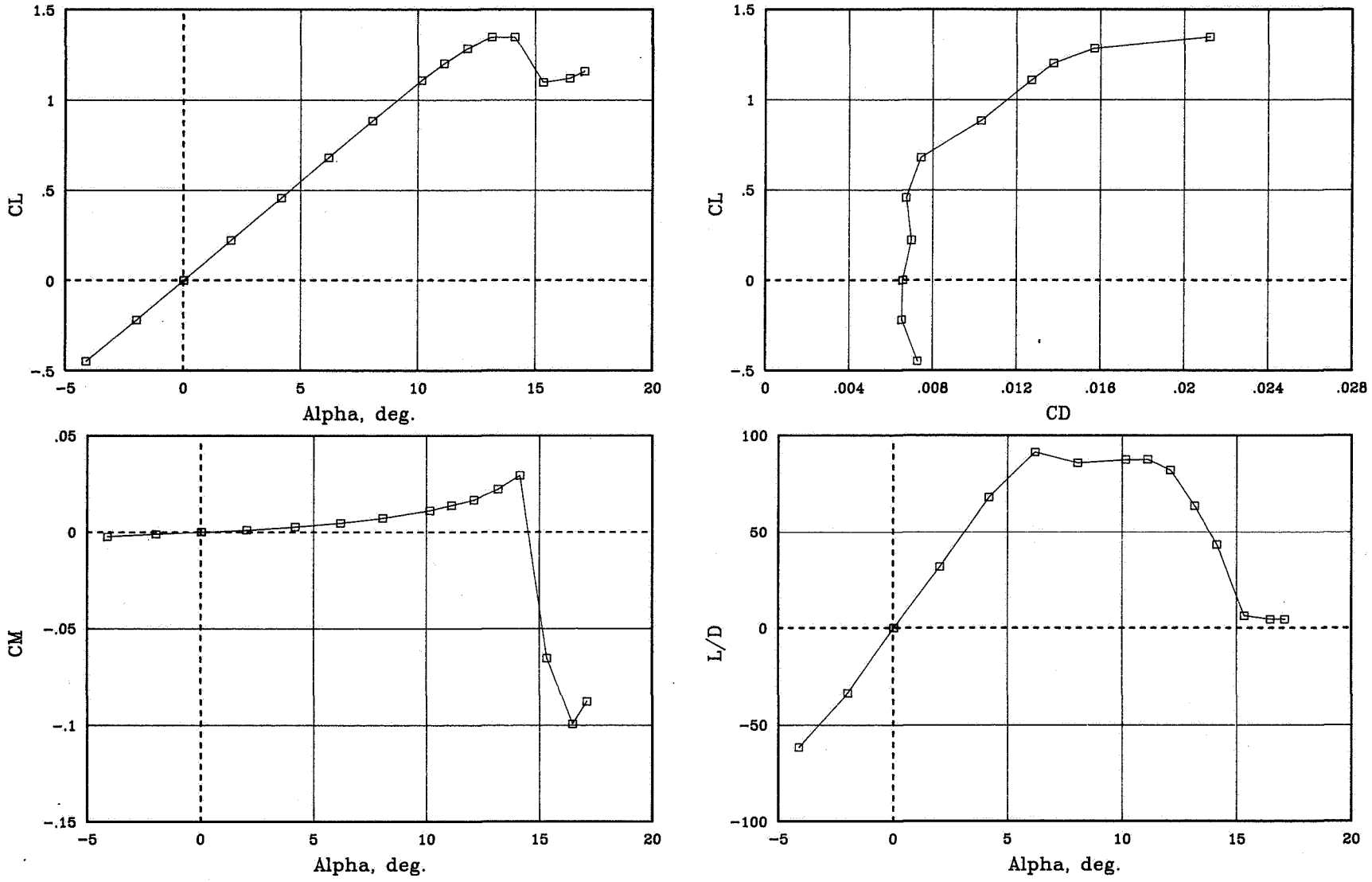

(a) $R = 3.9 \times 10^6$.

Figure 6. Variation of basic aerodynamic characteristics with angle of attack for various Reynolds numbers at $M = 0.30$ for free transition.

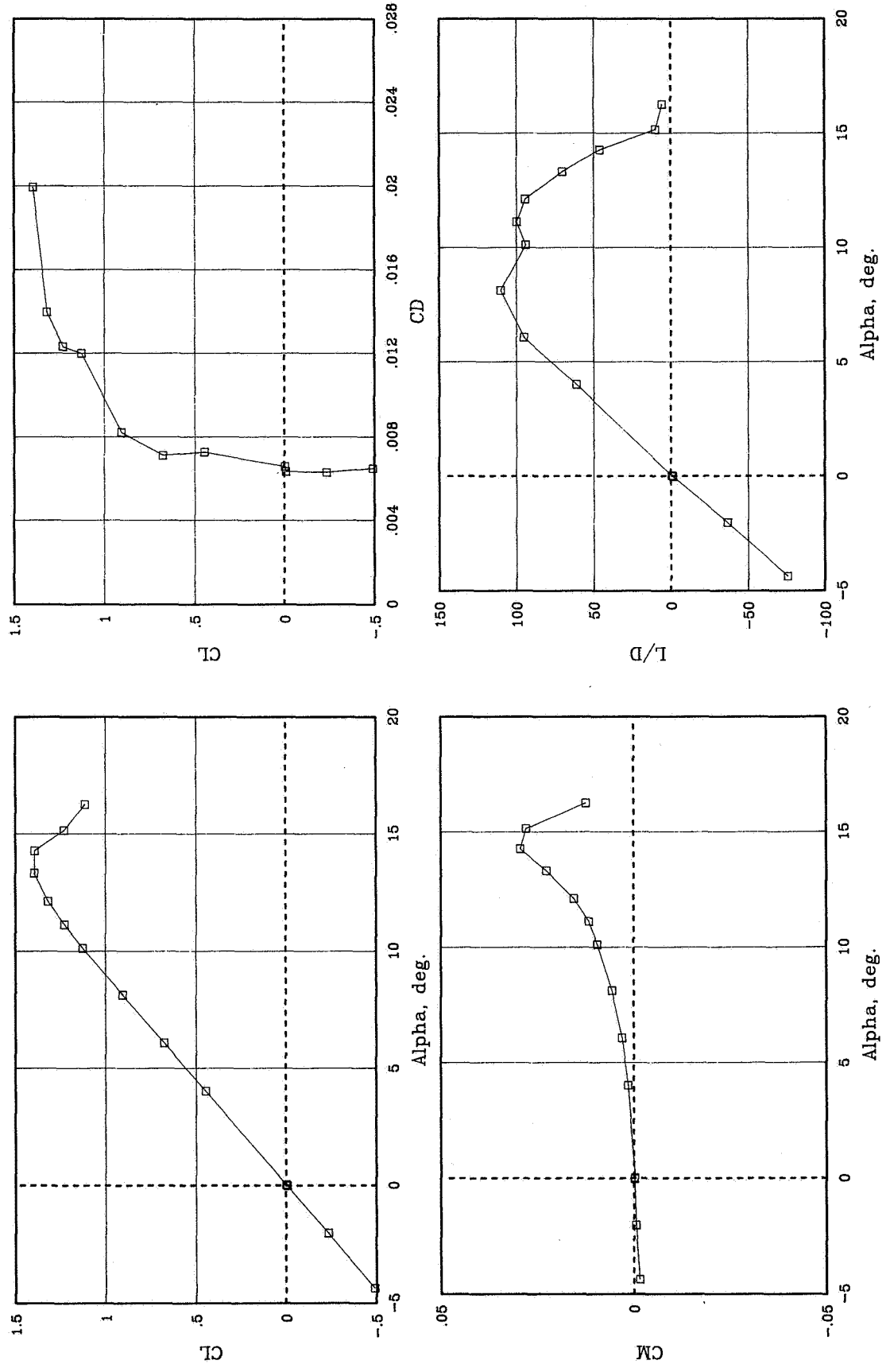

(b) $R = 5.9 \times 10^6$.

Figure 6. Continued.

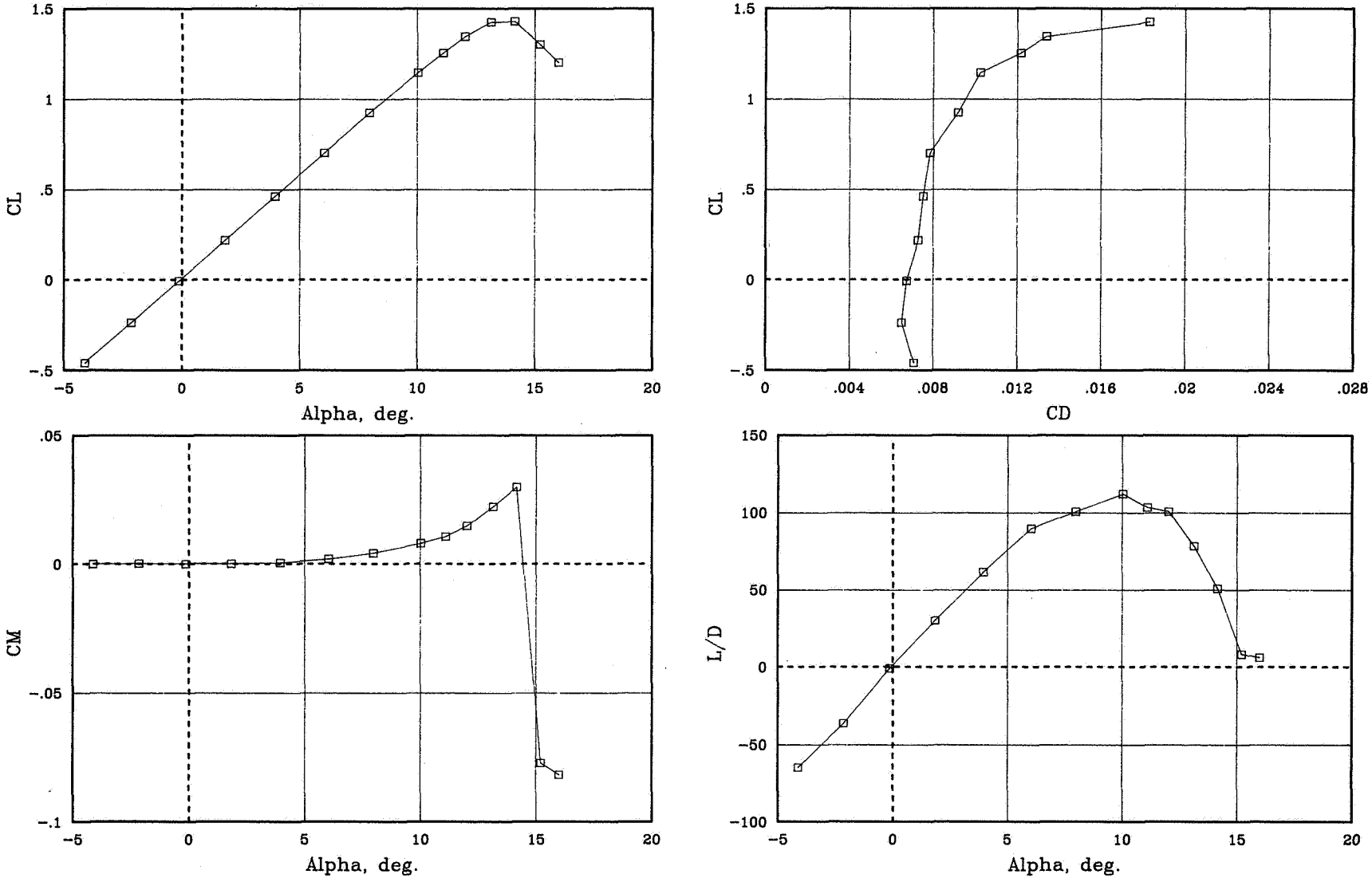

(c) $R = 9.0 \times 10^6$.

Figure 6. Continued.

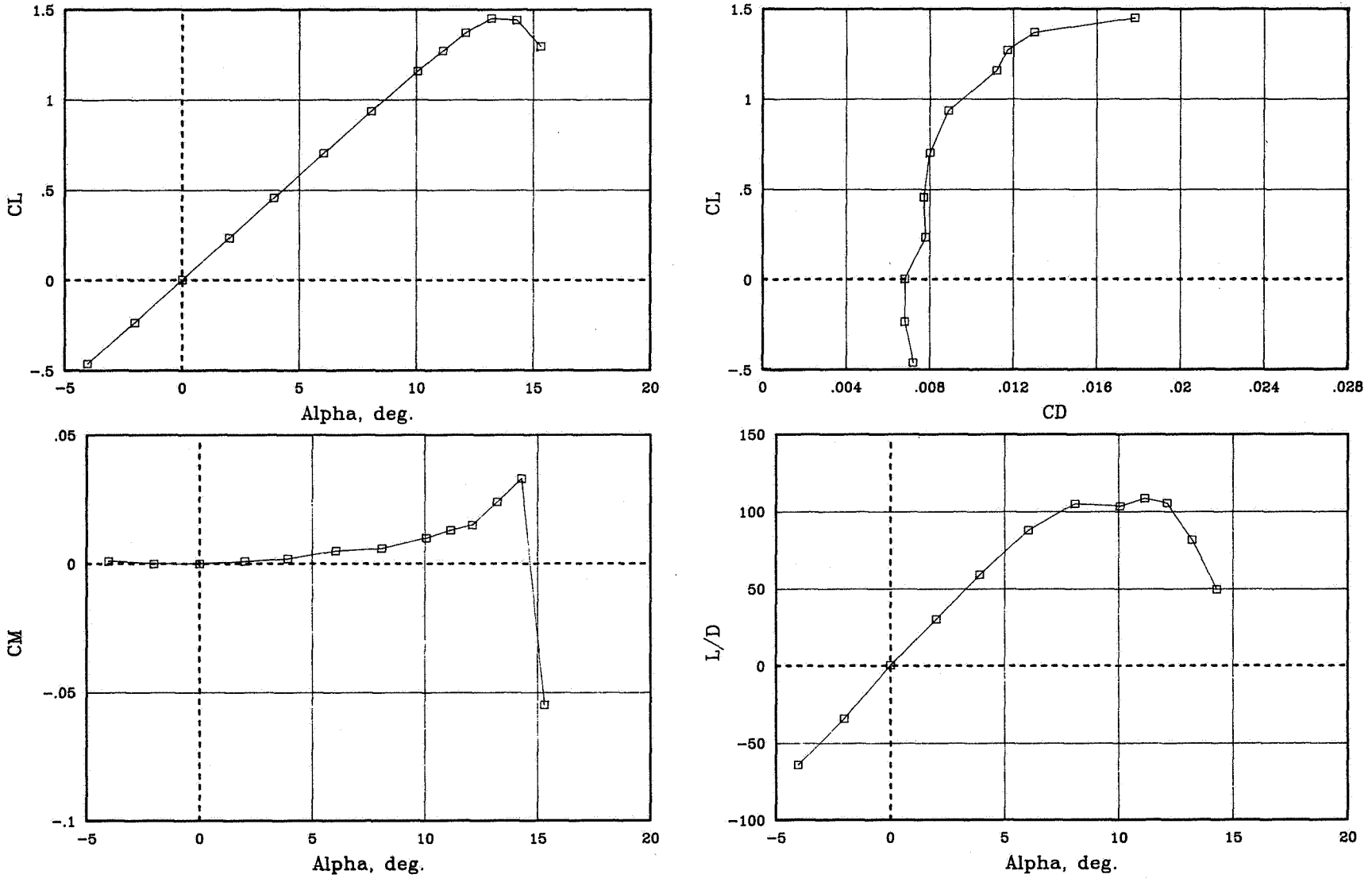

(d) $R = 11.9 \times 10^6$.

Figure 6. Concluded.

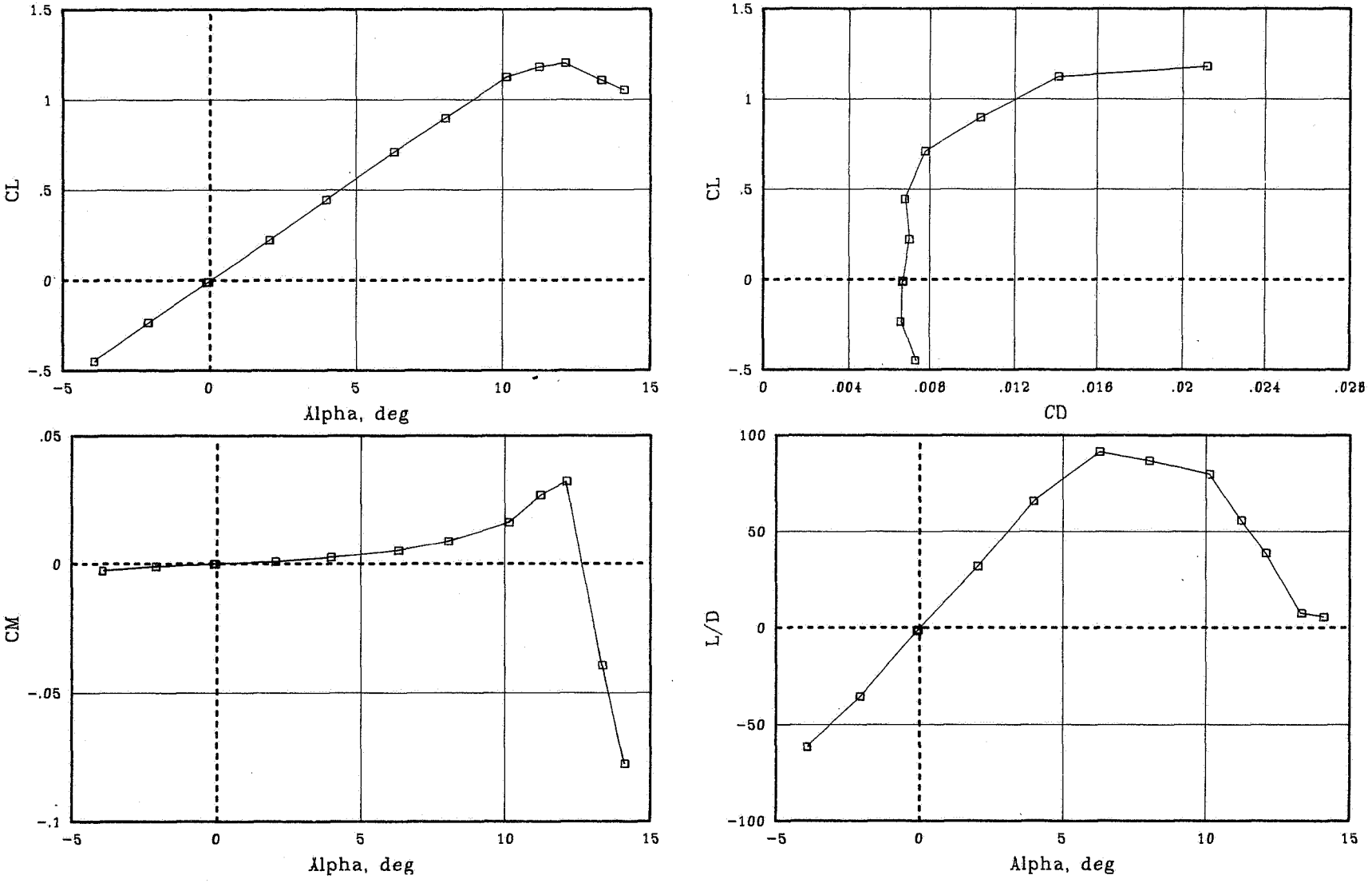

(a) $R = 3.9 \times 10^6$.

Figure 7. Variation of basic aerodynamic characteristics with angle of attack for various Reynolds numbers at $M = 0.36$ for free transition.

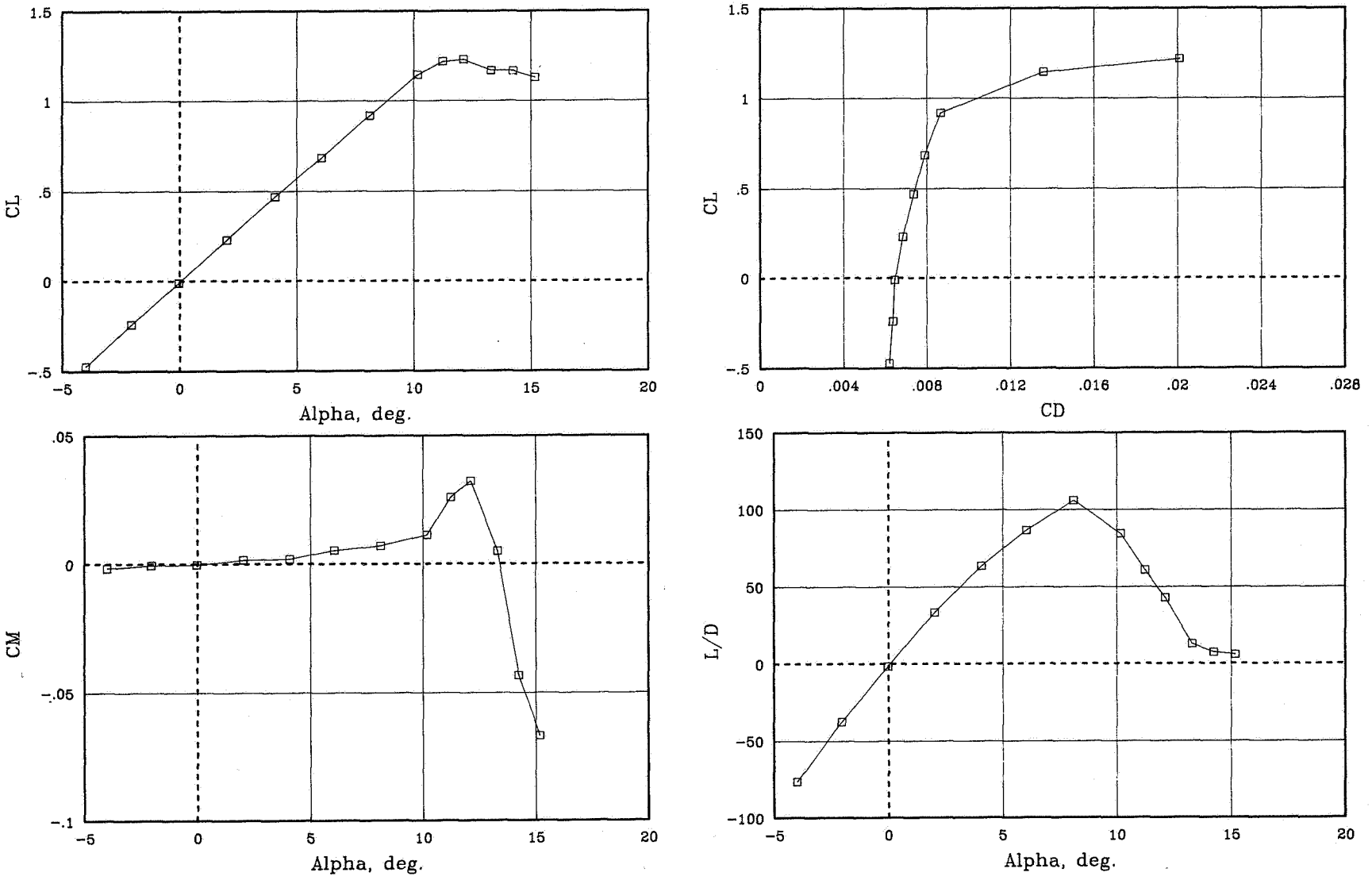

(b) $R = 5.9 \times 10^6$.

Figure 7. Continued.

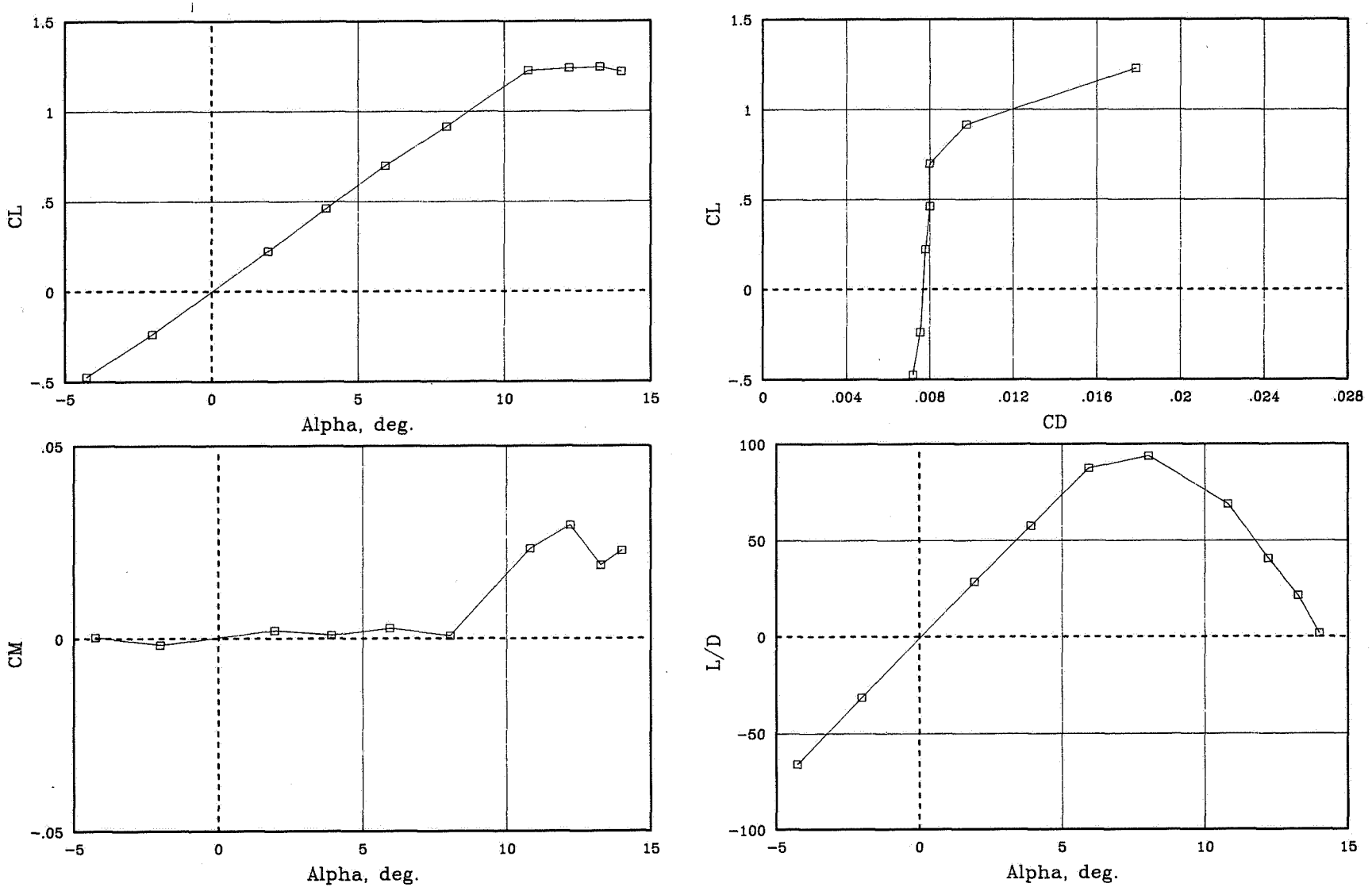

(c) $R = 8.9 \times 10^6$.

Figure 7. Concluded.

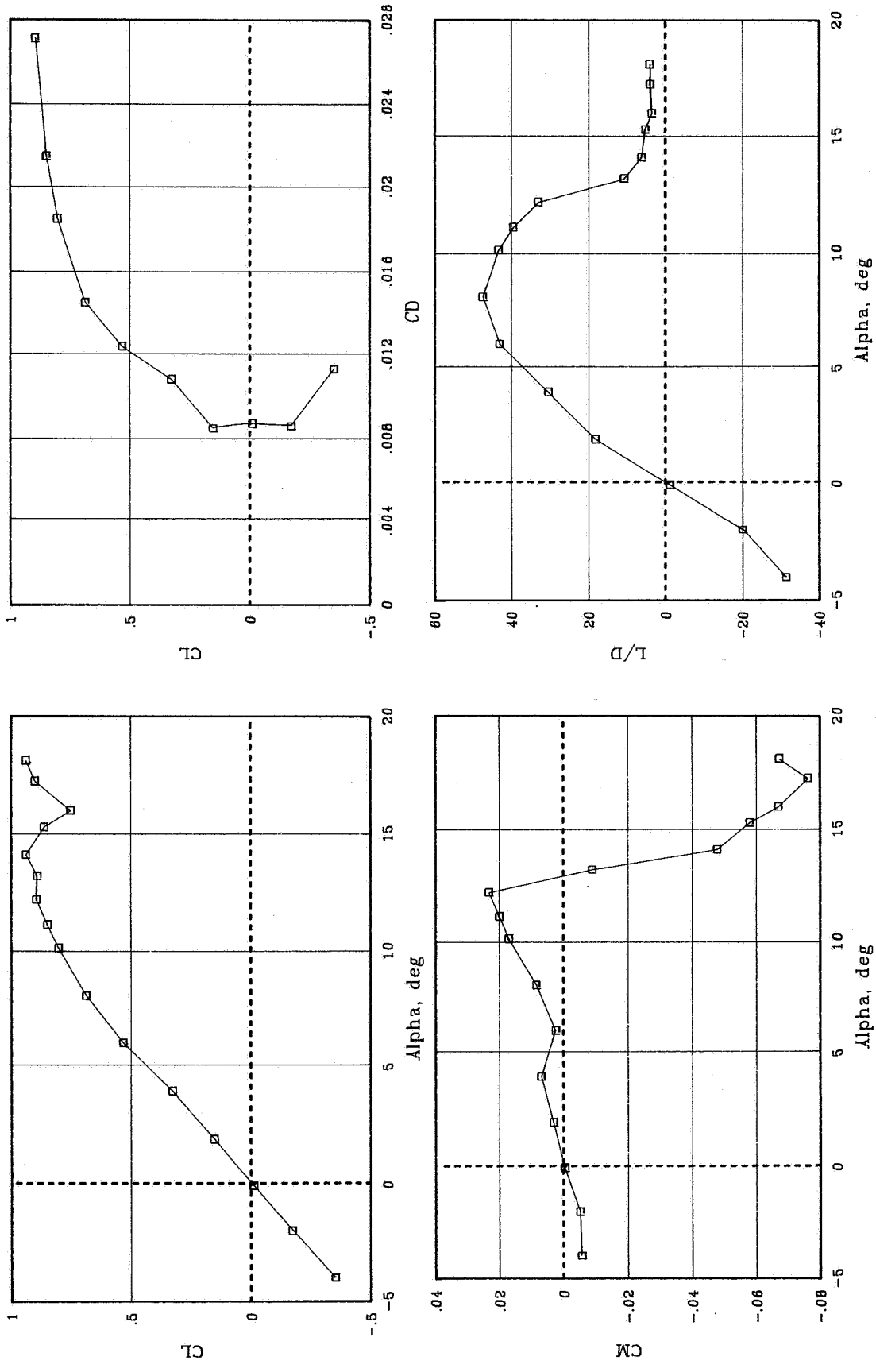

Figure 8. Variation of basic aerodynamic characteristics with angle of attack for $R = 0.7 \times 10^6$ and $M = 0.05$ for transition fixed with No. 60-W grit.

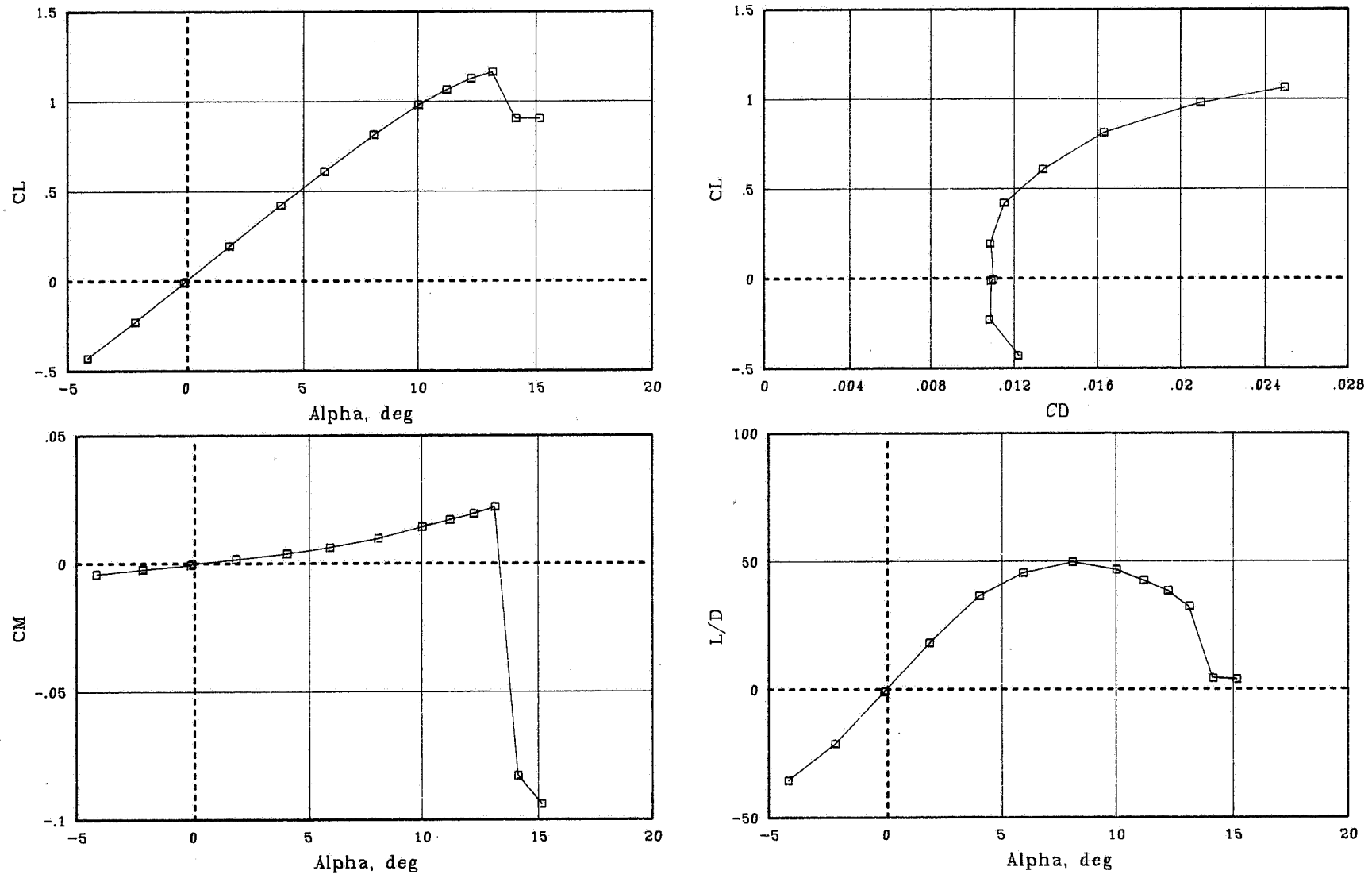

(a) $R = 2.0 \times 10^6$.

Figure 9. Variation of basic aerodynamic characteristics with angle of attack for various Reynolds numbers at $M = 0.15$ for transition fixed with No. 60-W grit.

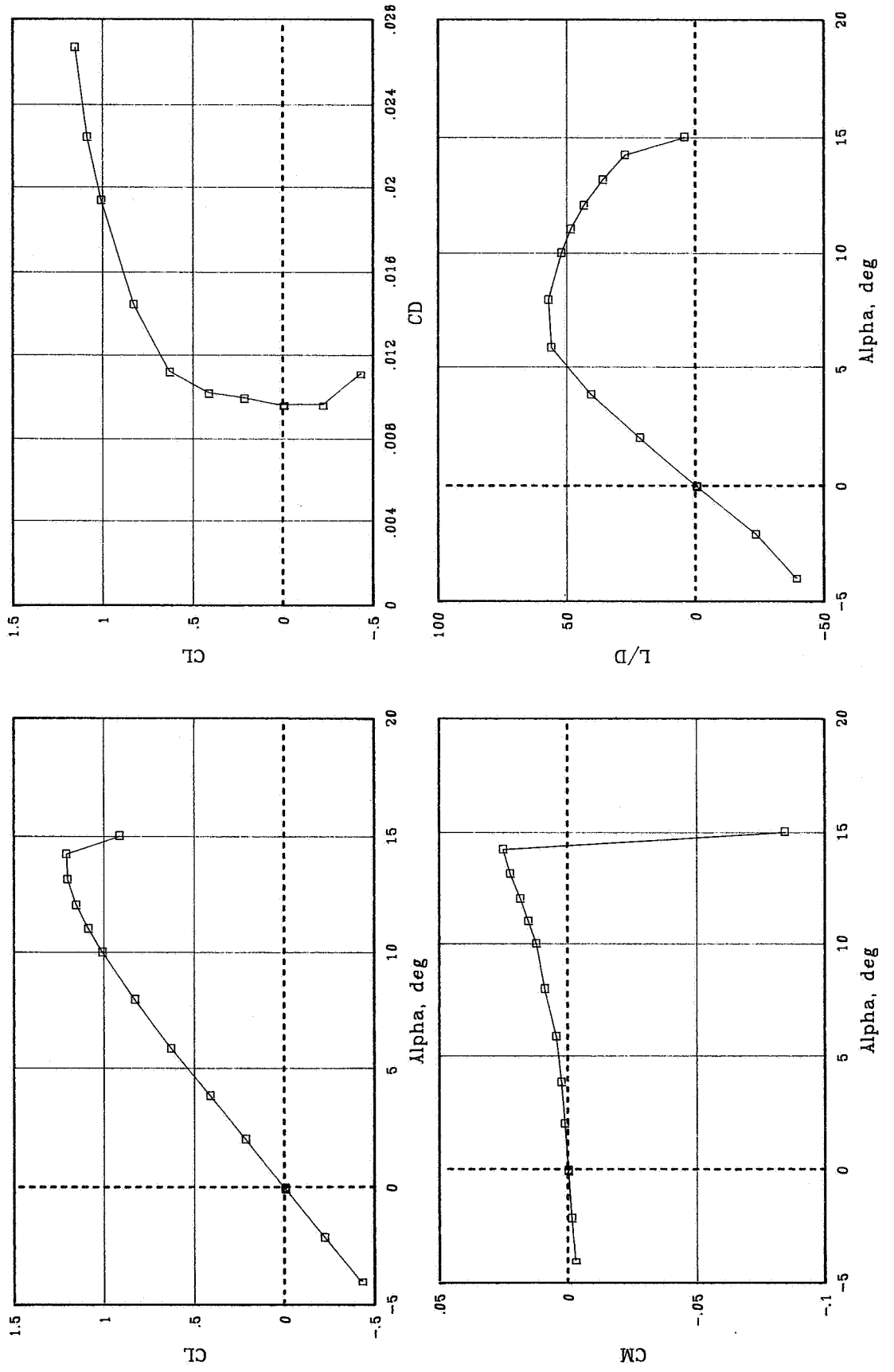

(b) $R = 4.0 \times 10^6$.

Figure 9. Continued.

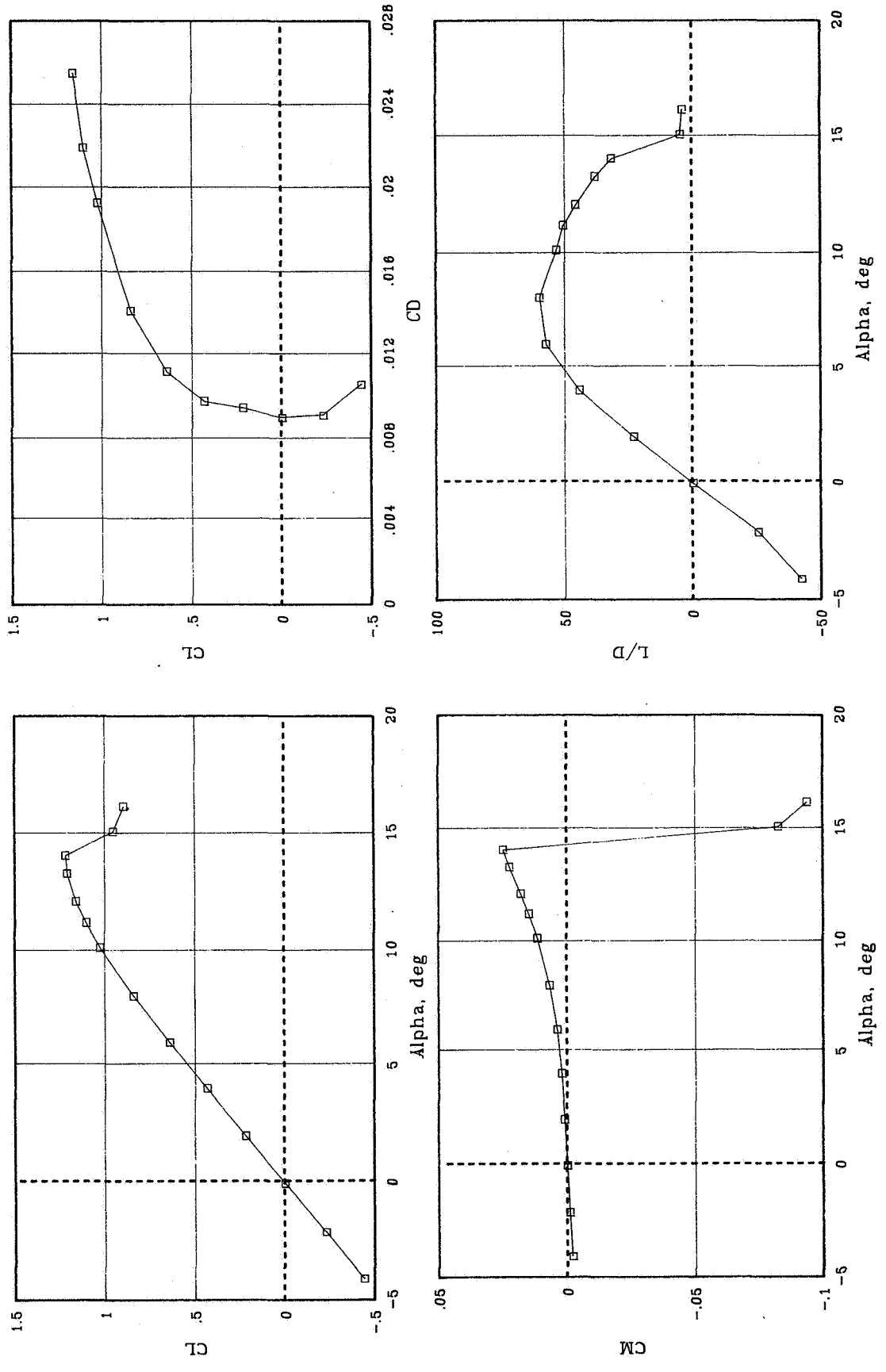

(c) $R = 6.0 \times 10^6$.

Figure 9. Continued.

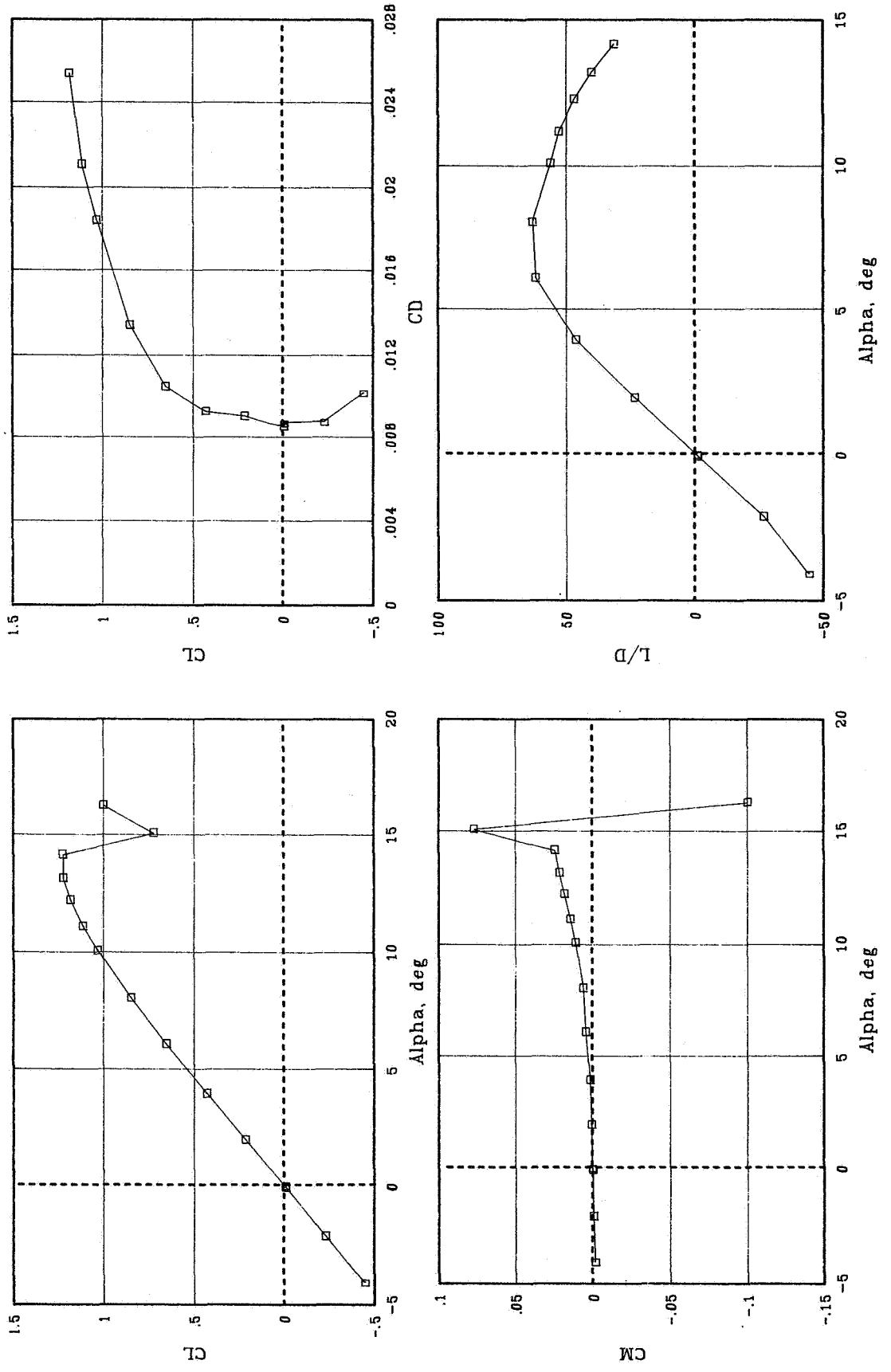

(d) $R = 9.0 \times 10^6$.

Figure 9. Continued.

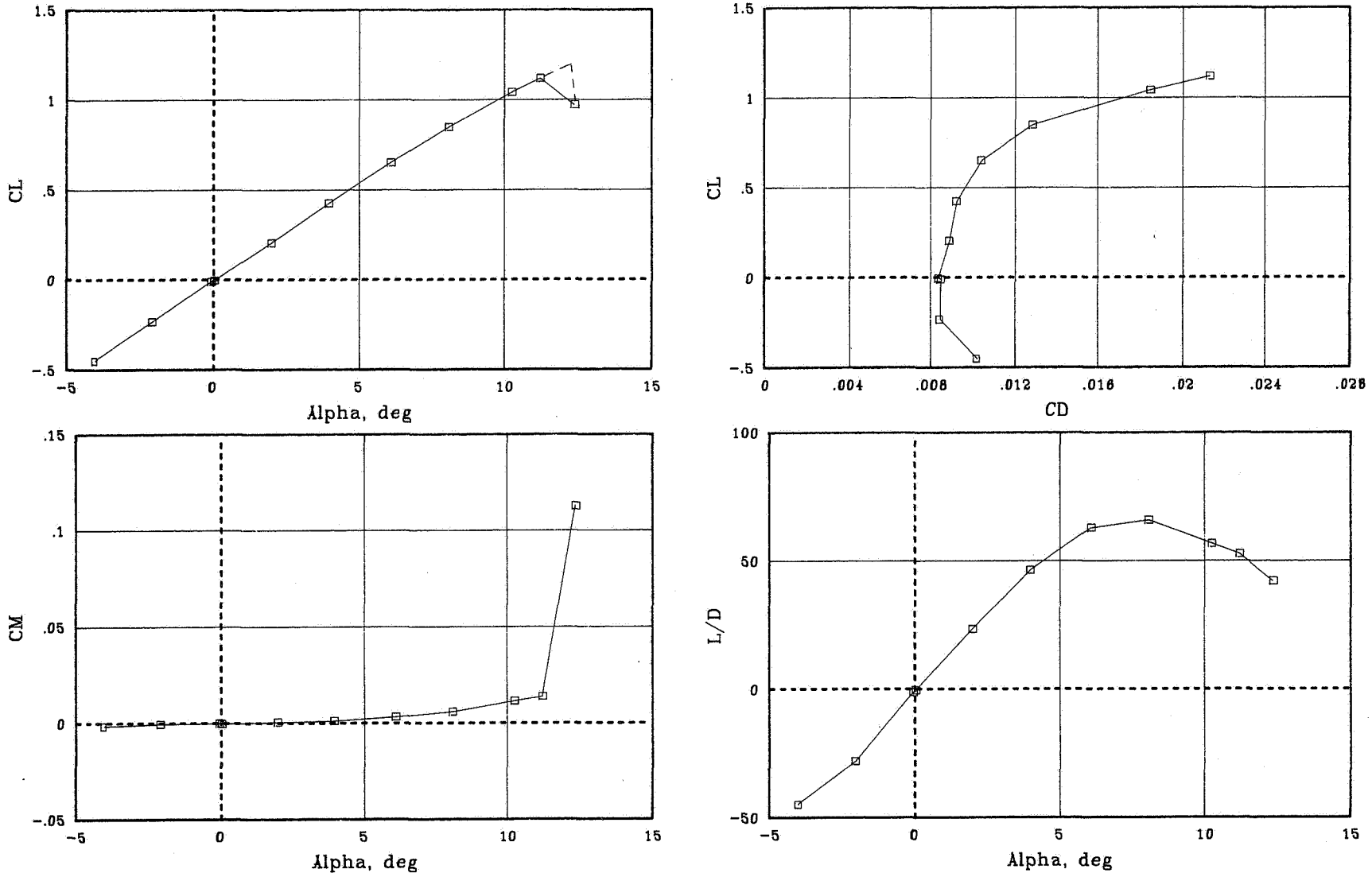

(e) $R = 12.1 \times 10^6$.

Figure 9. Concluded.

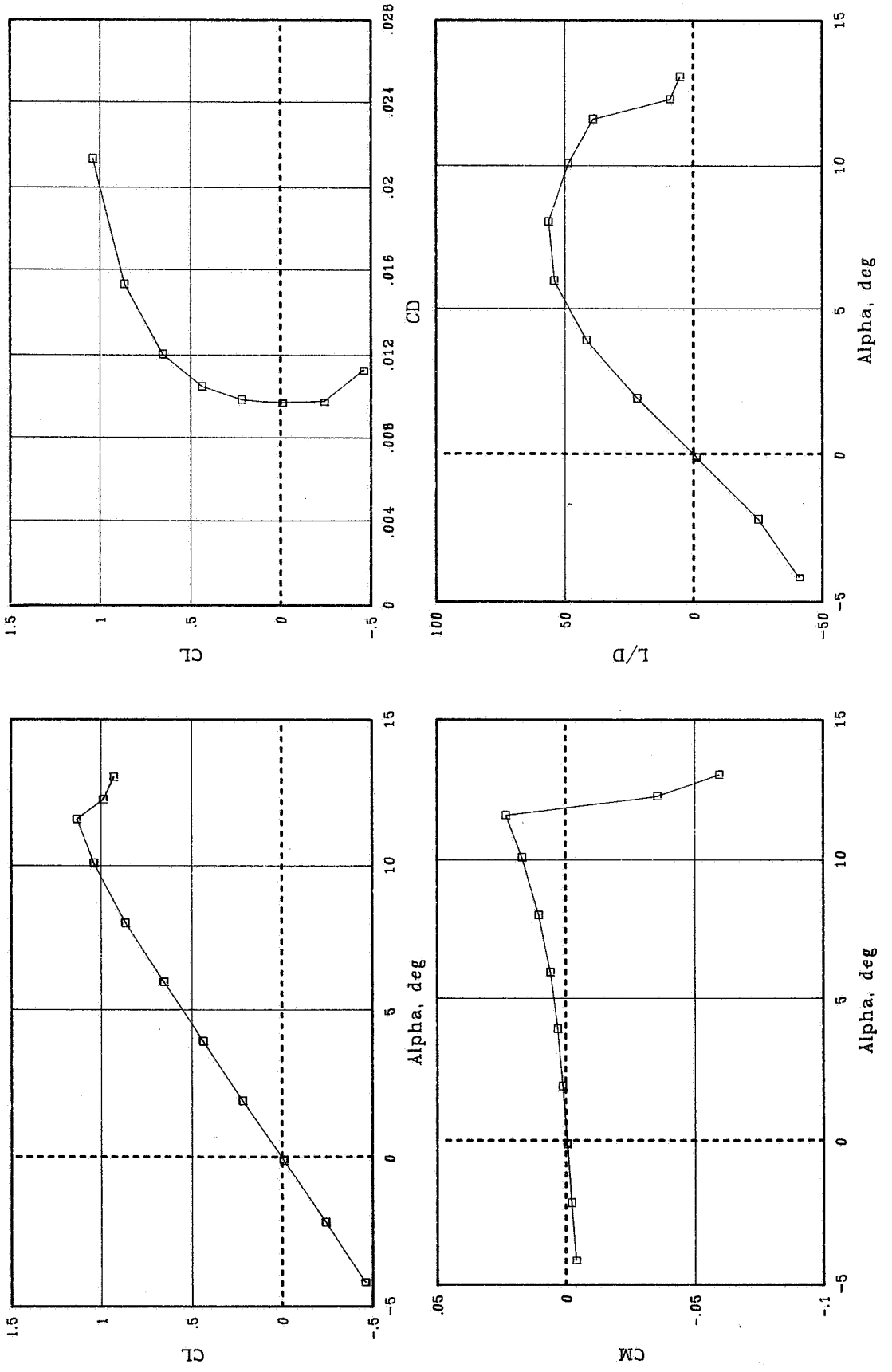

(a) $R = 4.0 \times 10^6$.

Figure 10. Variation of basic aerodynamic characteristics with angle of attack for various Reynolds numbers at $M = 0.30$ for transition fixed with No. 60-W grit.

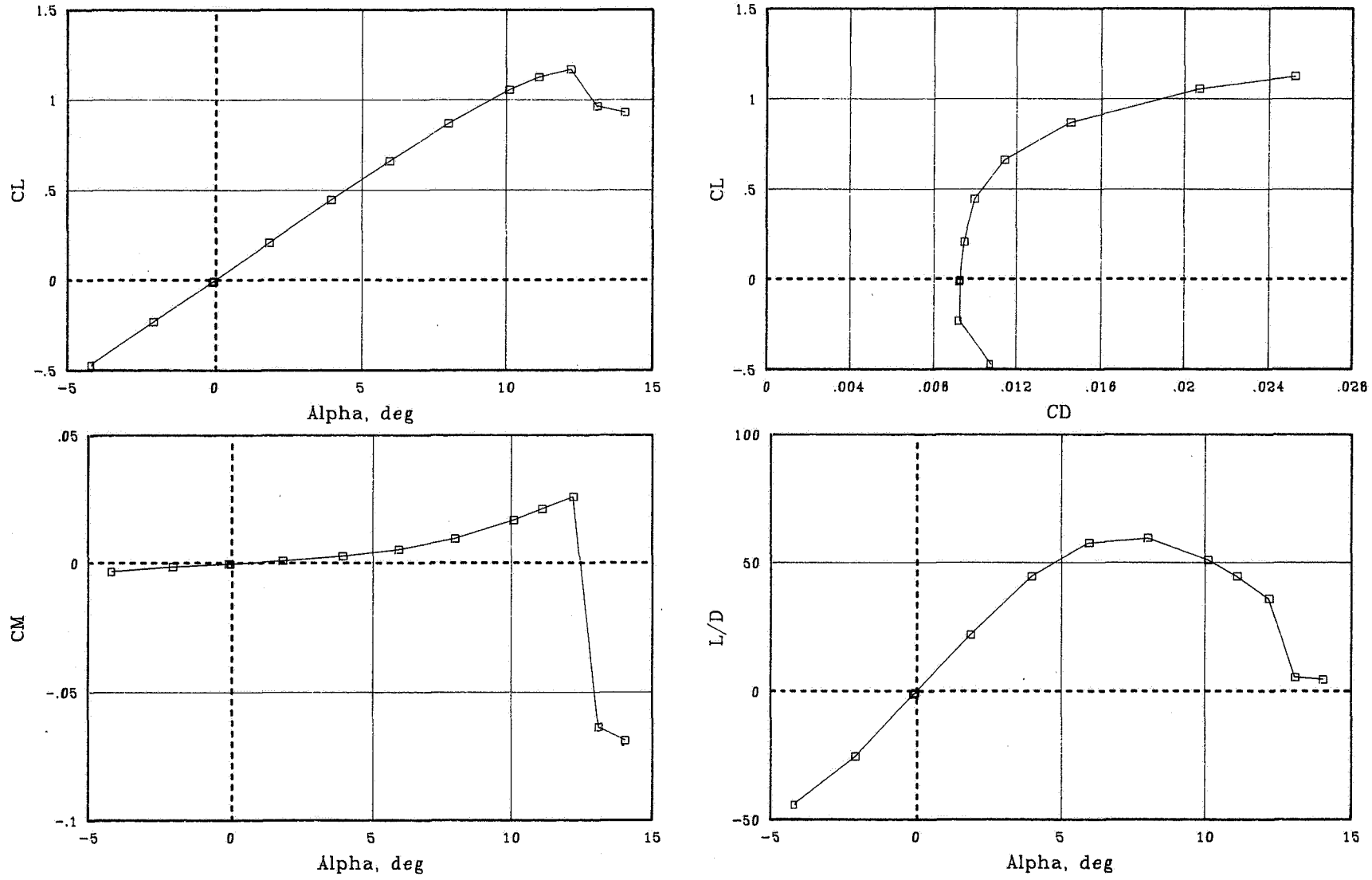

(b) $R = 6.0 \times 10^6$.

Figure 10. Continued.

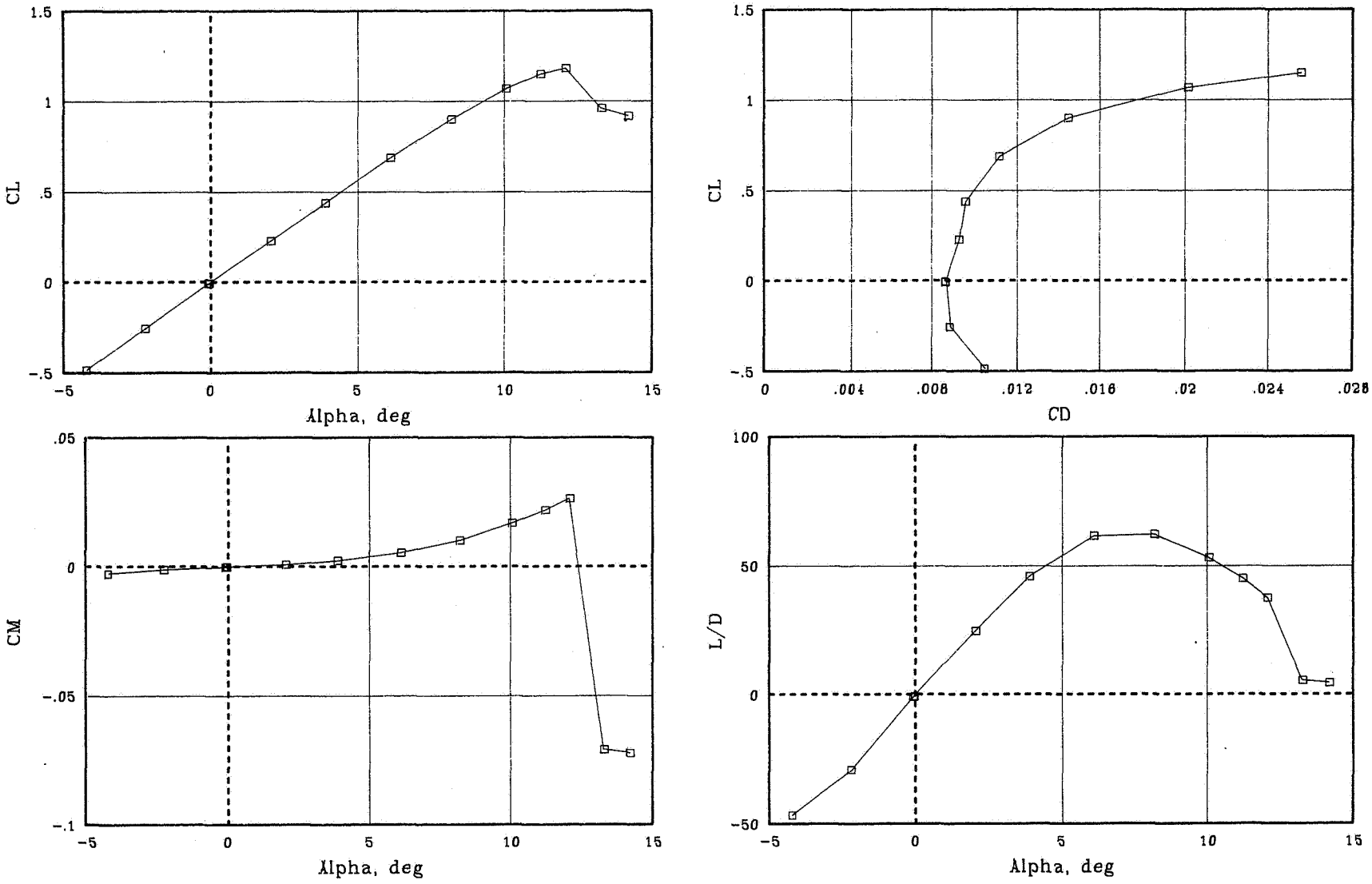

(c) $R = 9.0 \times 10^6$.

Figure 10. Continued.

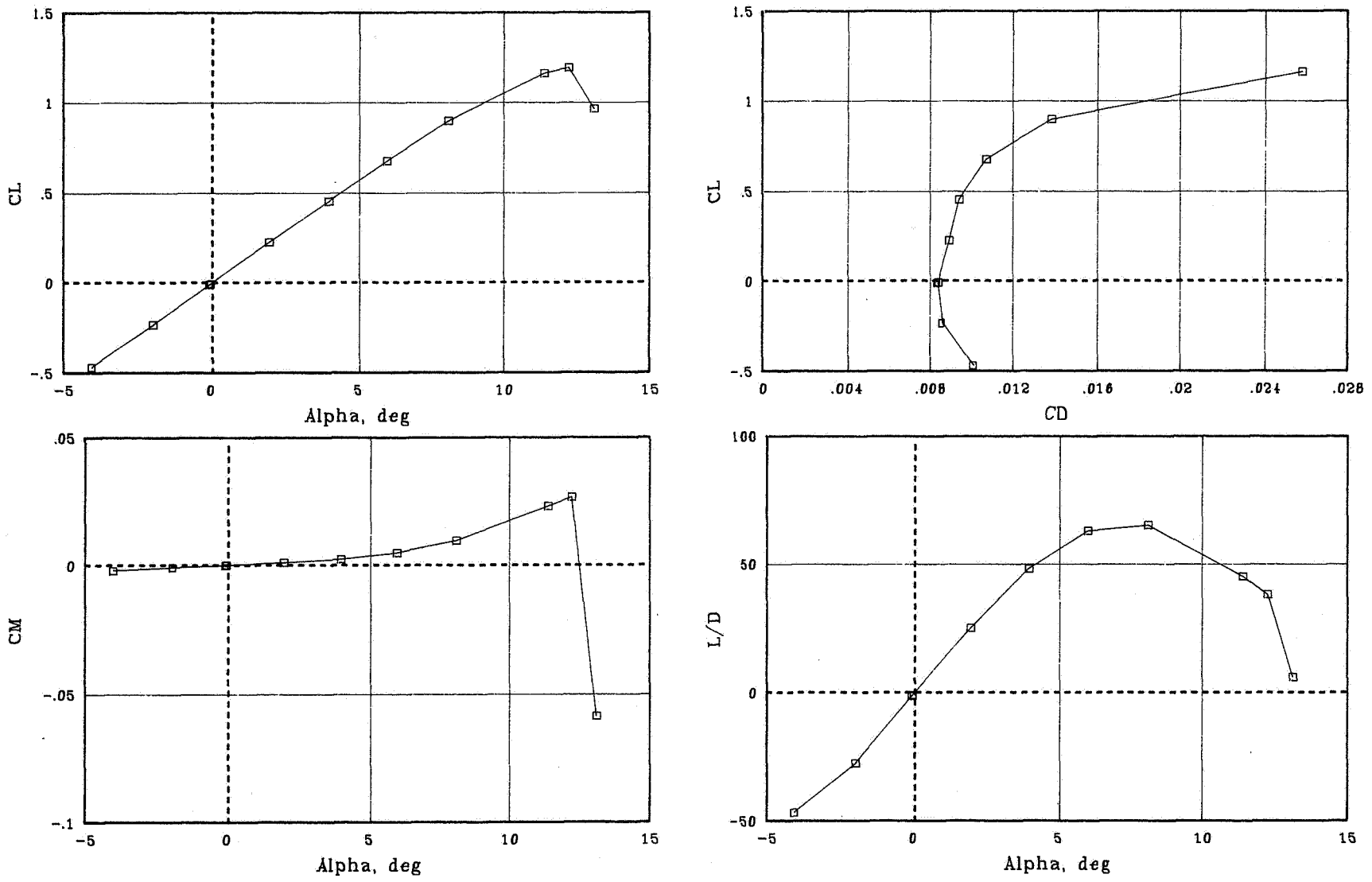

(d) $R = 12.0 \times 10^6$.

Figure 10. Concluded.

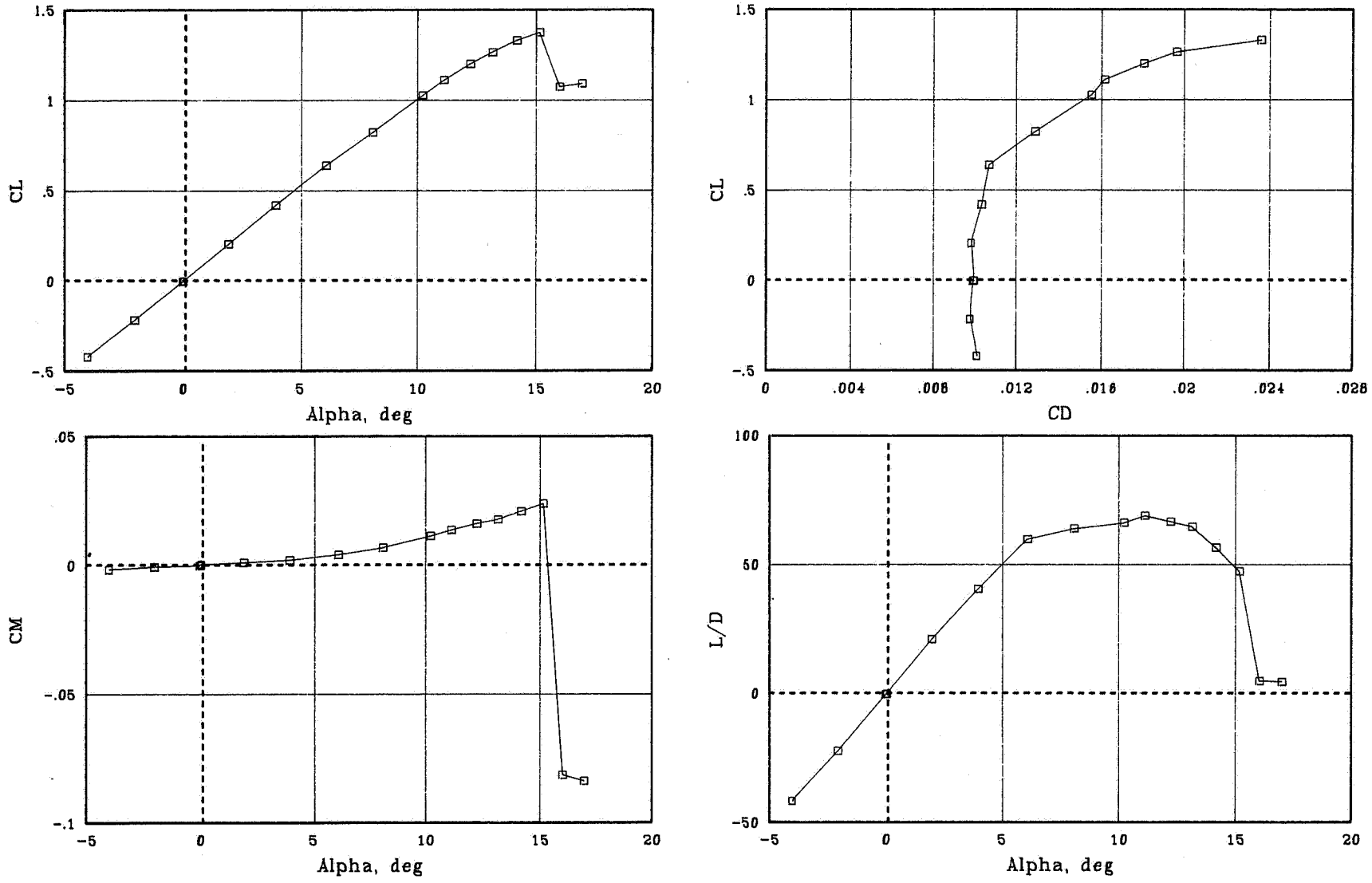

(a) $R = 2.0 \times 10^6$.

Figure 11. Variation of basic aerodynamic characteristics with angle of attack for various Reynolds numbers at $M = 0.15$ for transition fixed with No. 80 grit.

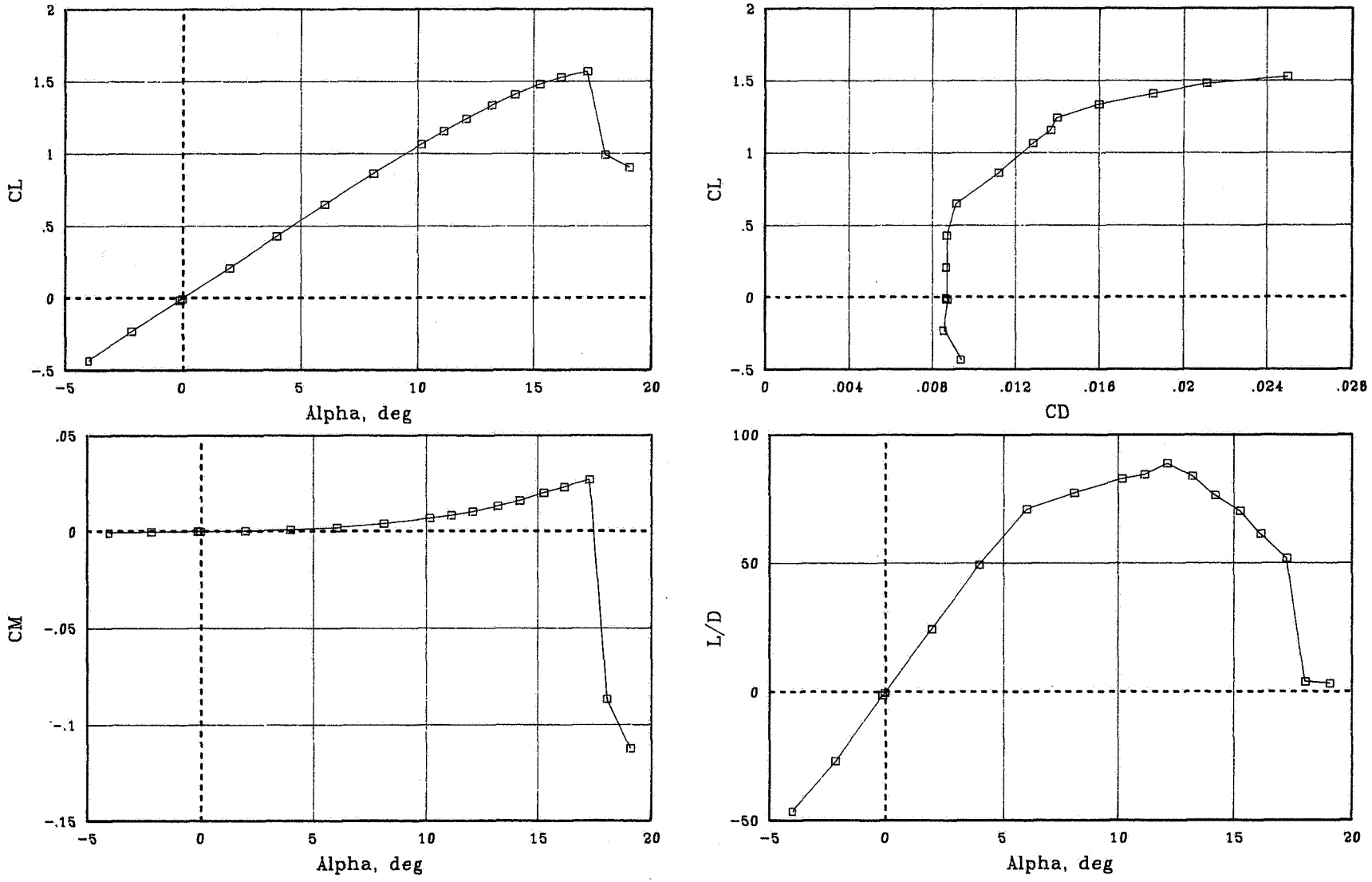

(b) $R = 4.0 \times 10^6$.

Figure 11. Continued.

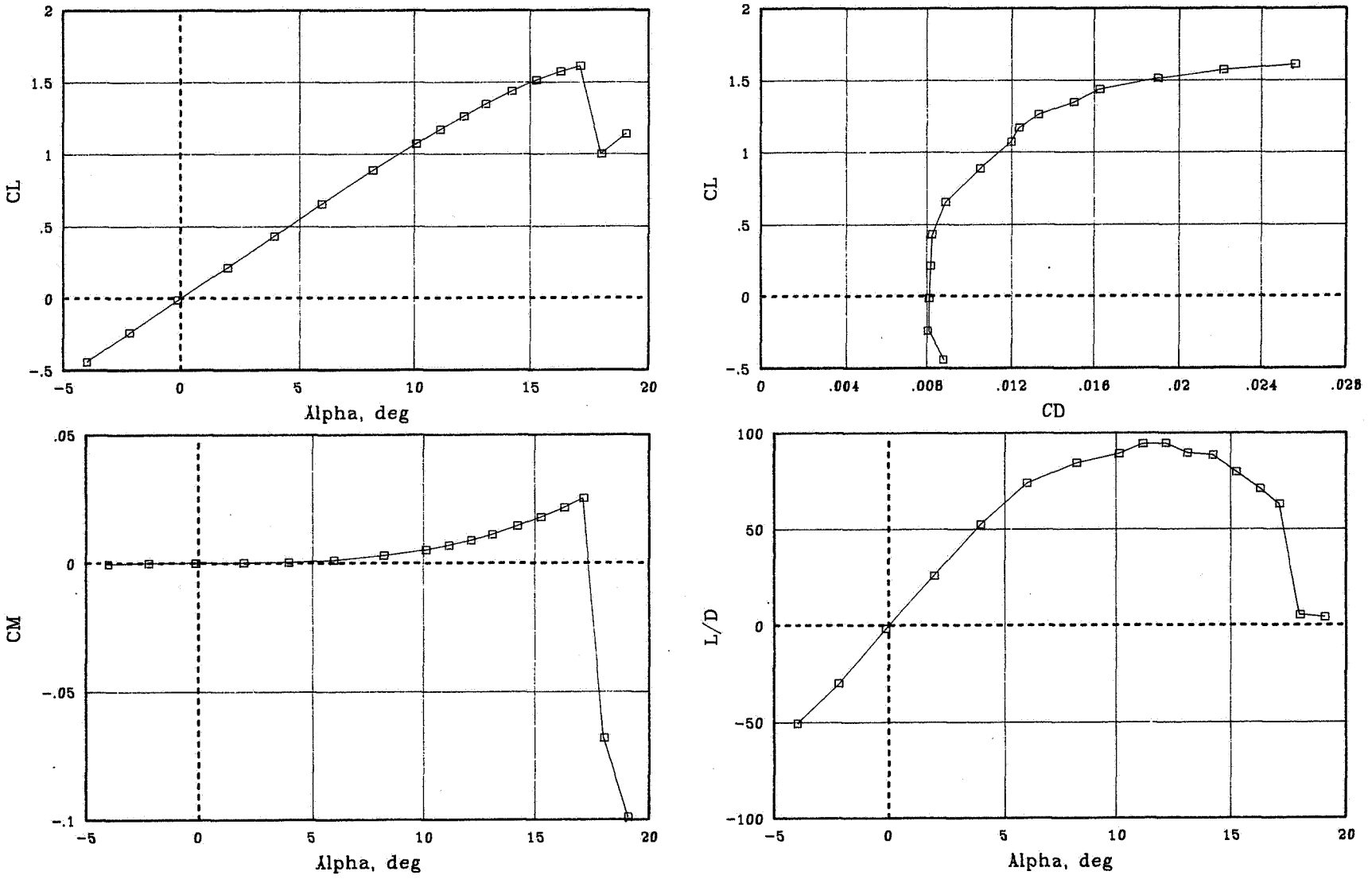

(c) $R = 6.0 \times 10^6$.

Figure 11. Concluded.

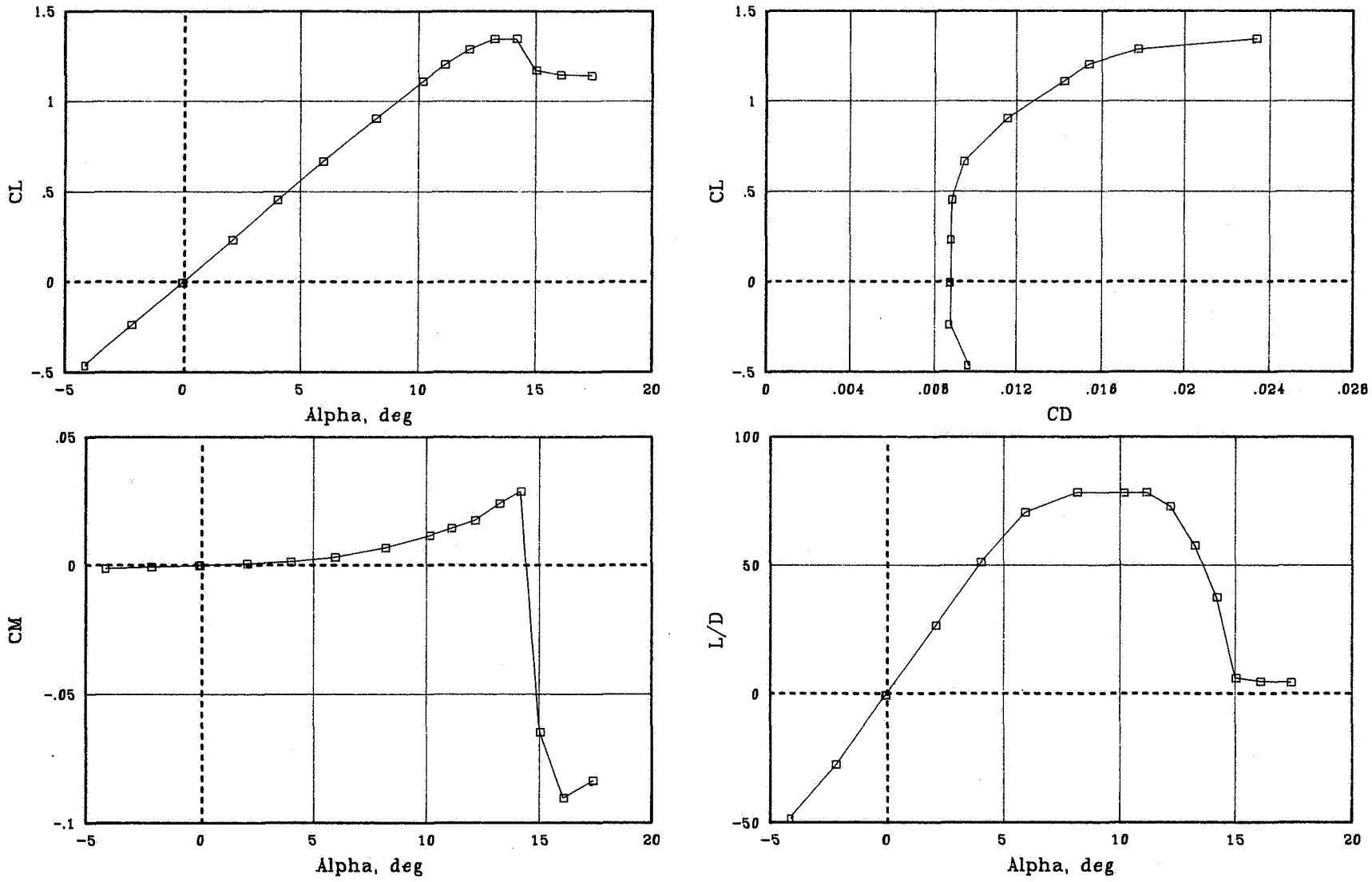

(a) $R = 4.0 \times 10^6$.

Figure 12. Variation of basic aerodynamic characteristics with angle of attack for various Reynolds numbers at $M = 0.30$ for transition fixed with No. 80 grit.

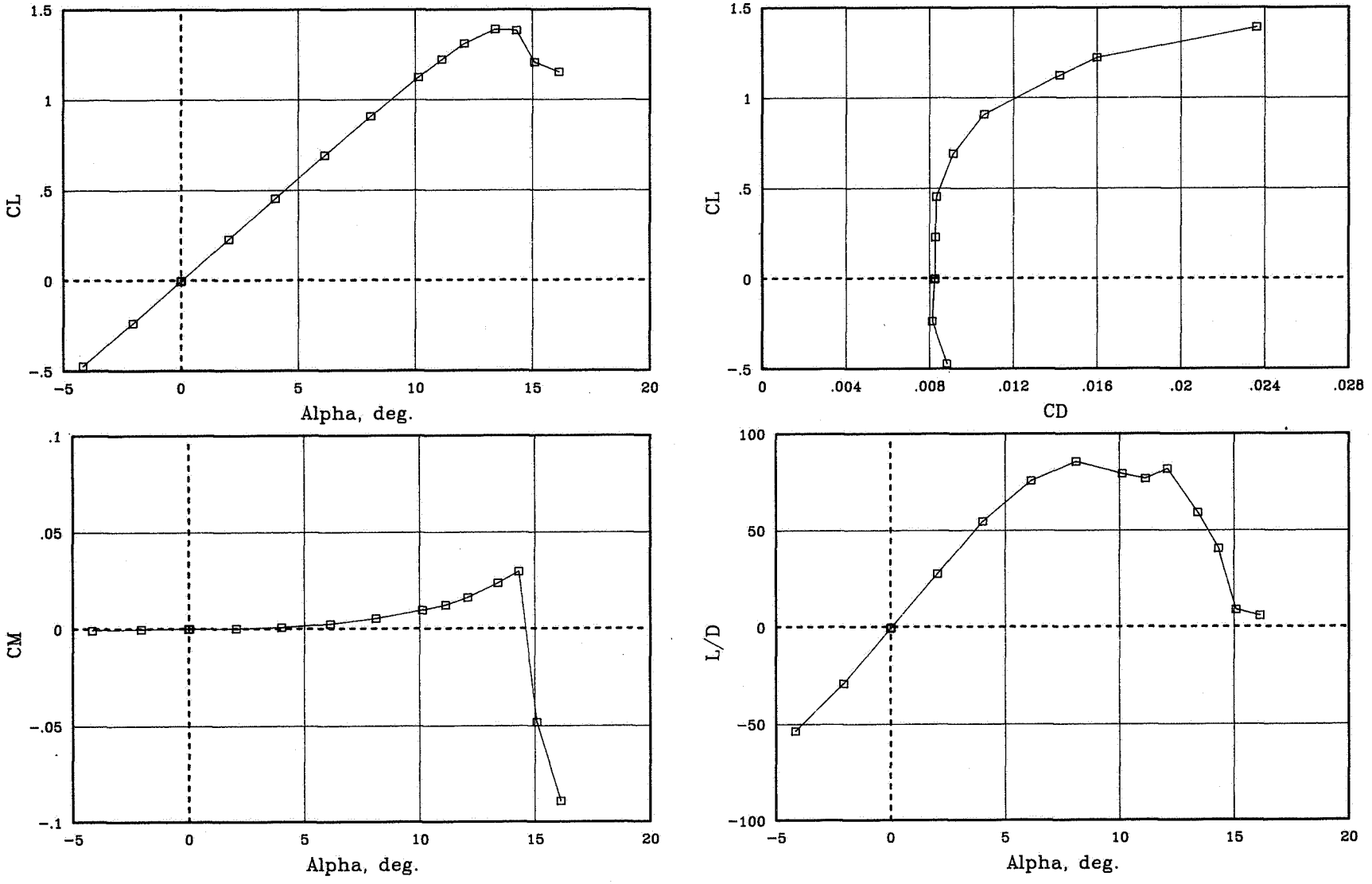

(b) $R = 6.0 \times 10^6$.

Figure 12. Concluded.

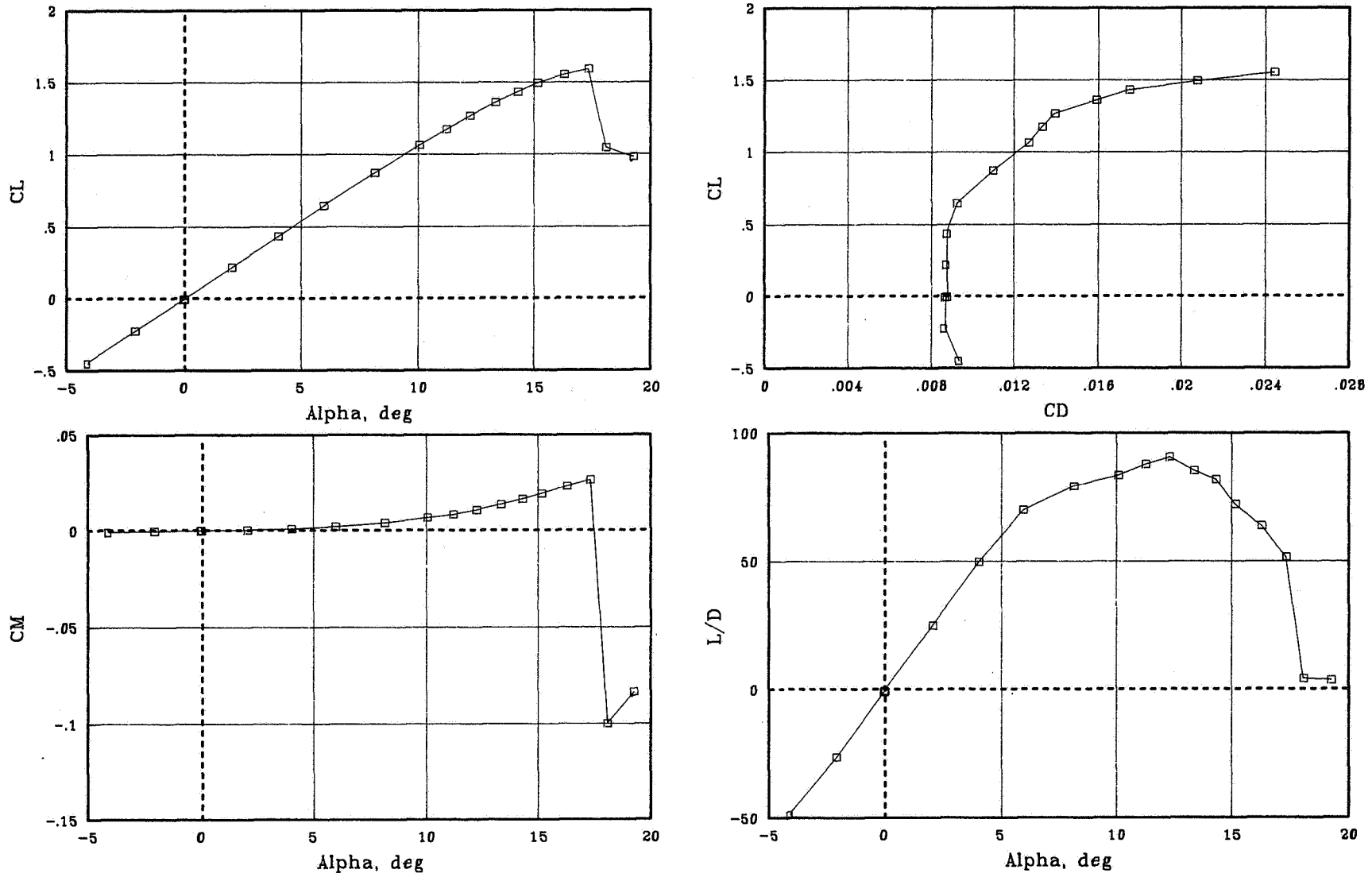

(a) $R = 4.0 \times 10^6$.

Figure 13. Variation of basic aerodynamic characteristics with angle of attack for various Reynolds numbers at $M = 0.15$ for transition fixed with No. 120 grit.

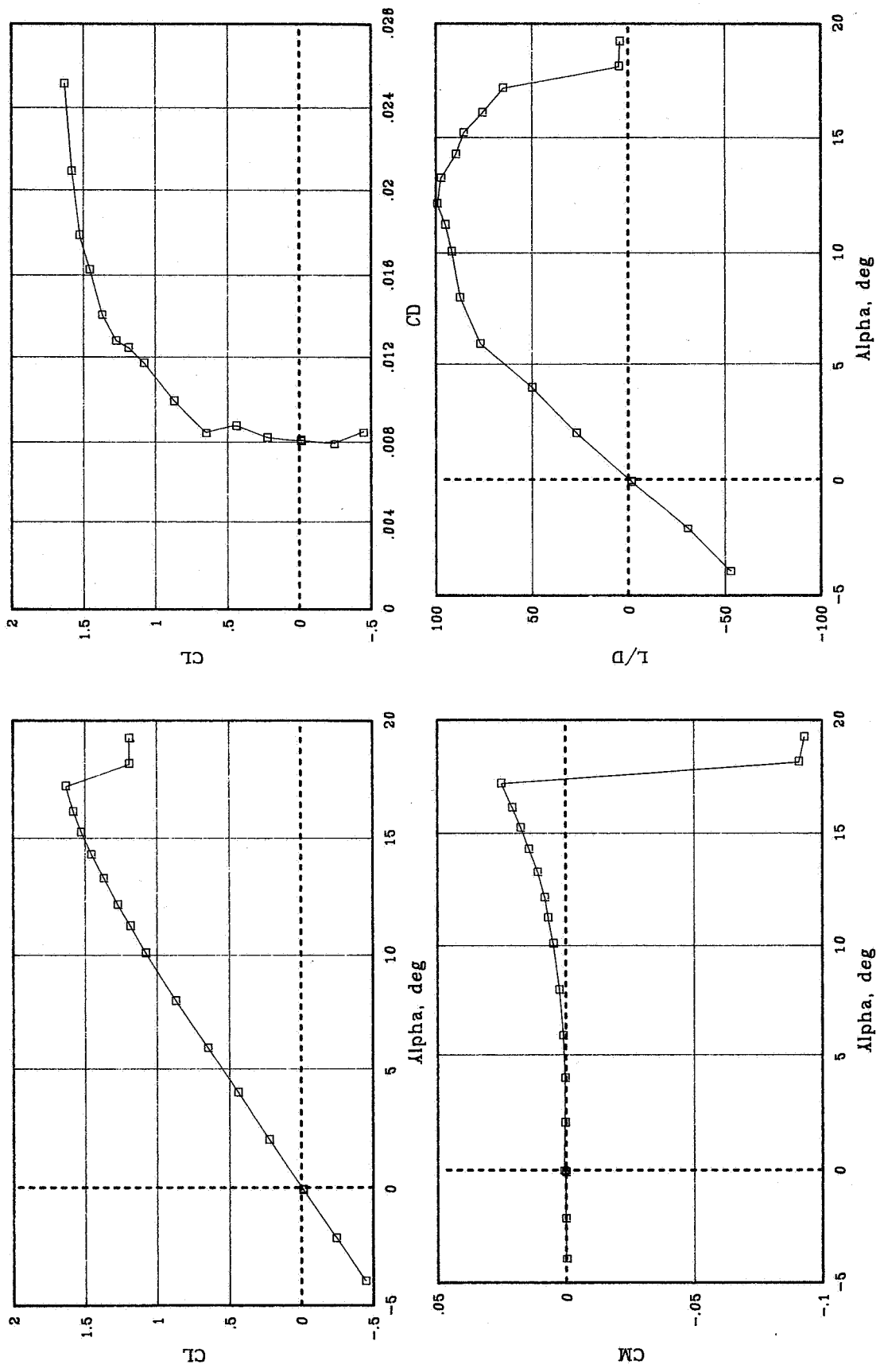

(b) $R = 6.0 \times 10^6$.

Figure 13. Continued.

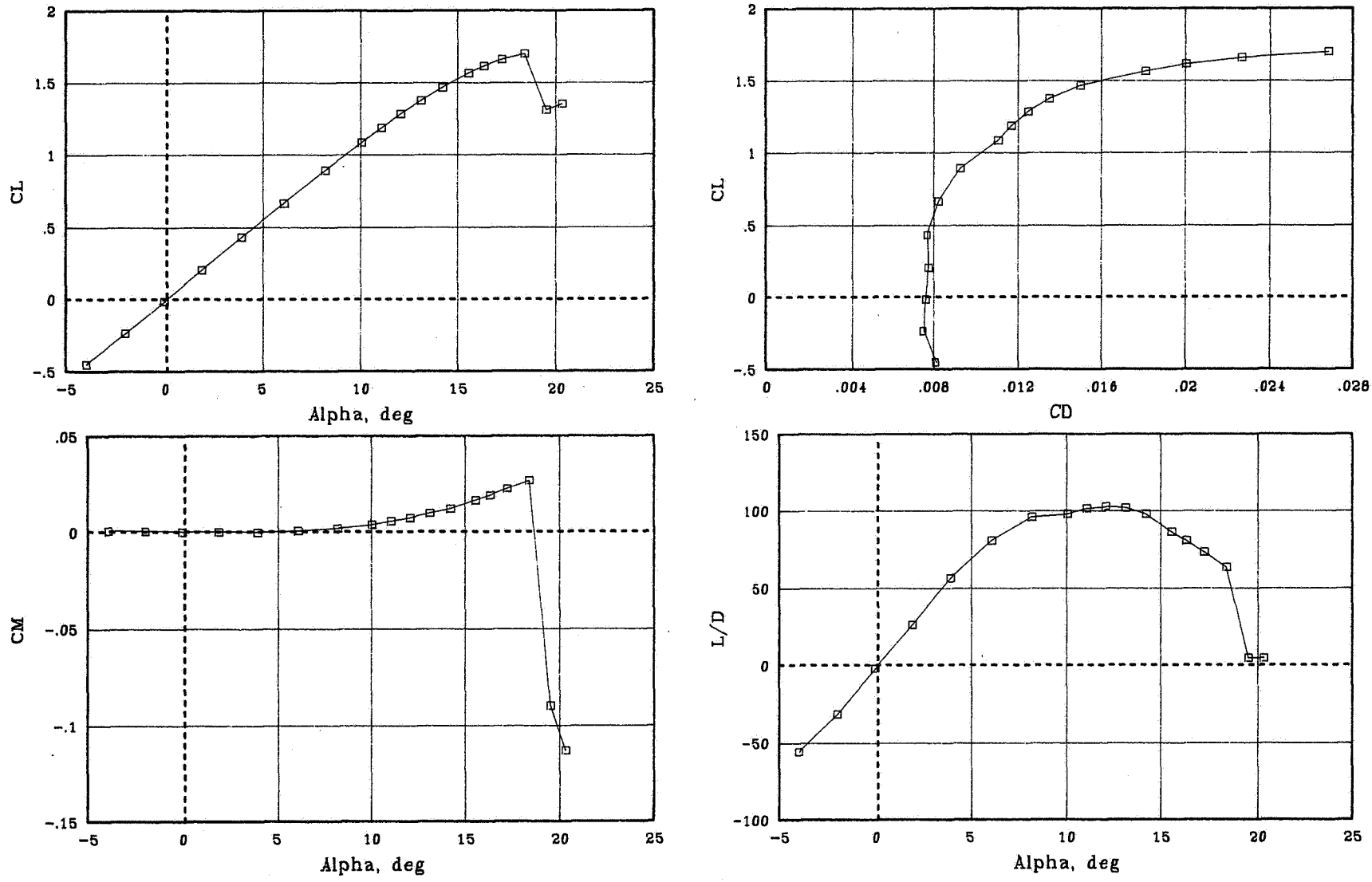

(c) $R = 8.9 \times 10^6$.

Figure 13. Concluded.

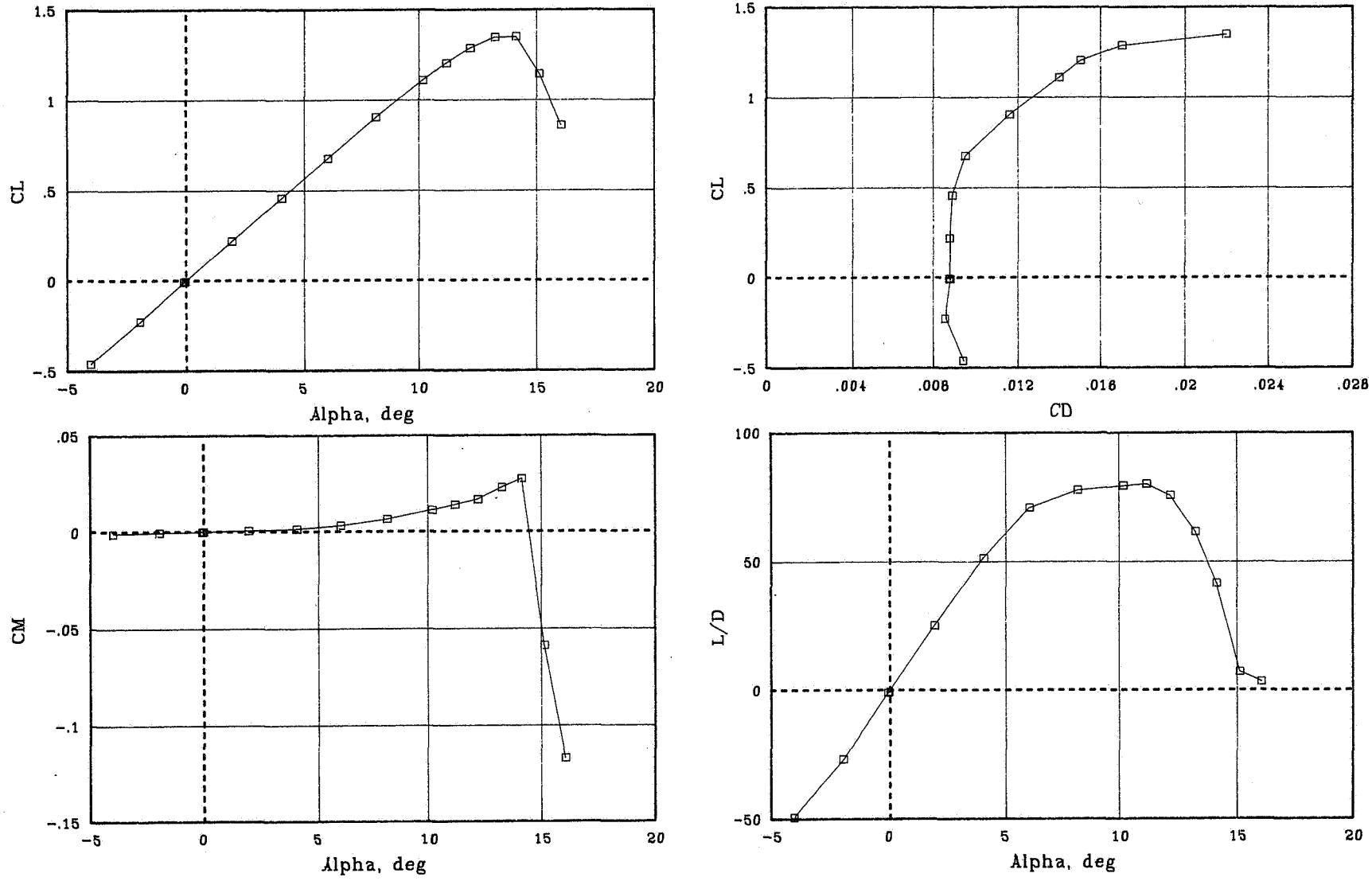

(a) $R = 3.9 \times 10^6$.

Figure 14. Variation of basic aerodynamic characteristics with angle of attack for various Reynolds numbers at $M = 0.30$ for transition fixed with No. 120 grit.

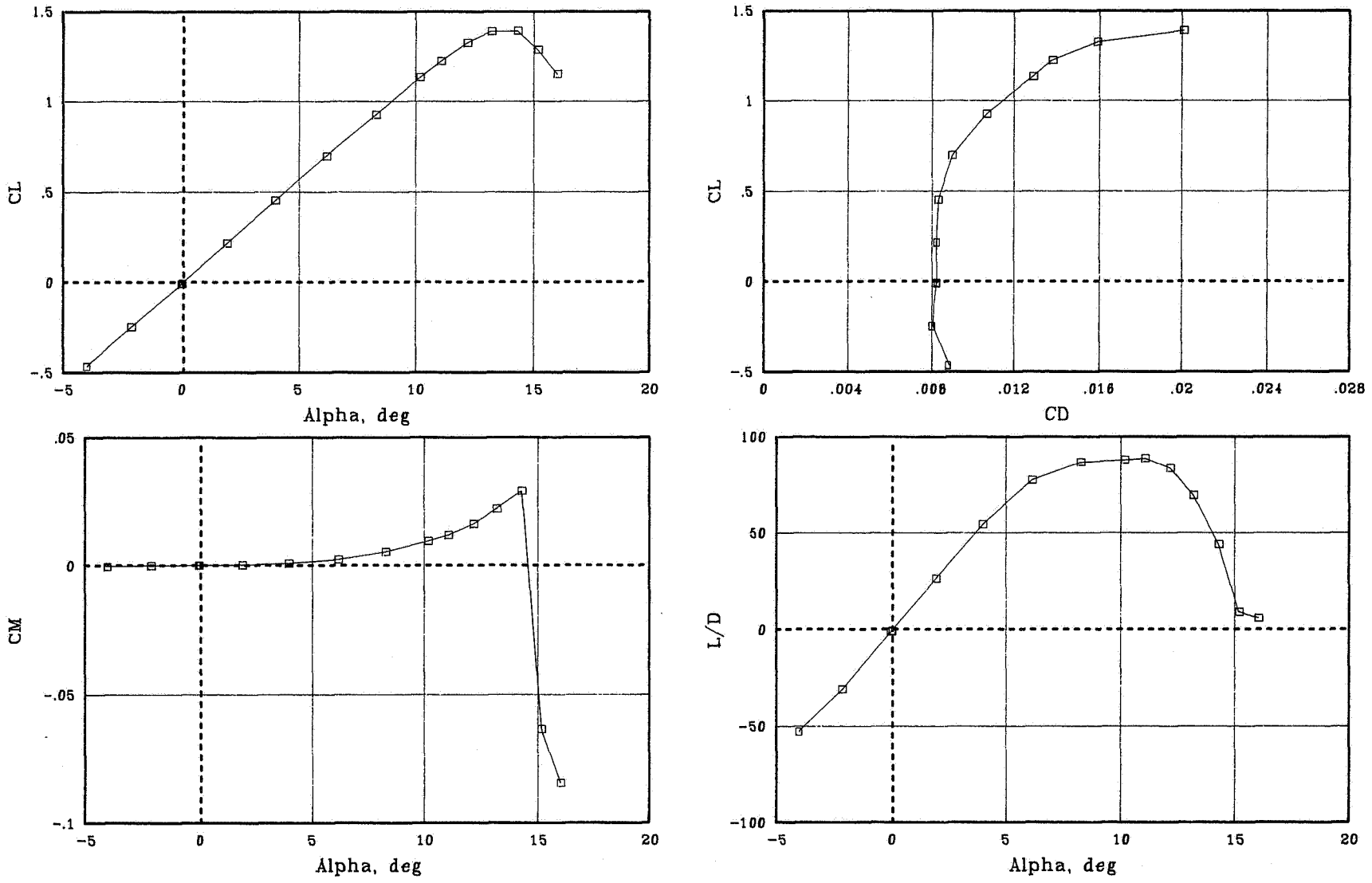

(b) $R = 6.0 \times 10^6$.

Figure 14. Continued.

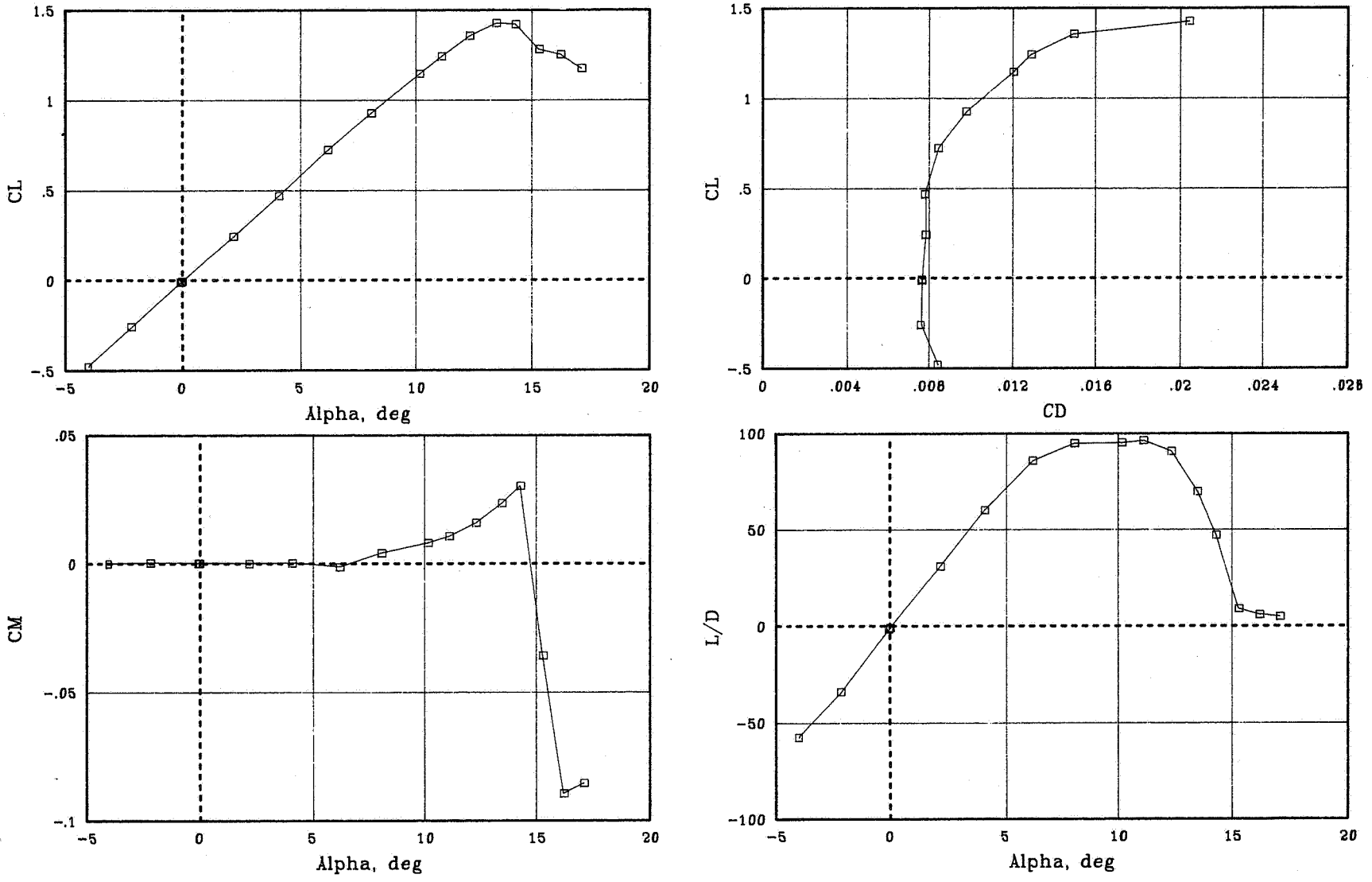

(c) $R = 8.9 \times 10^6$.

Figure 14. Concluded.

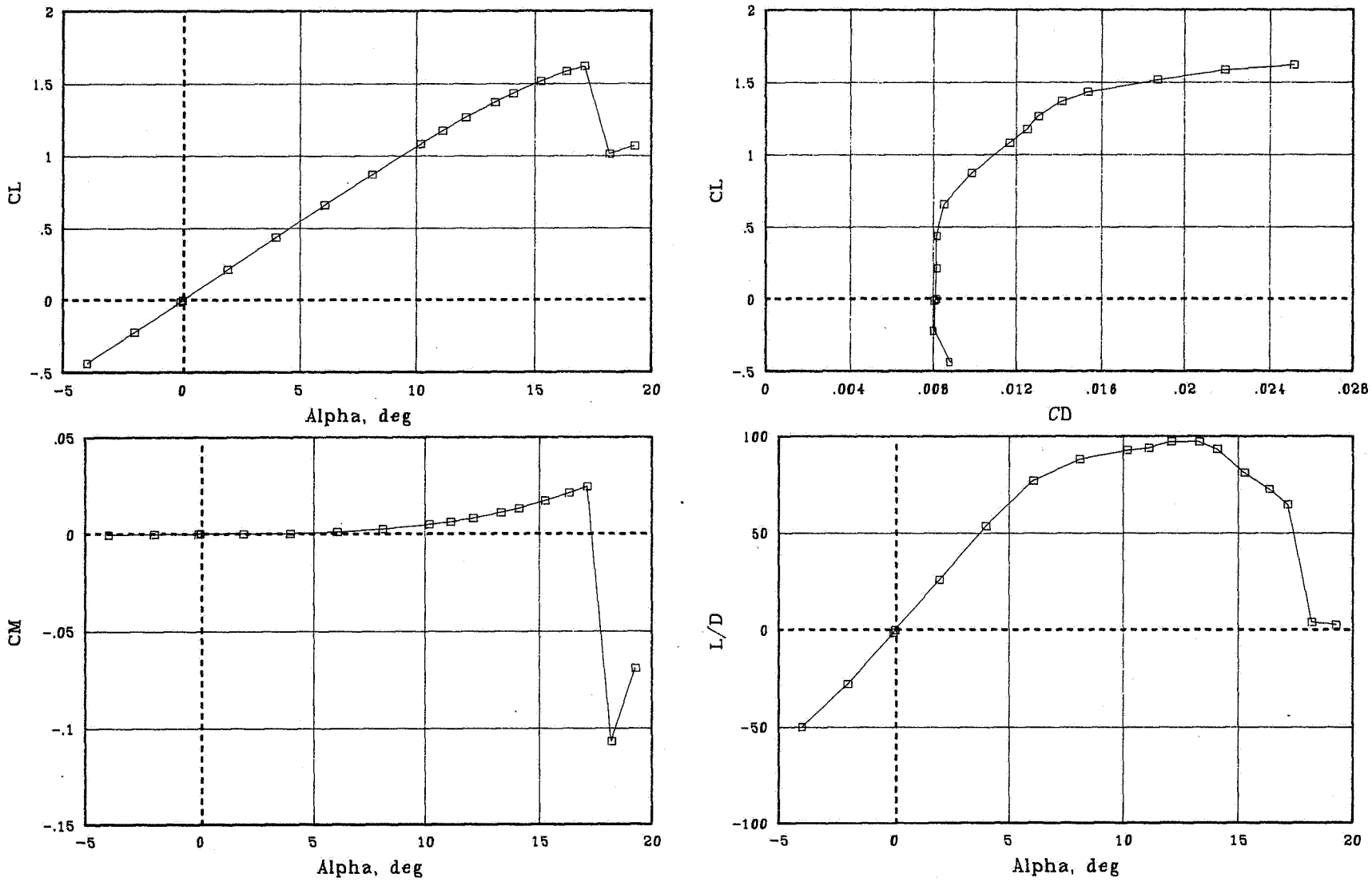

(a) $R = 6.0 \times 10^6$.

Figure 15. Variation of basic aerodynamic characteristics with angle of attack for various Reynolds numbers at $M = 0.15$ for transition fixed with No. 180 grit.

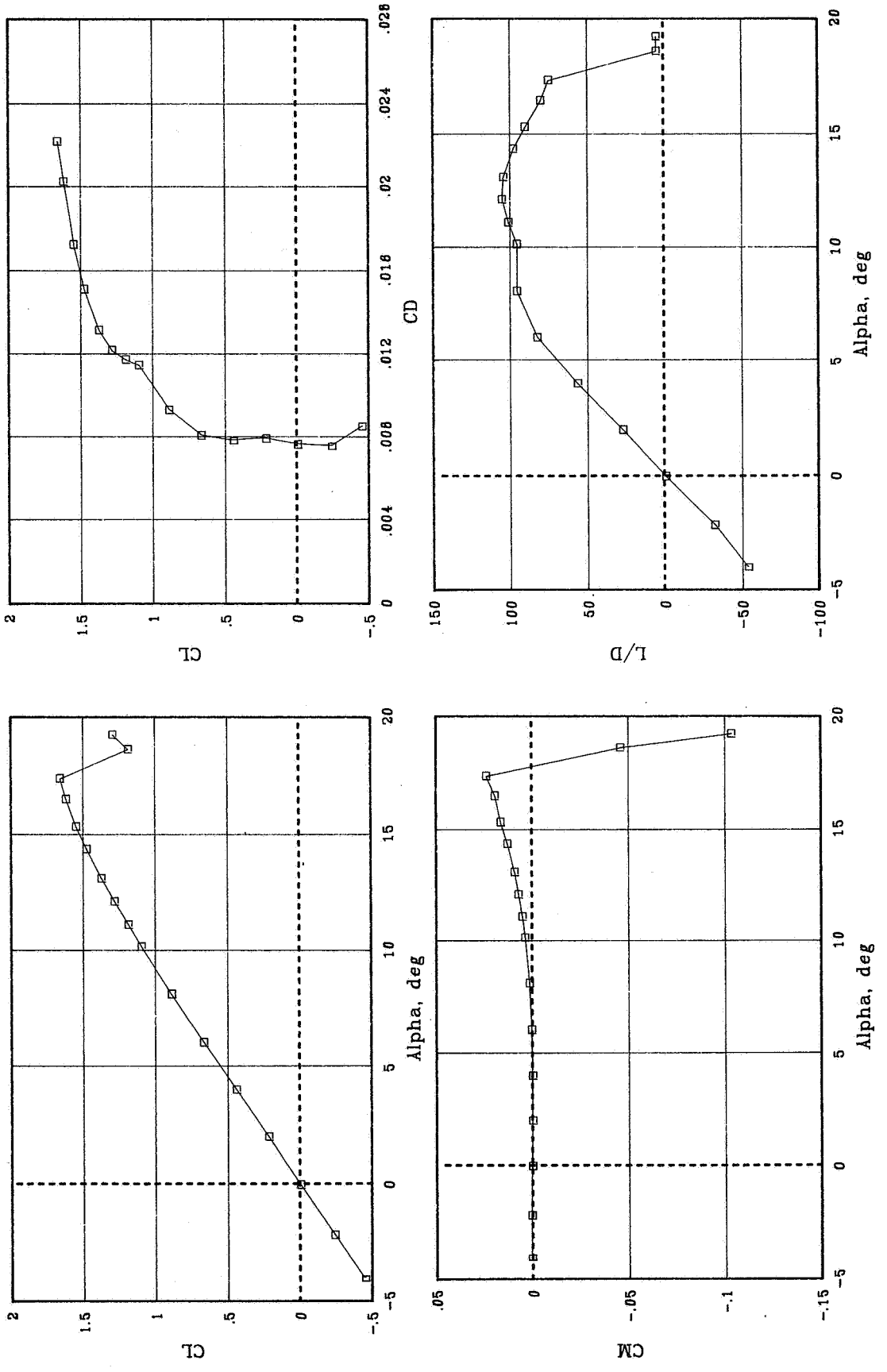

(b) $R = 9.0 \times 10^6$.

Figure 15. Continued.

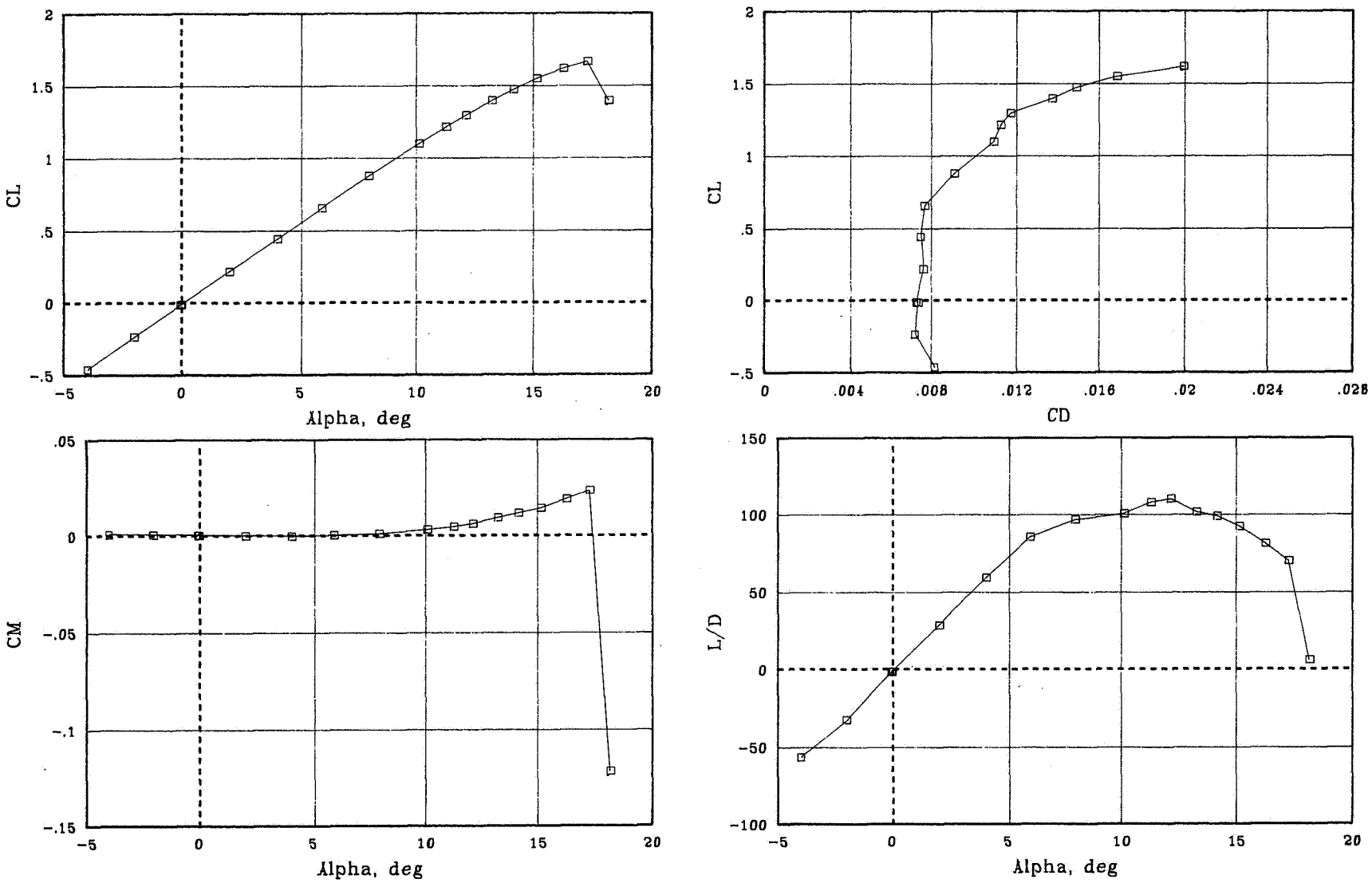

(c) $R = 12.0 \times 10^6$.

Figure 15. Concluded.

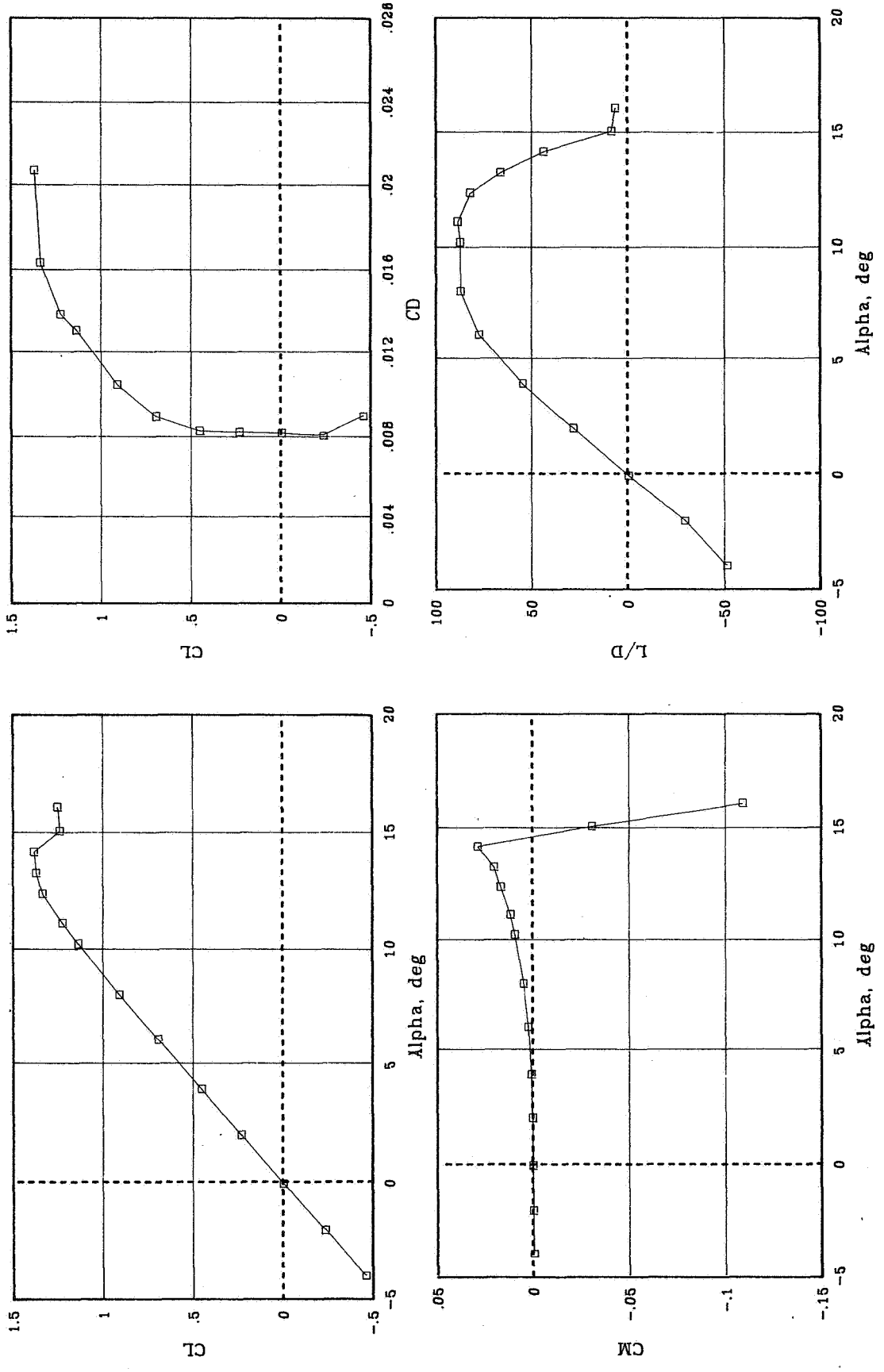

(a) $R = 6.0 \times 10^6$.

Figure 16. Variation of basic aerodynamic characteristics with angle of attack for various Reynolds numbers at $M = 0.30$ for transition fixed with No. 180 grit.

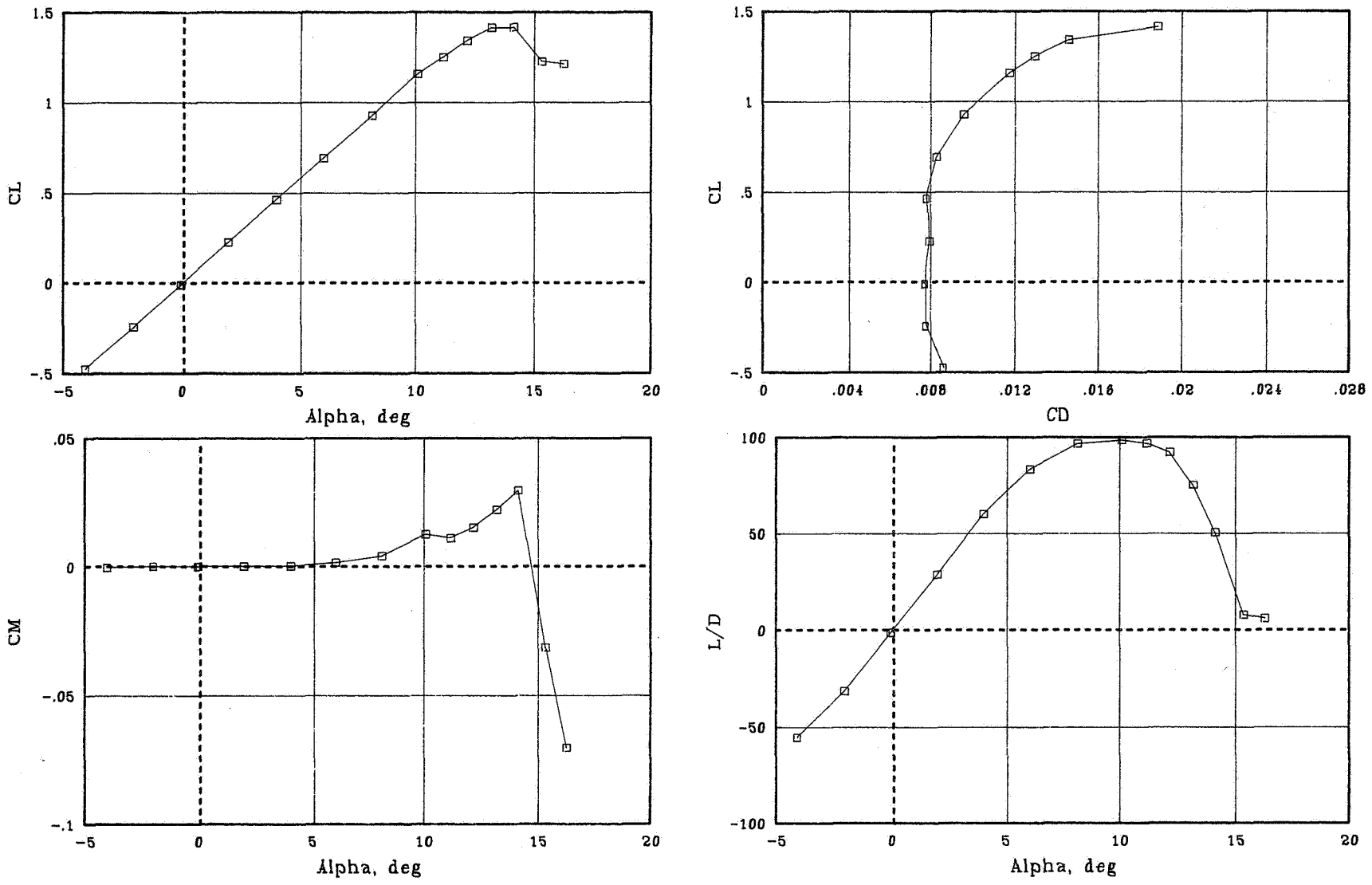

(b) $R = 8.9 \times 10^6$.

Figure 16. Continued.

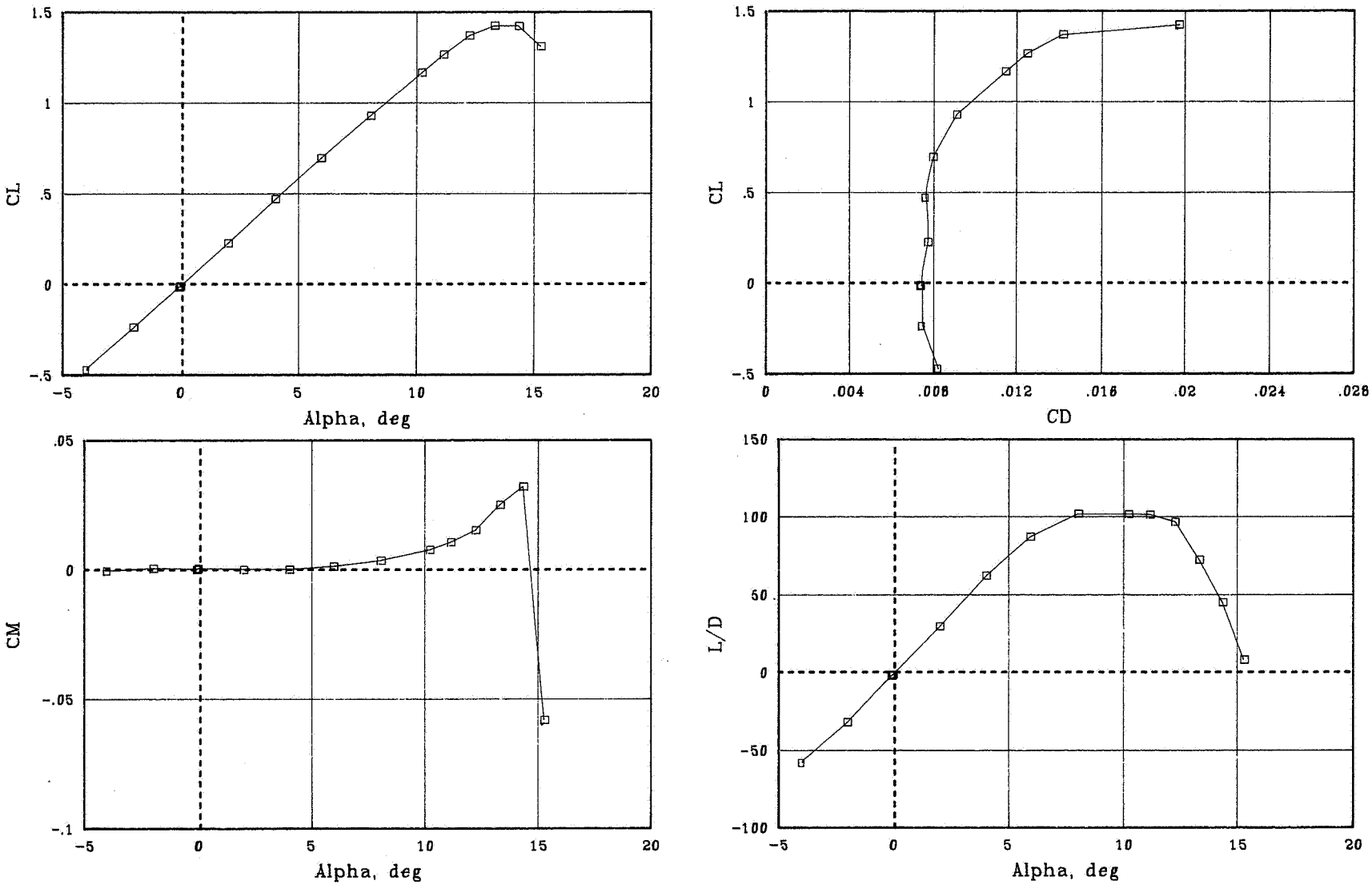

(c) $R = 11.9 \times 10^6$.

Figure 16. Concluded.

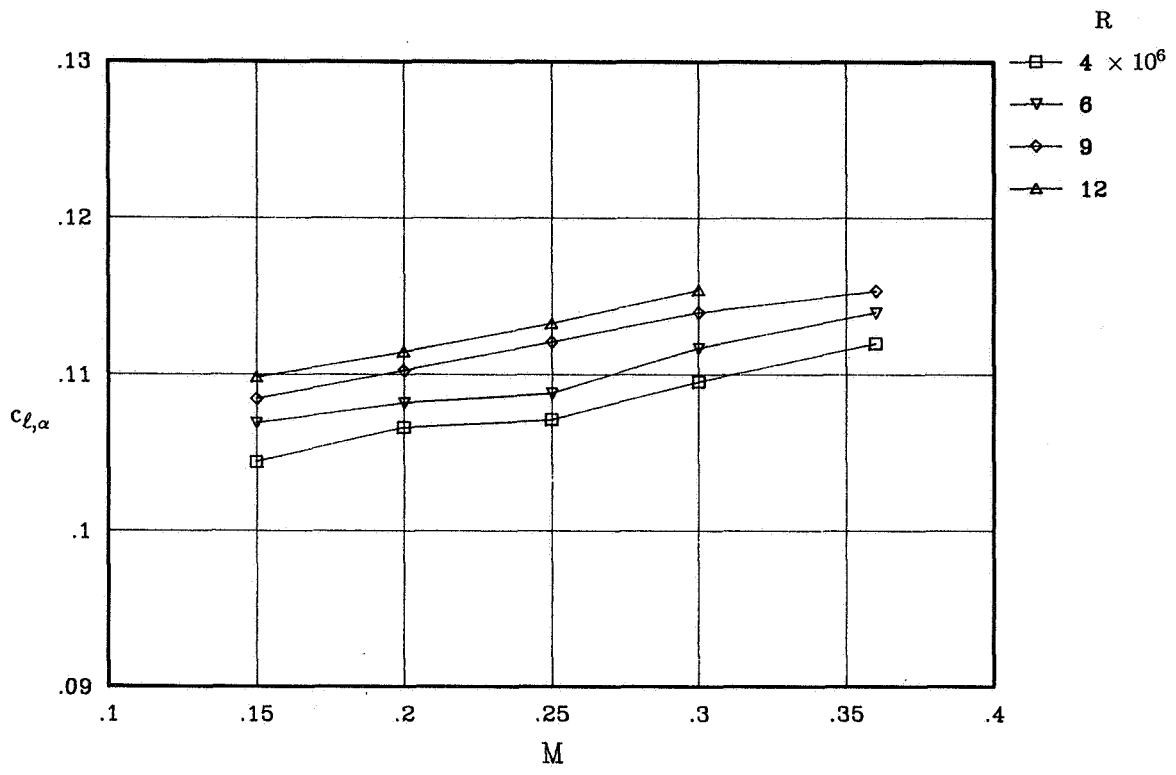

(a) Variation with Mach number.

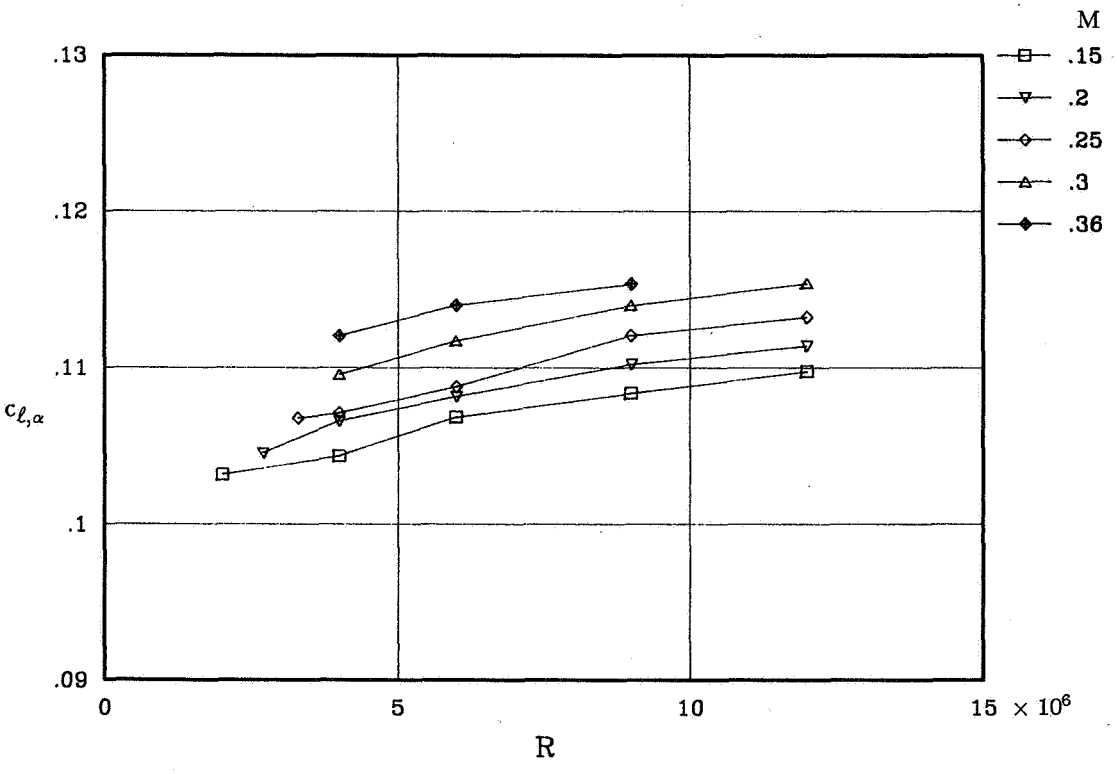

(b) Variation with Reynolds number.

Figure 17. Variation of lift-curve slope with Mach number and Reynolds number for free-transition case.

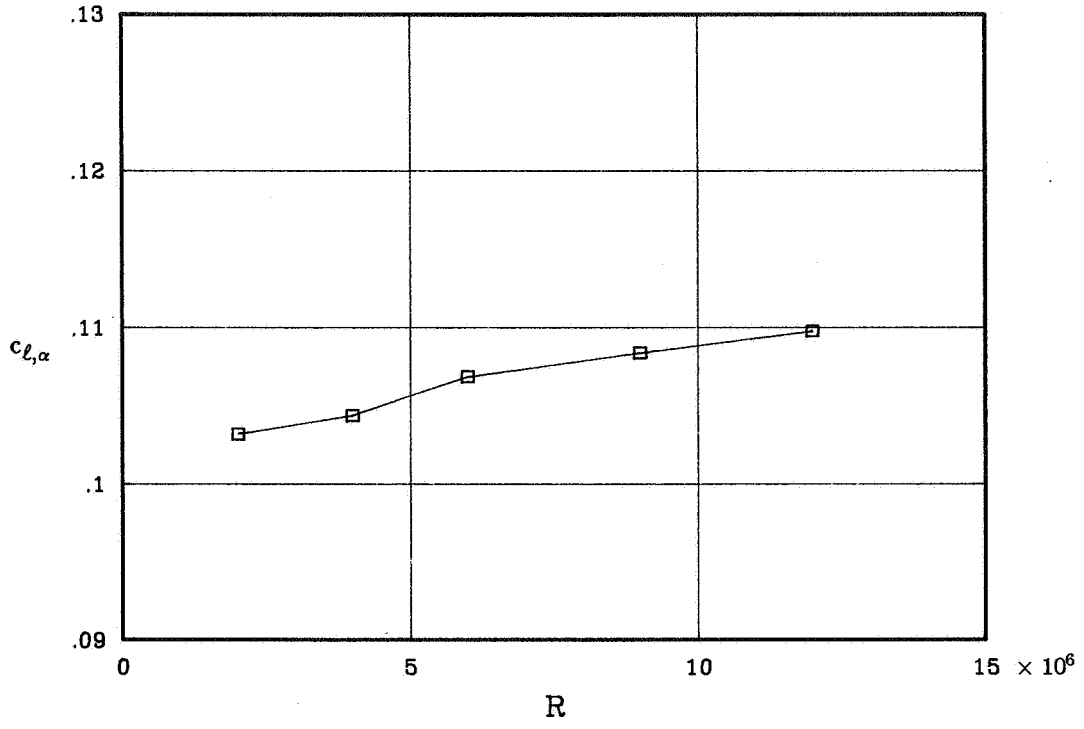

(a) Free transition.

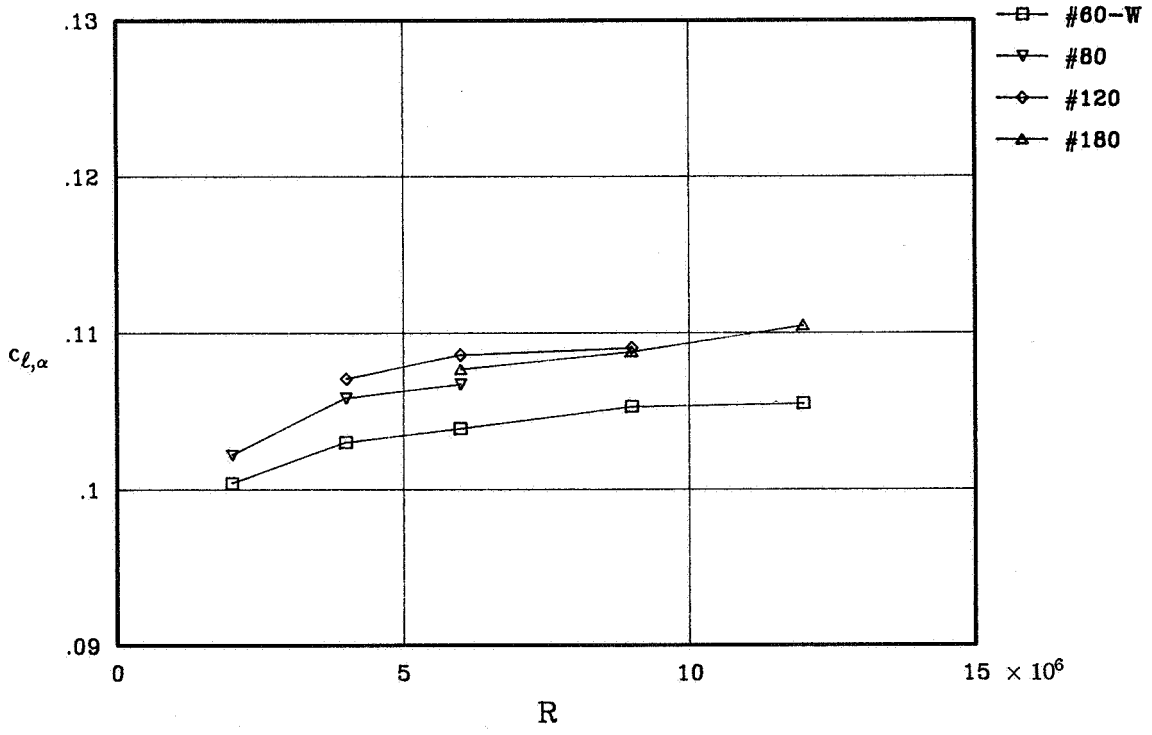

(b) Fixed transition.

Figure 18. Variation of lift-curve slope with Reynolds number for free and fixed transition at $M = 0.15$.

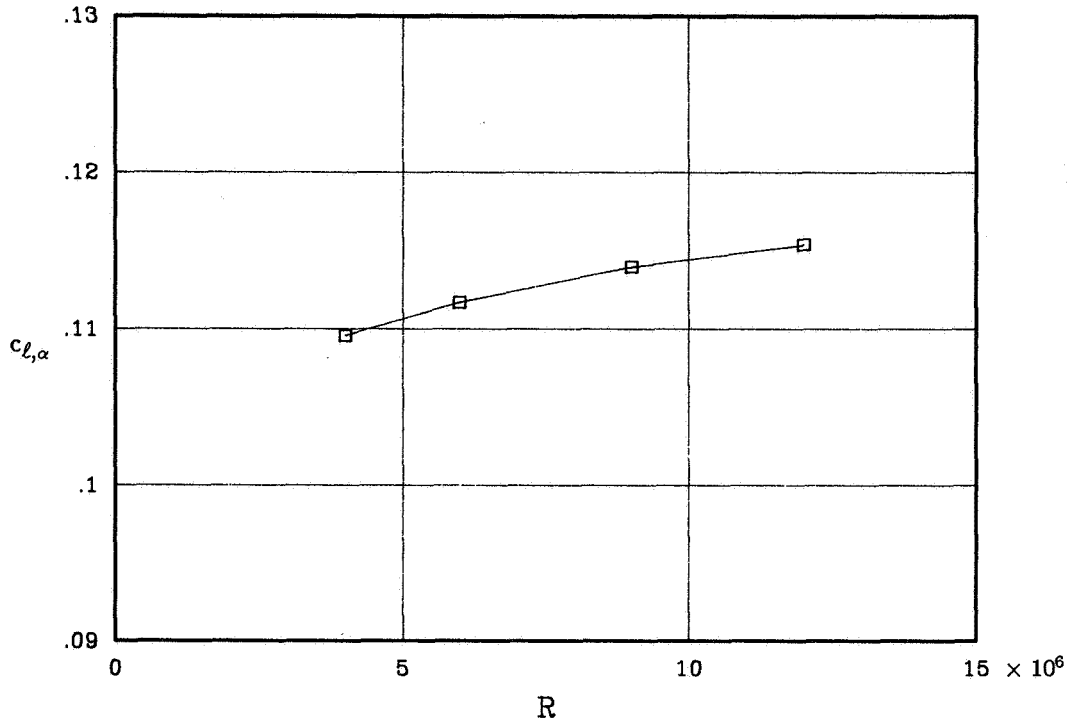

(a) Free transition.

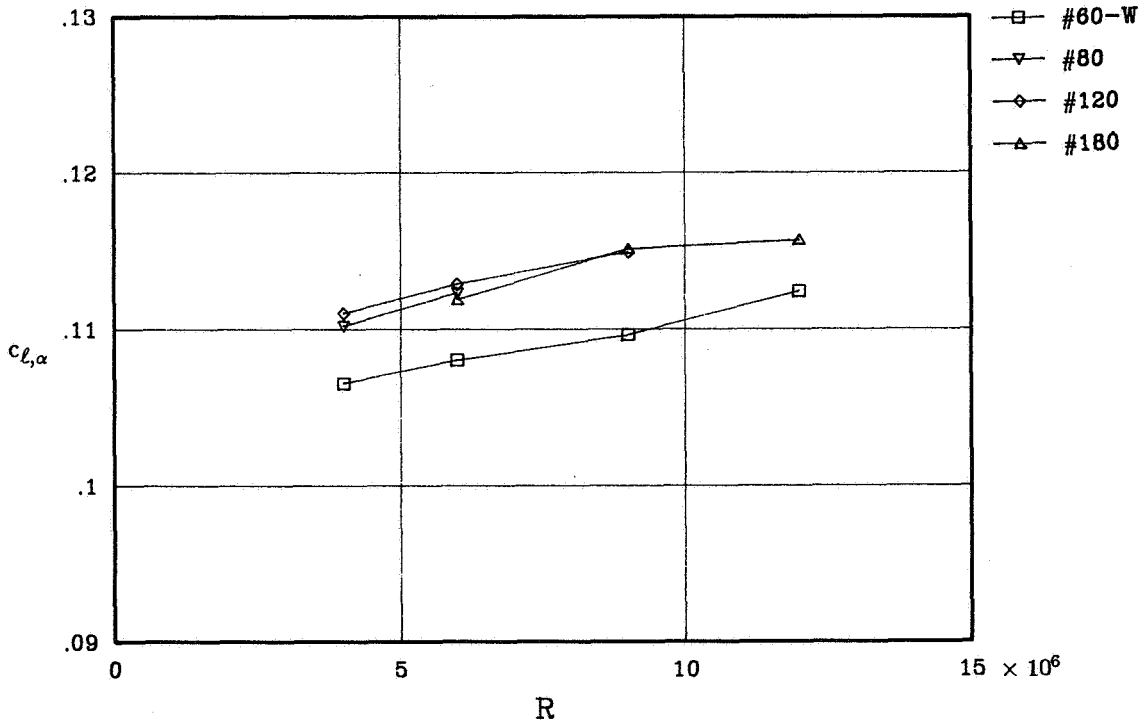

(b) Fixed transition.

Figure 19. Variation of lift-curve slope with Reynolds number for free and fixed transition at $M = 0.30$.

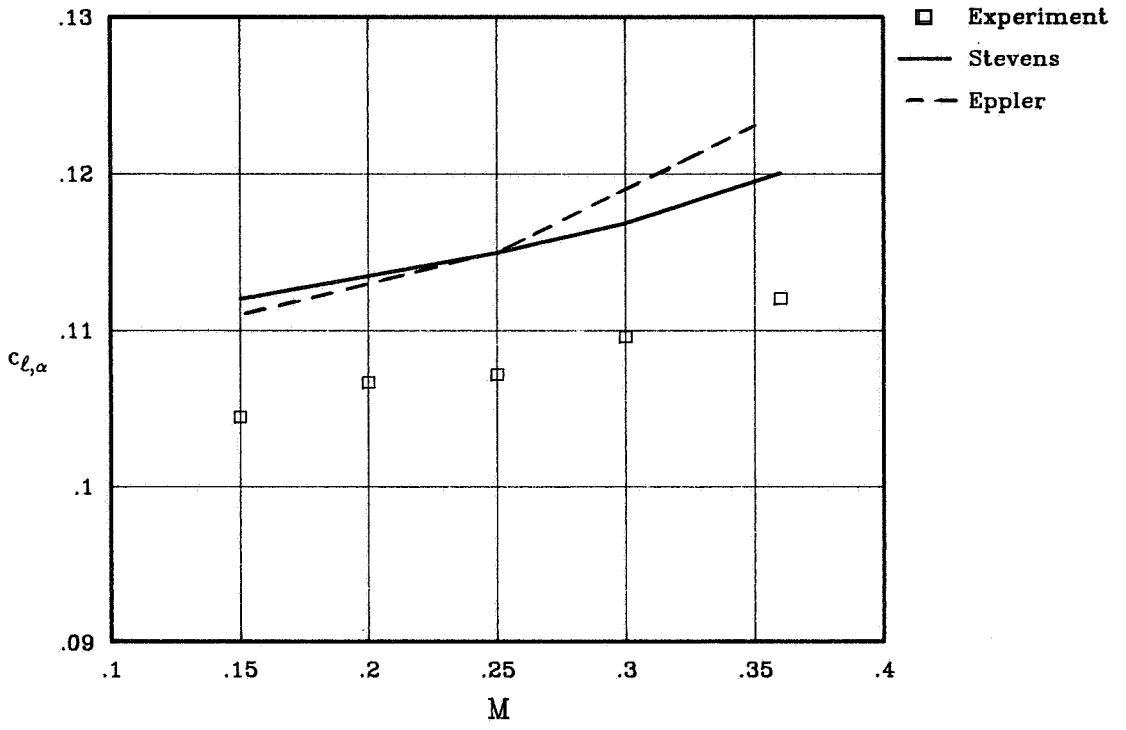

(a) $R = 4 \times 10^6$

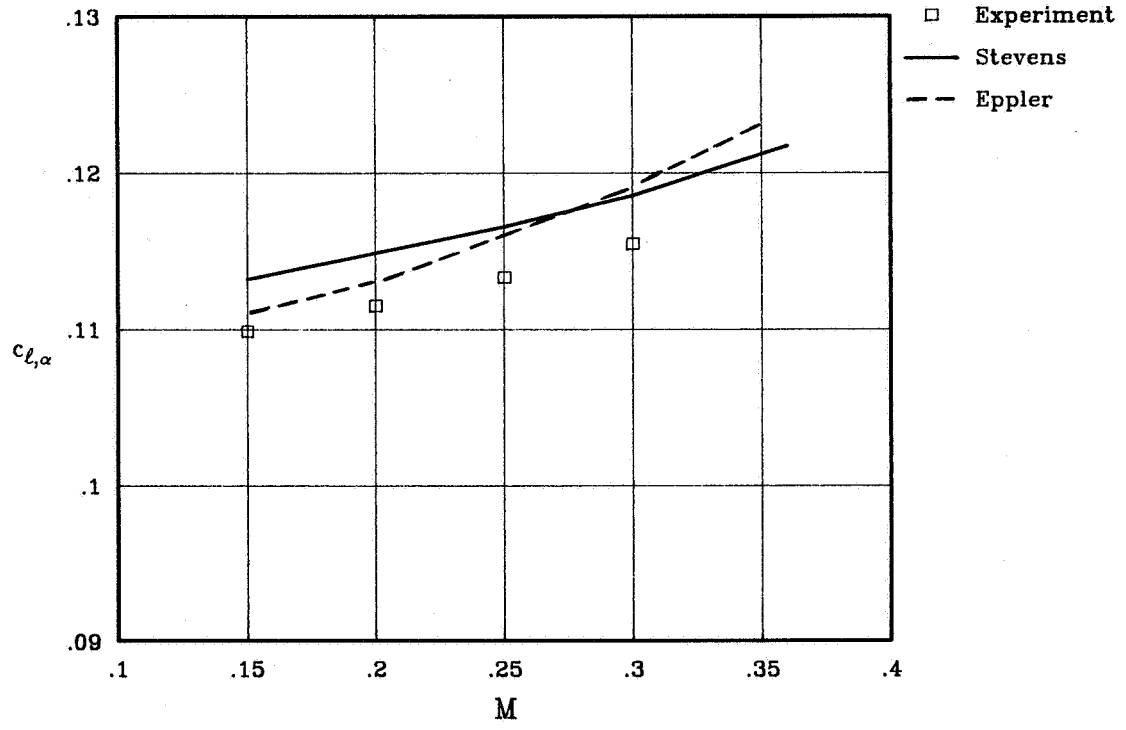

(b) $R = 12 \times 10^6$.

Figure 20. Theoretical and experimental lift-curve slopes as function of Mach number for free-transition case.

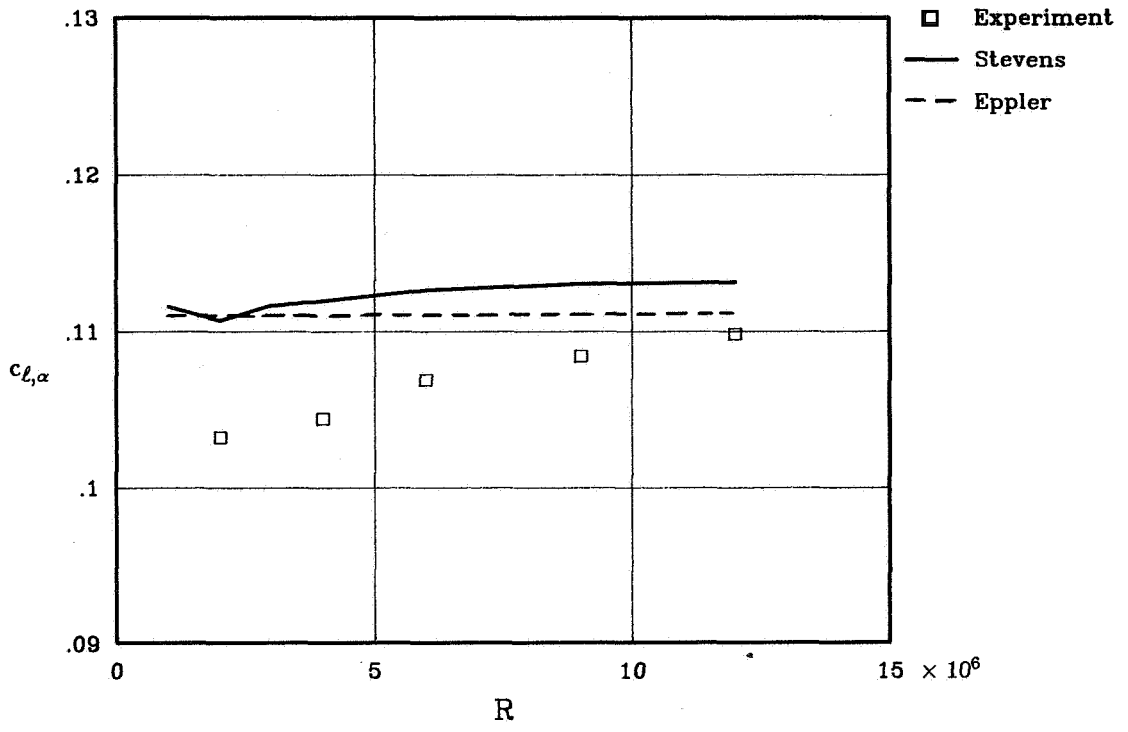

(a) $M = 0.15$.

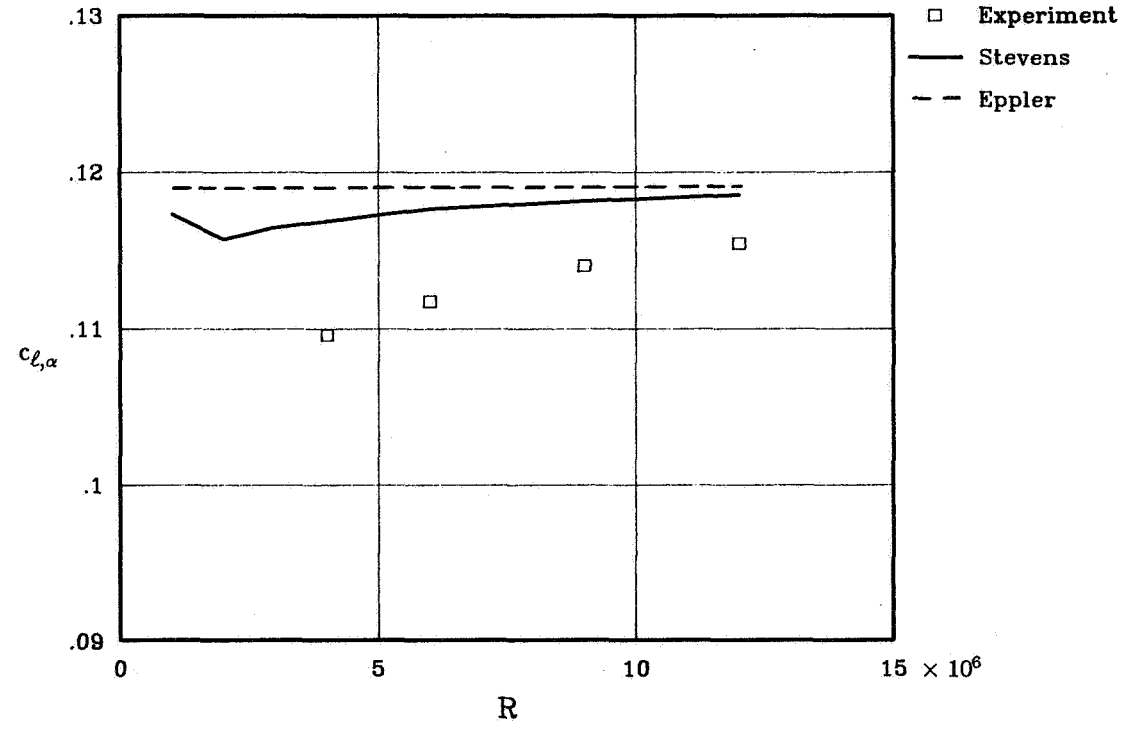

(b) $M = 0.30$.

Figure 21. Theoretical and experimental lift-curve slopes as function of Reynolds number for free-transition case.

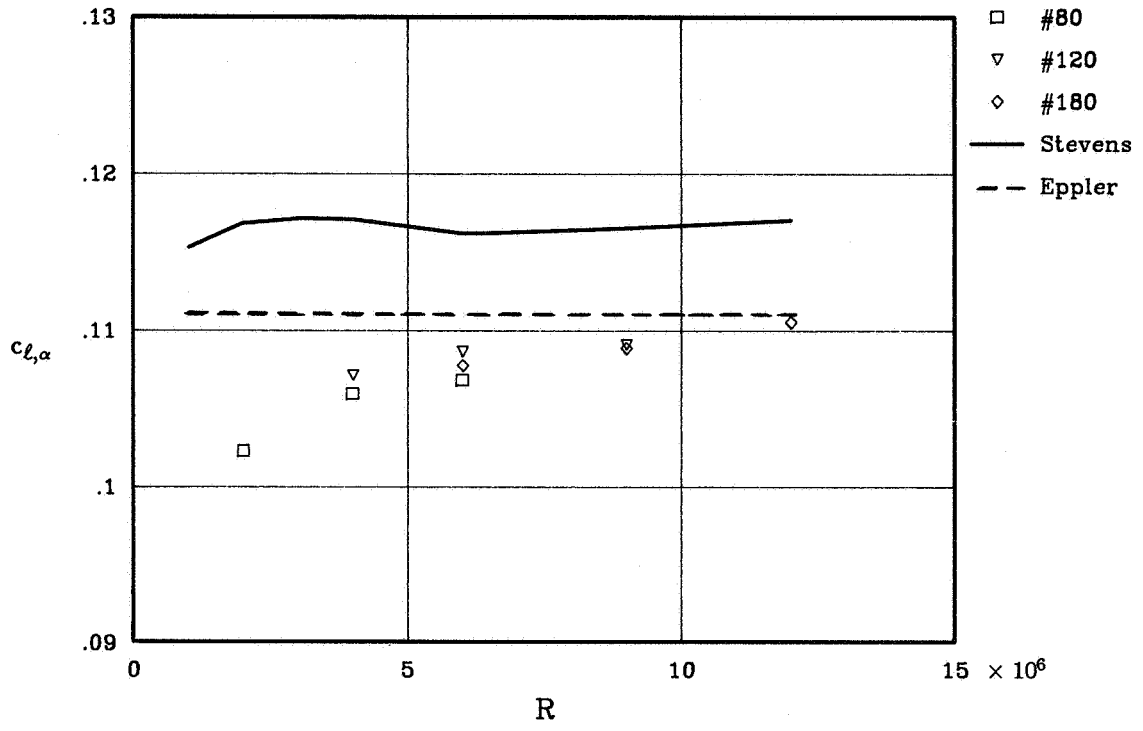

(a) $M = 0.15$.

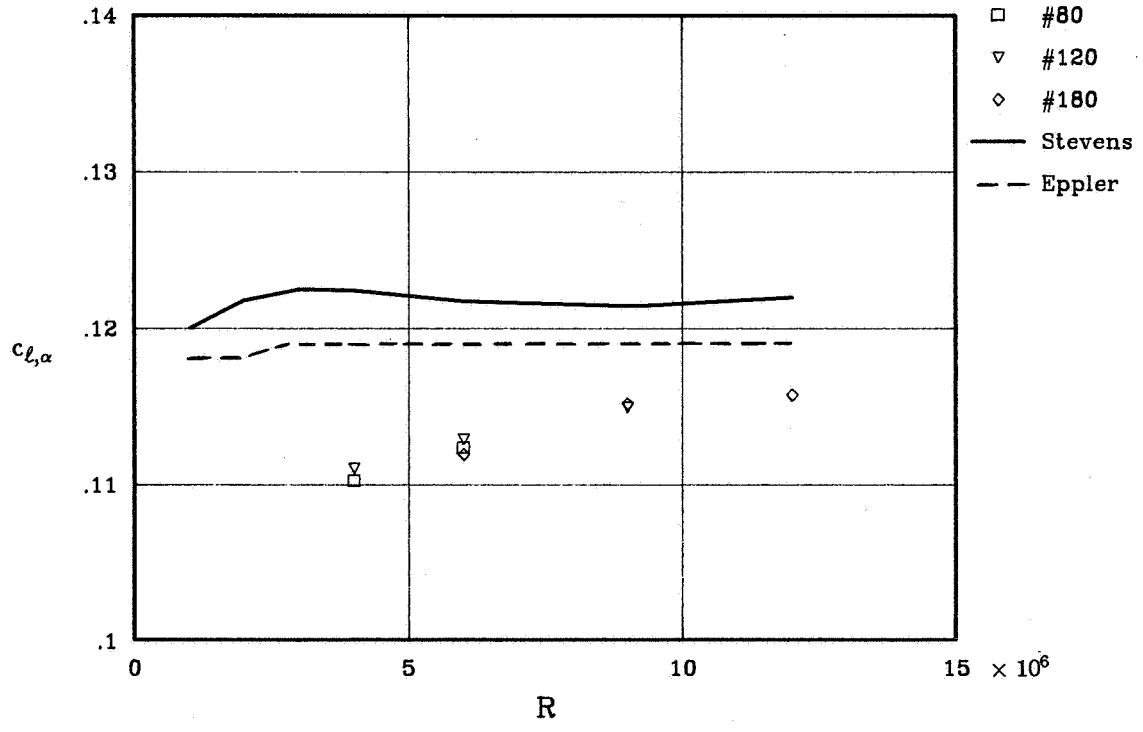

(b) $M = 0.30$.

Figure 22. Theoretical and experimental lift-curve slopes as function of Reynolds number for fixed-transition case.

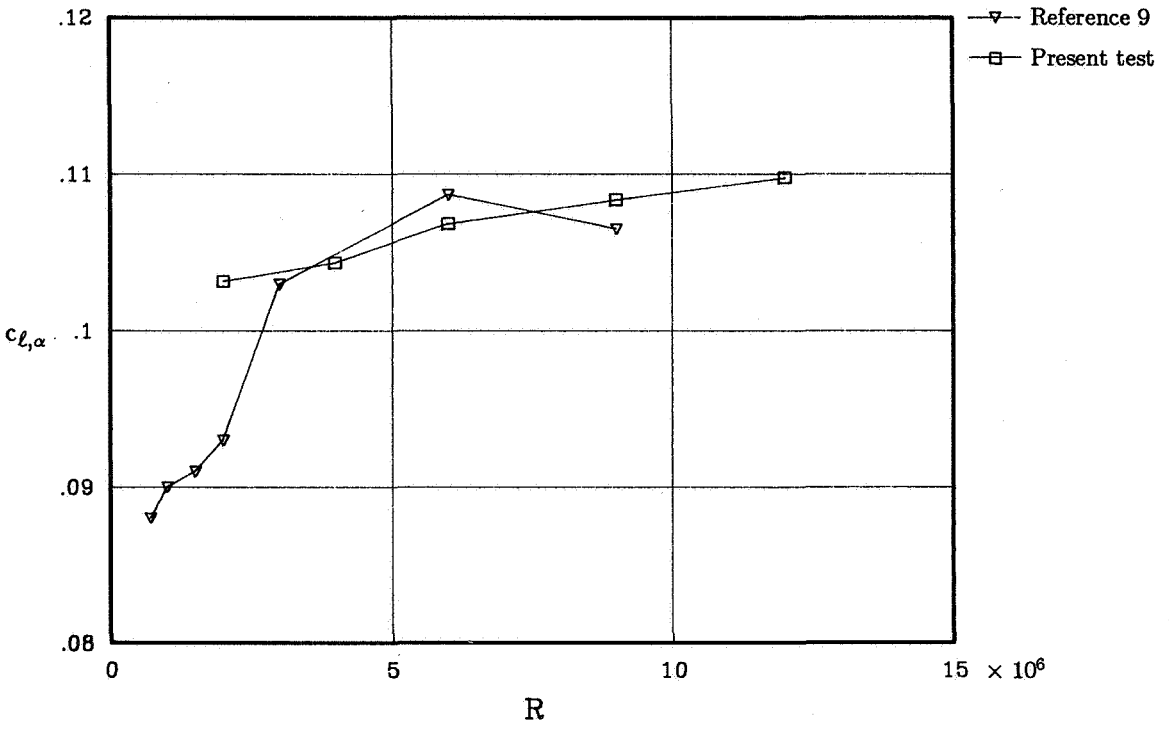

(a) Free transition.

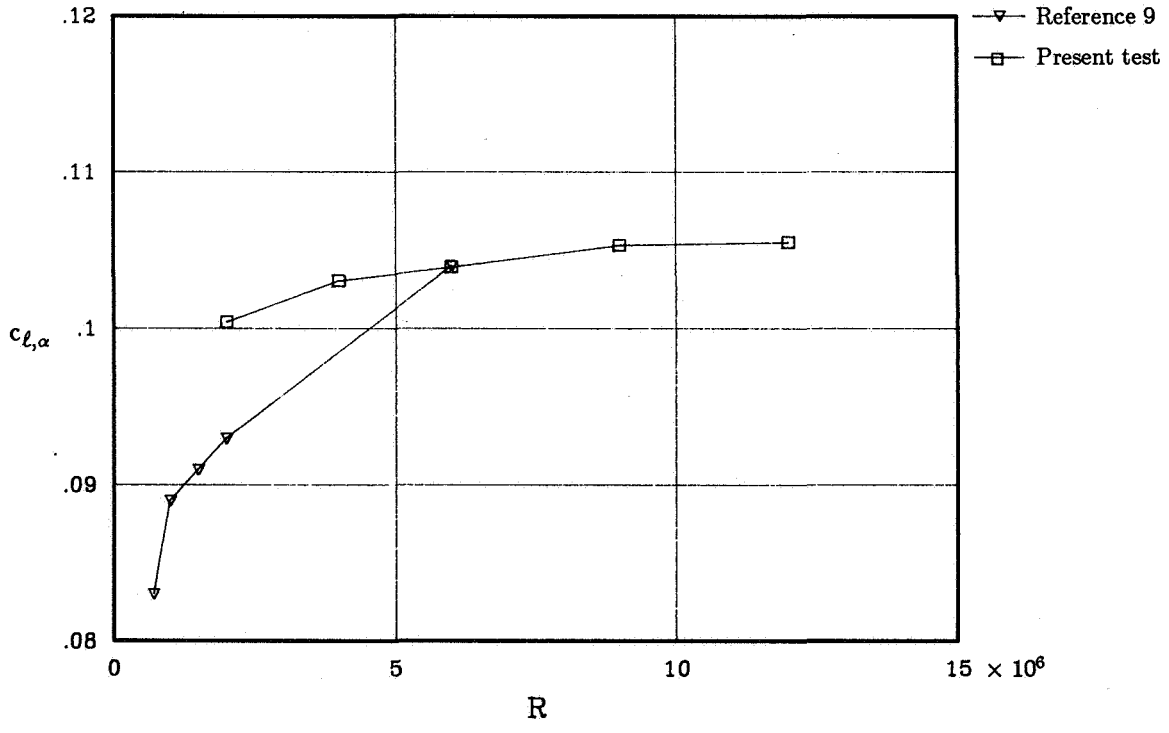

(b) Fixed transition (No. 60-W grit).

Figure 23. Comparison of lift-curve slope with previously published data (ref. 9) from same facility as function of Reynolds number for $M \leq 0.15$.

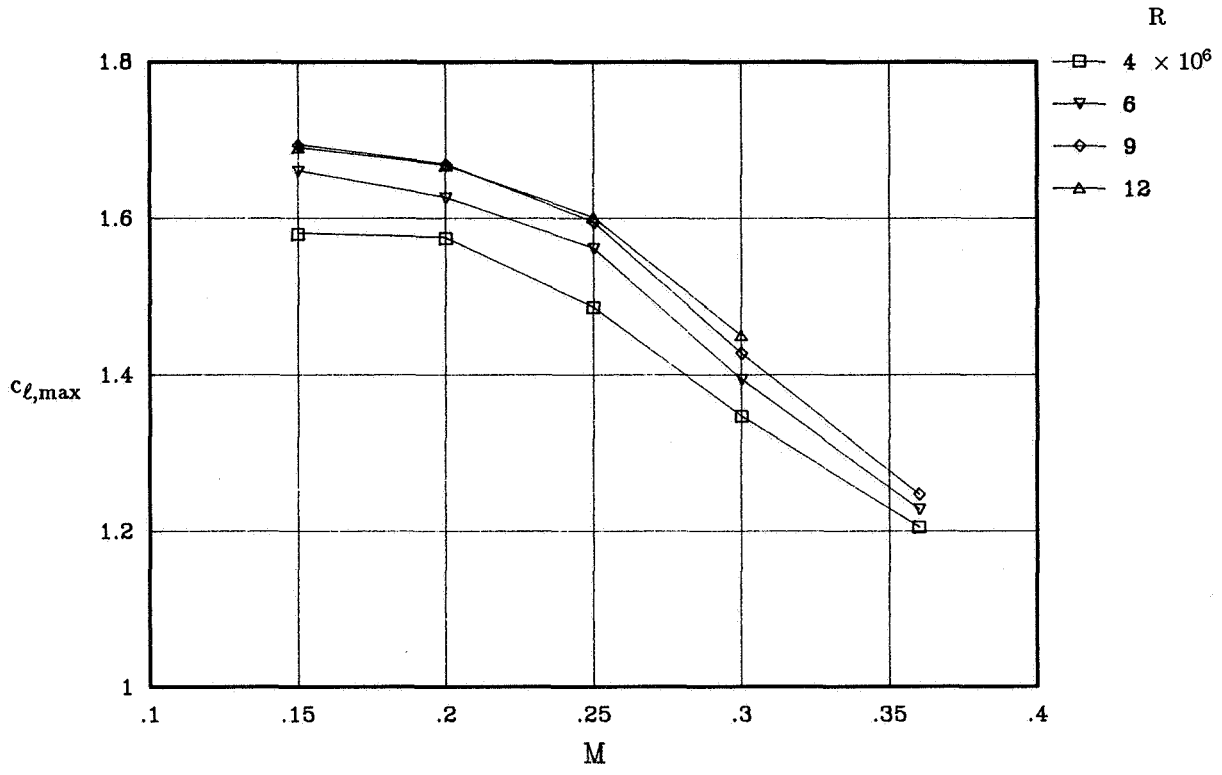

(a) Variation with Mach number.

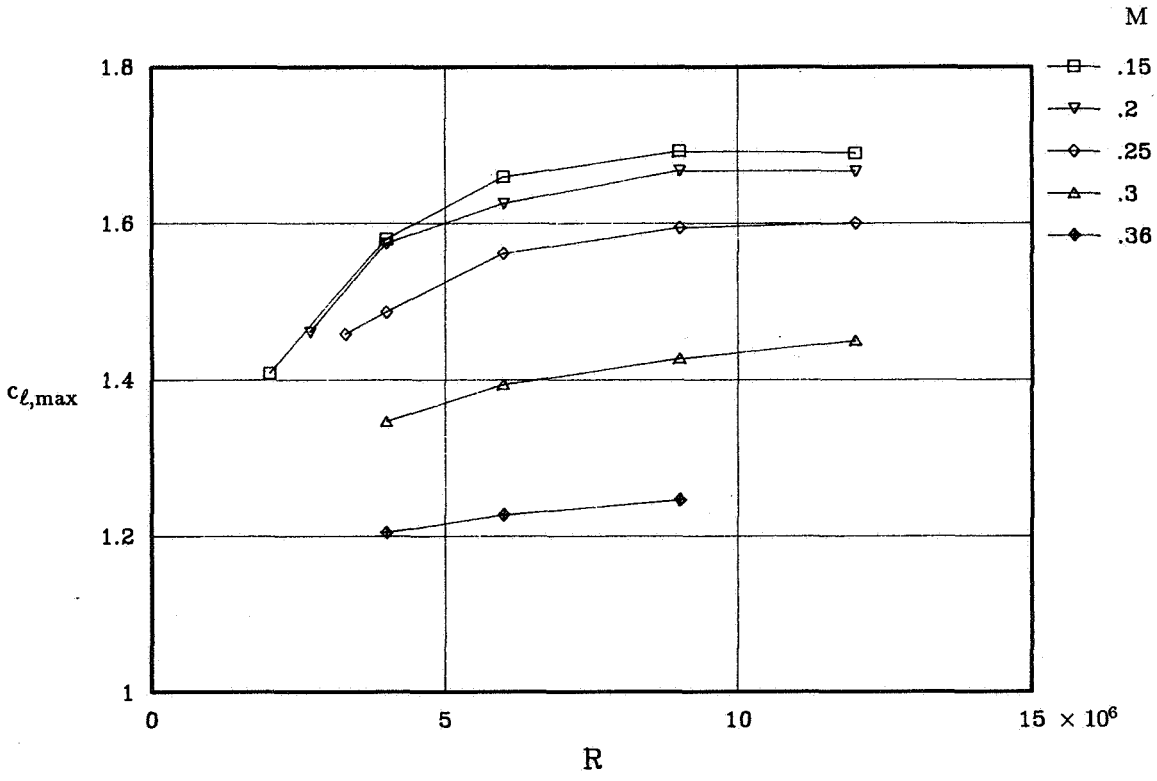

(b) Variation with Reynolds number.

Figure 24. Variation of maximum lift coefficient with Mach number and Reynolds number for free-transition case.

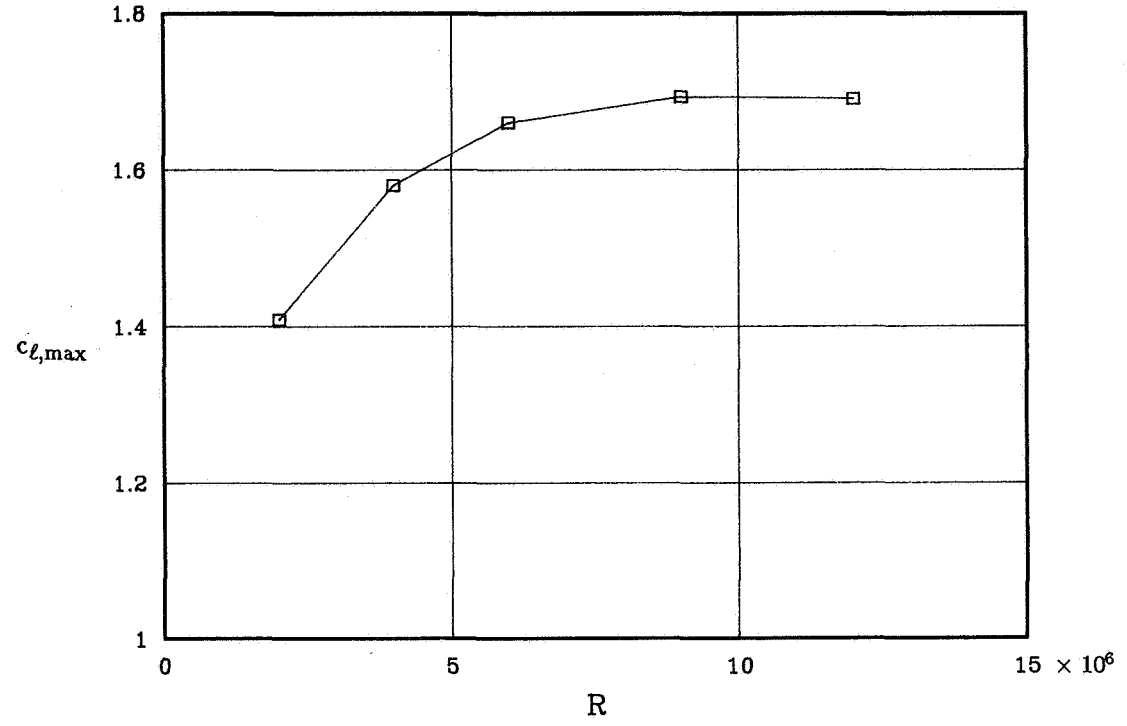

(a) Free transition.

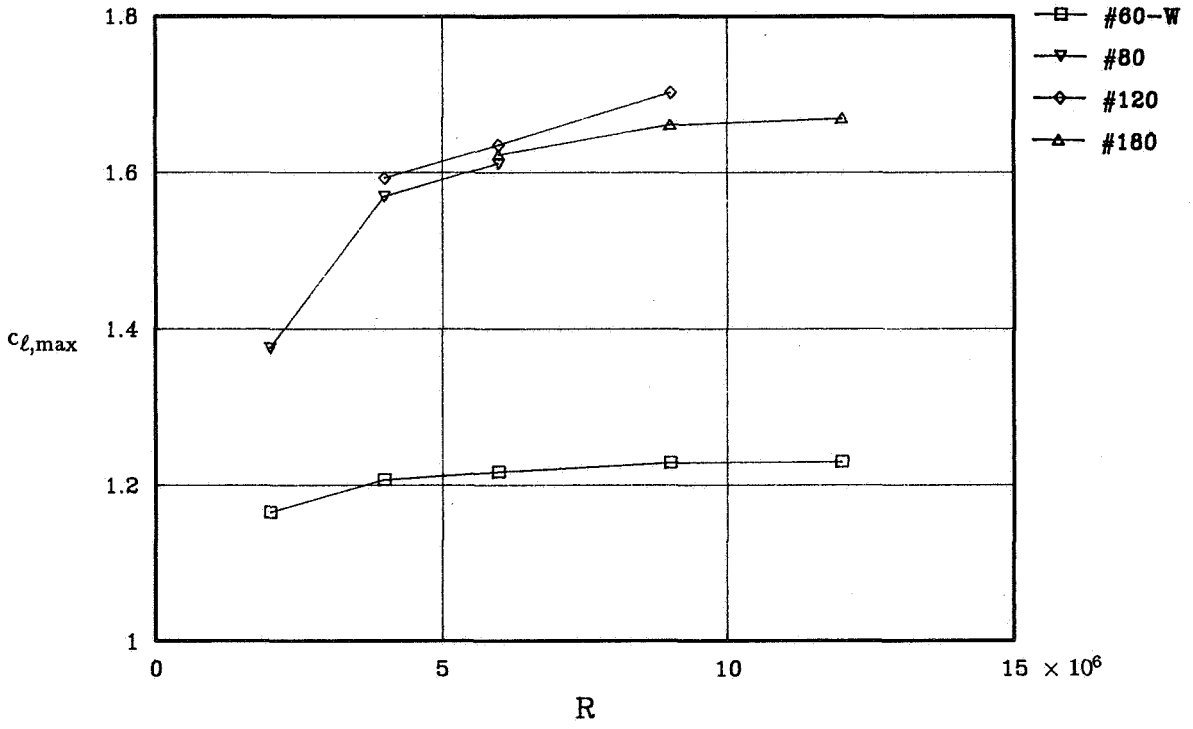

(b) Fixed transition.

Figure 25. Variation of maximum lift coefficient with Reynolds number for free and fixed transition at $M = 0.15$.

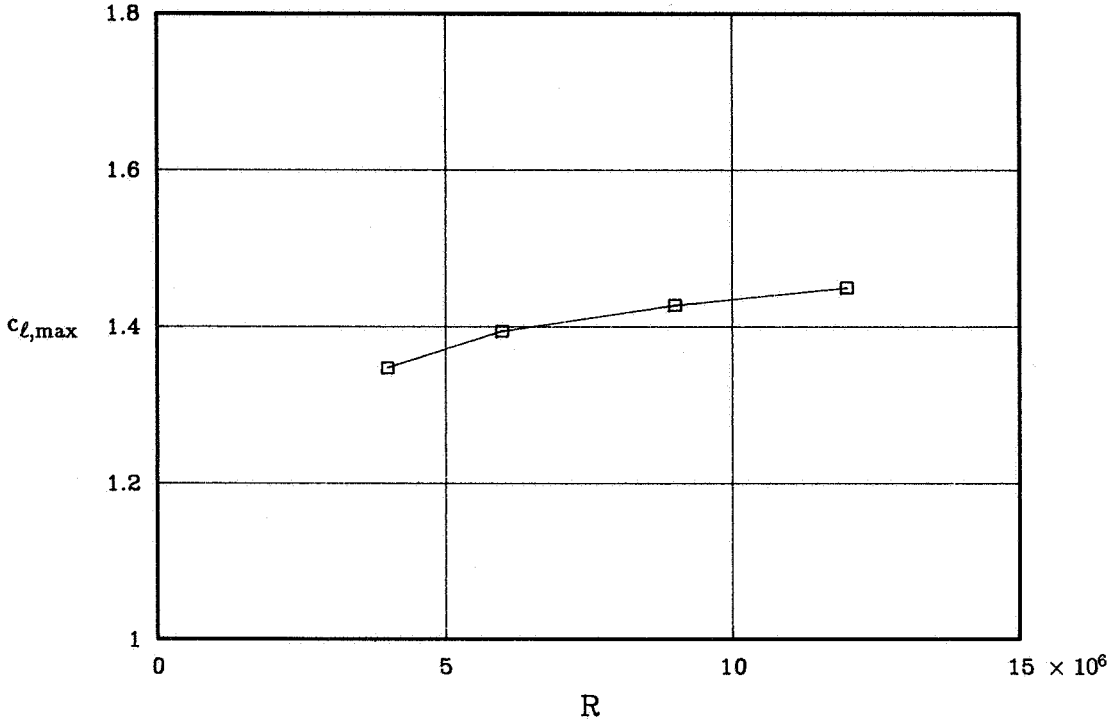

(a) Free transition.

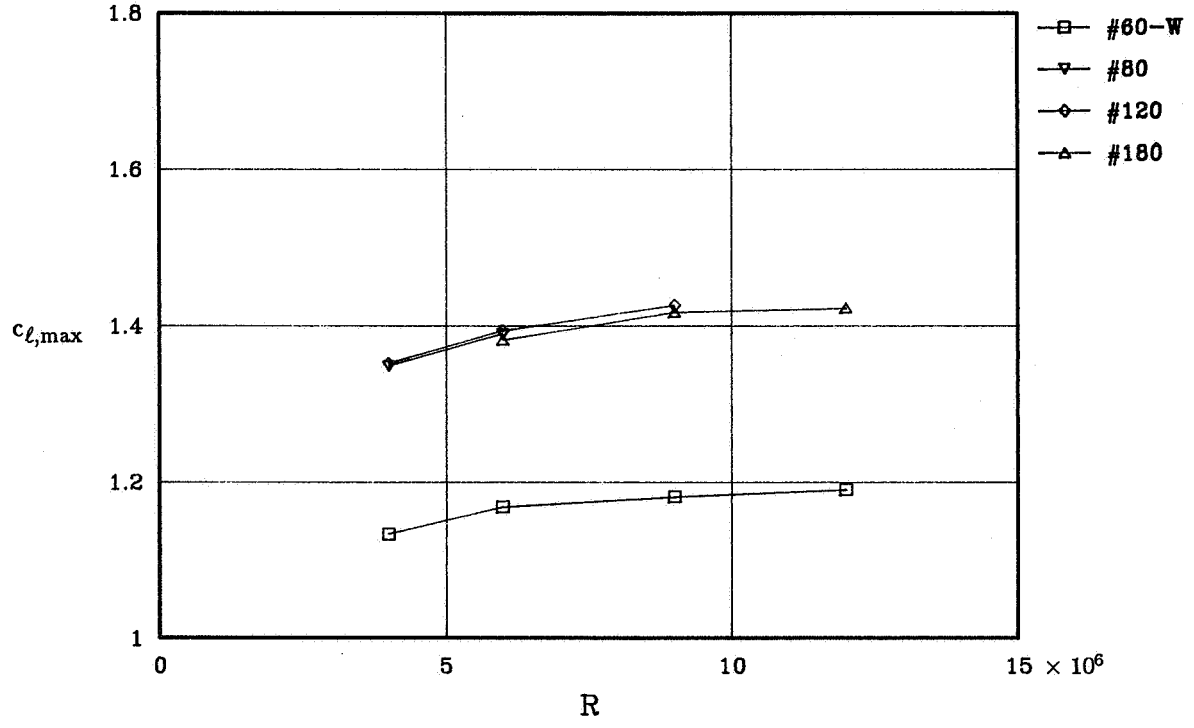

(b) Fixed transition.

Figure 26. Variation of maximum lift coefficient with Reynolds number for free and fixed transition at $M = 0.30$.

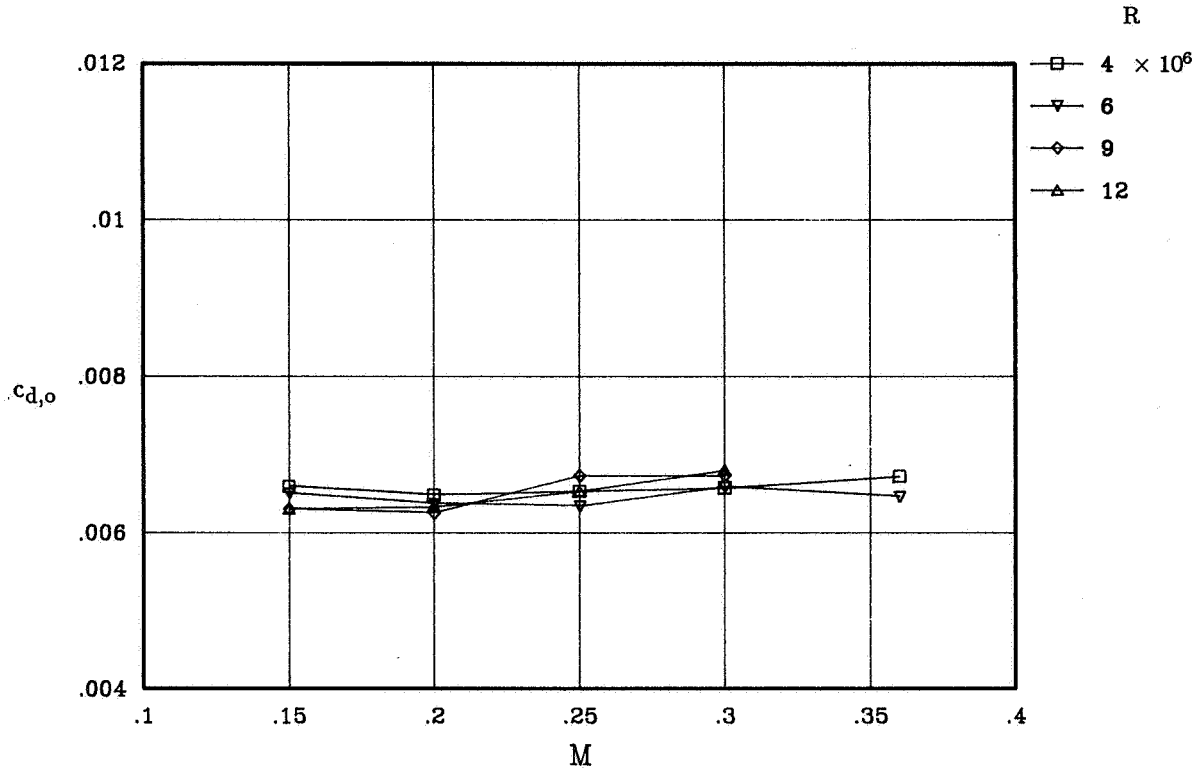

(a) Variation with Mach number.

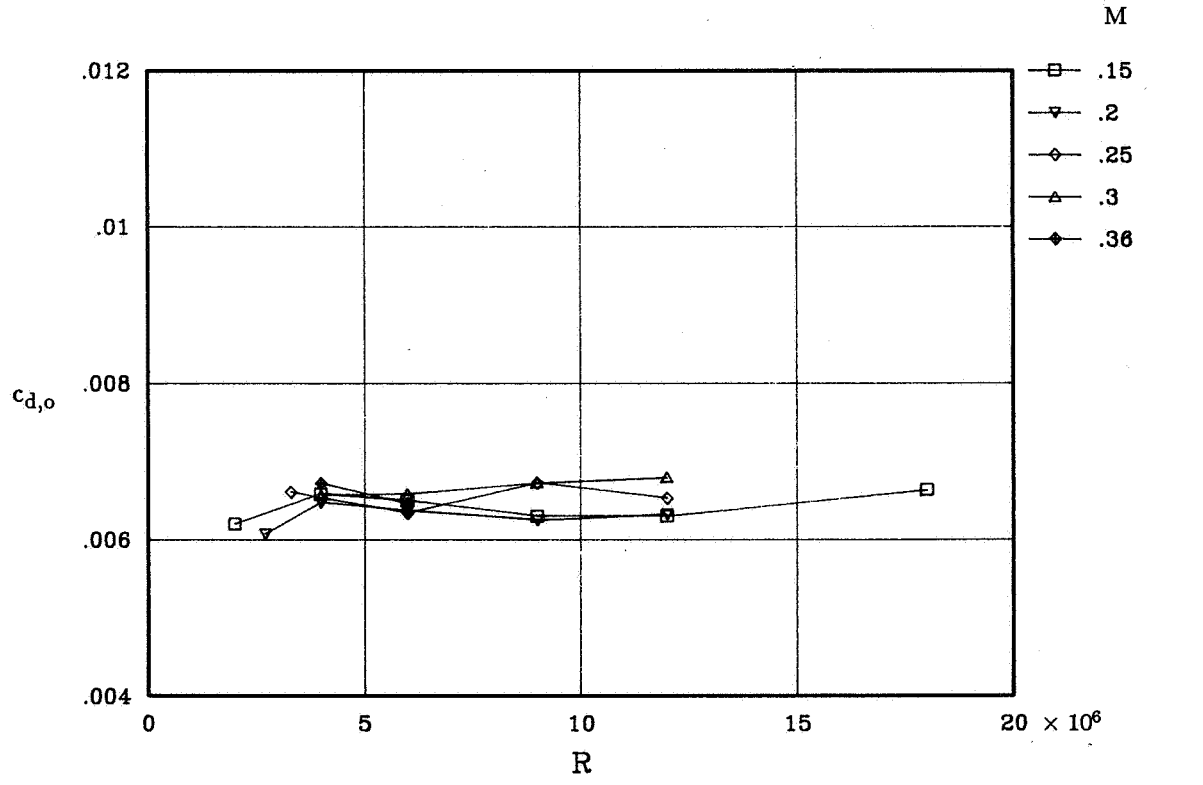

(b) Variation with Reynolds number.

Figure 27. Variation of drag coefficient at zero lift with Mach number and Reynolds number for free-transition case.

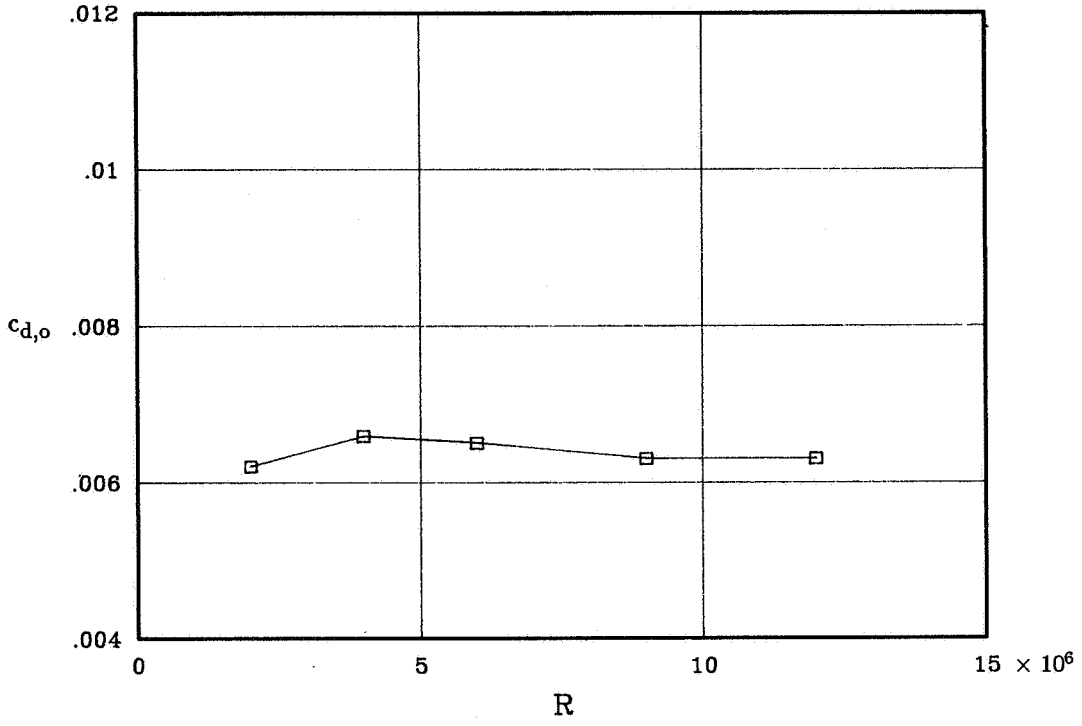

(a) Free transition.

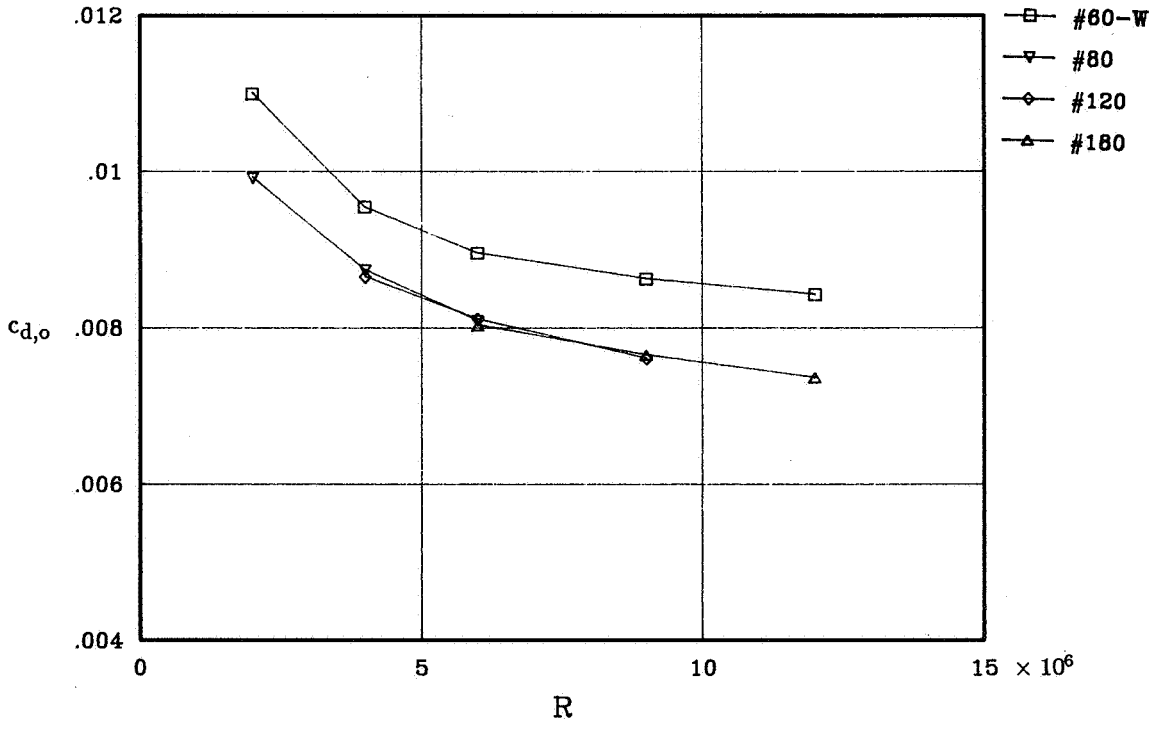

(b) Fixed transition.

Figure 28. Variation of drag coefficient at zero lift with Reynolds number for free and fixed transition at $M = 0.15$.

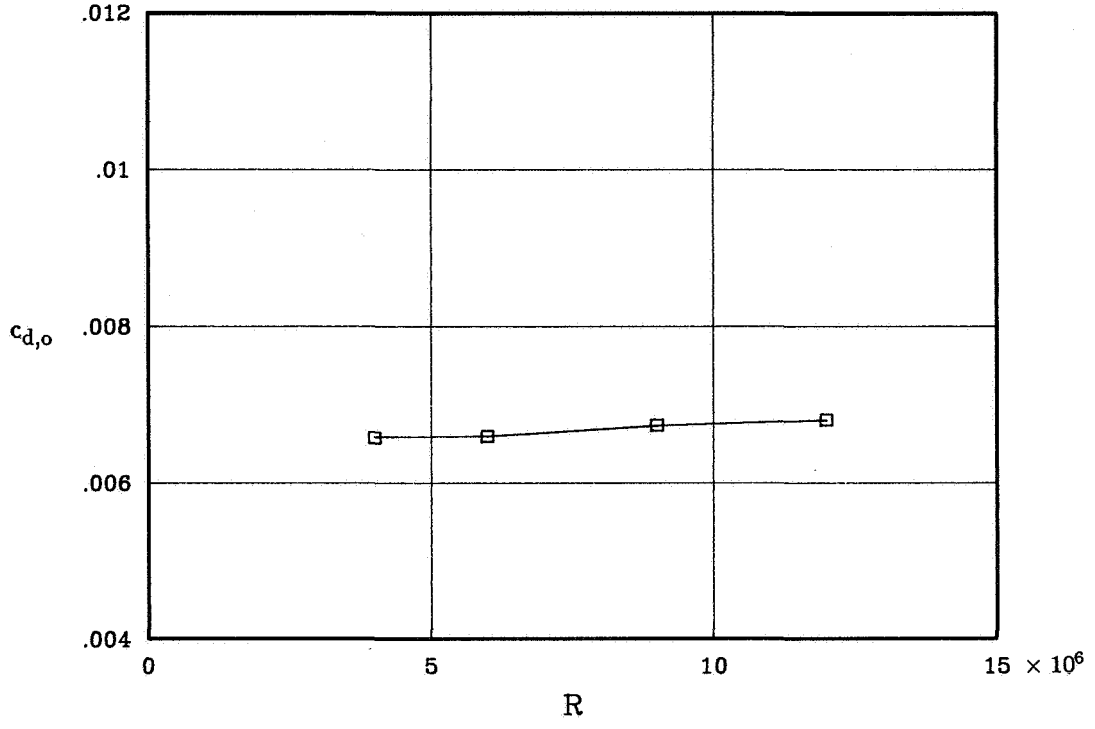

(a) Free transition.

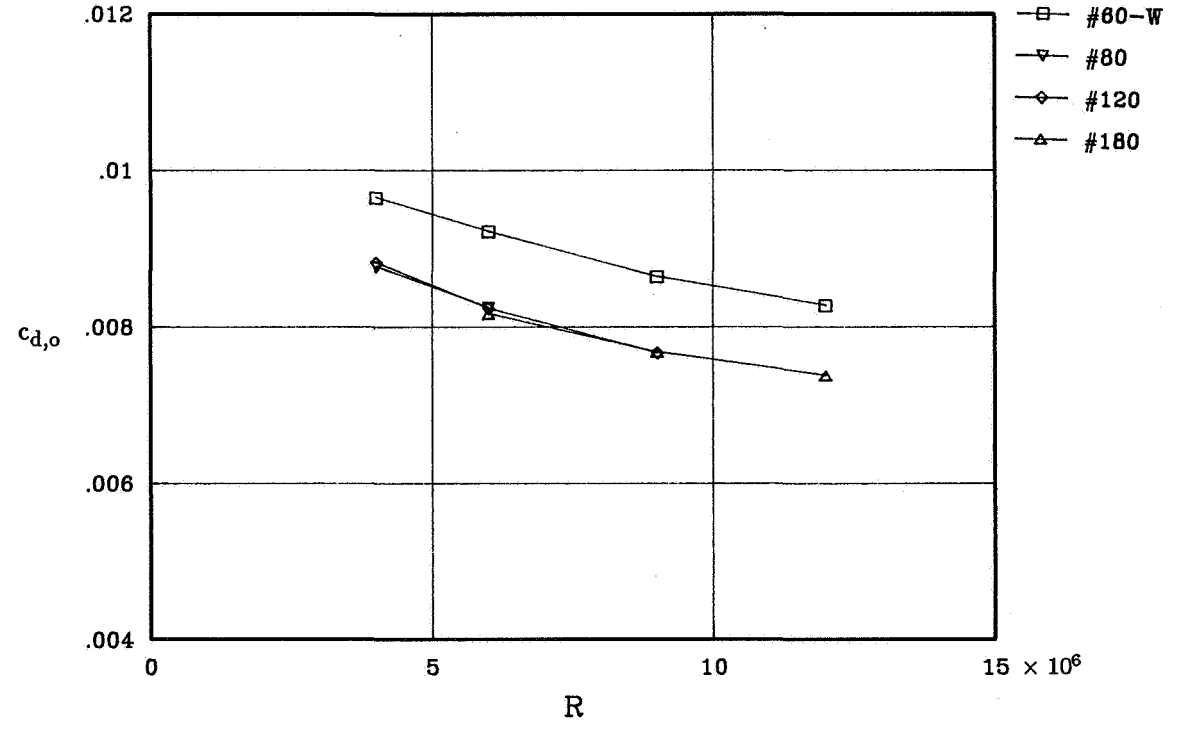

(b) Fixed transition.

Figure 29. Variation of drag coefficient at zero lift with Reynolds number for free and fixed transition at $M = 0.30$.

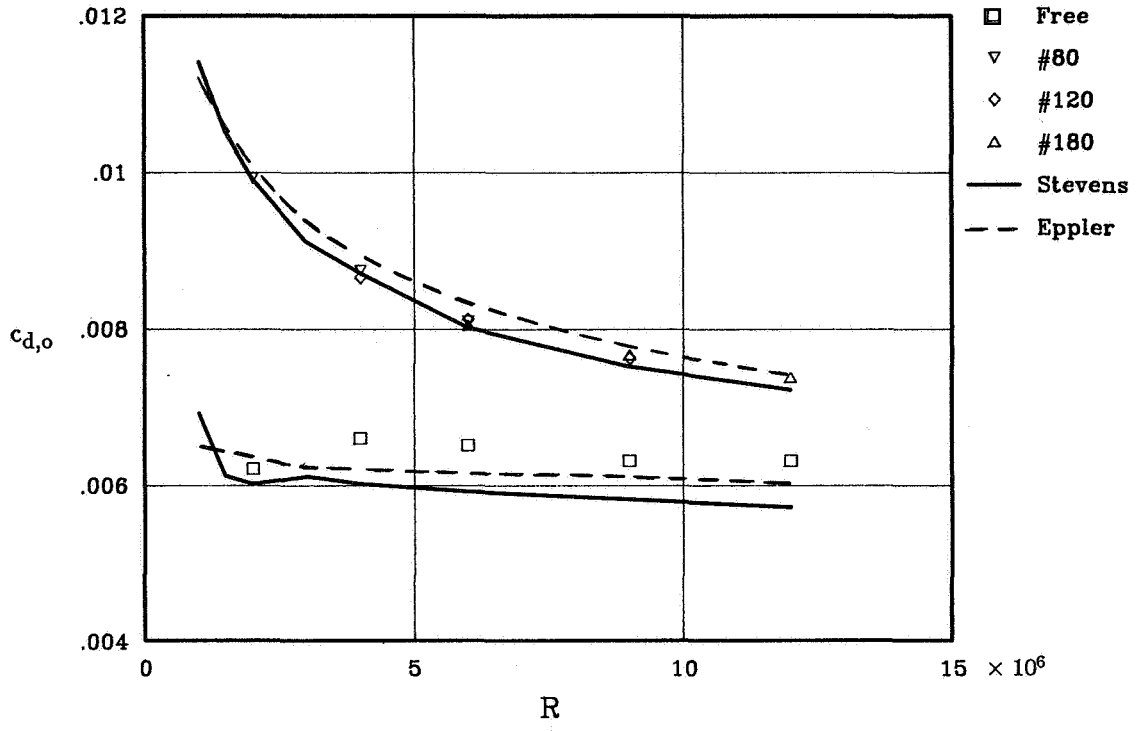

(a) $M = 0.15$.

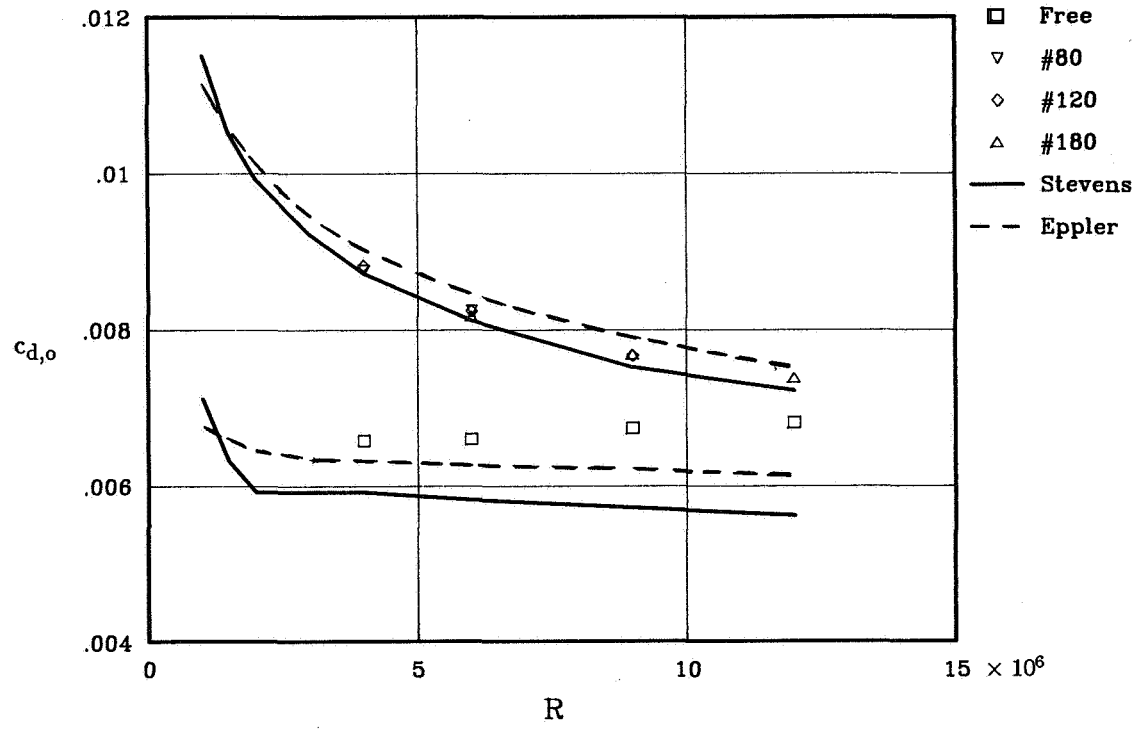

(b) $M = 0.30$.

Figure 30. Theoretical and experimental drag coefficients at zero lift as function of Reynolds number.

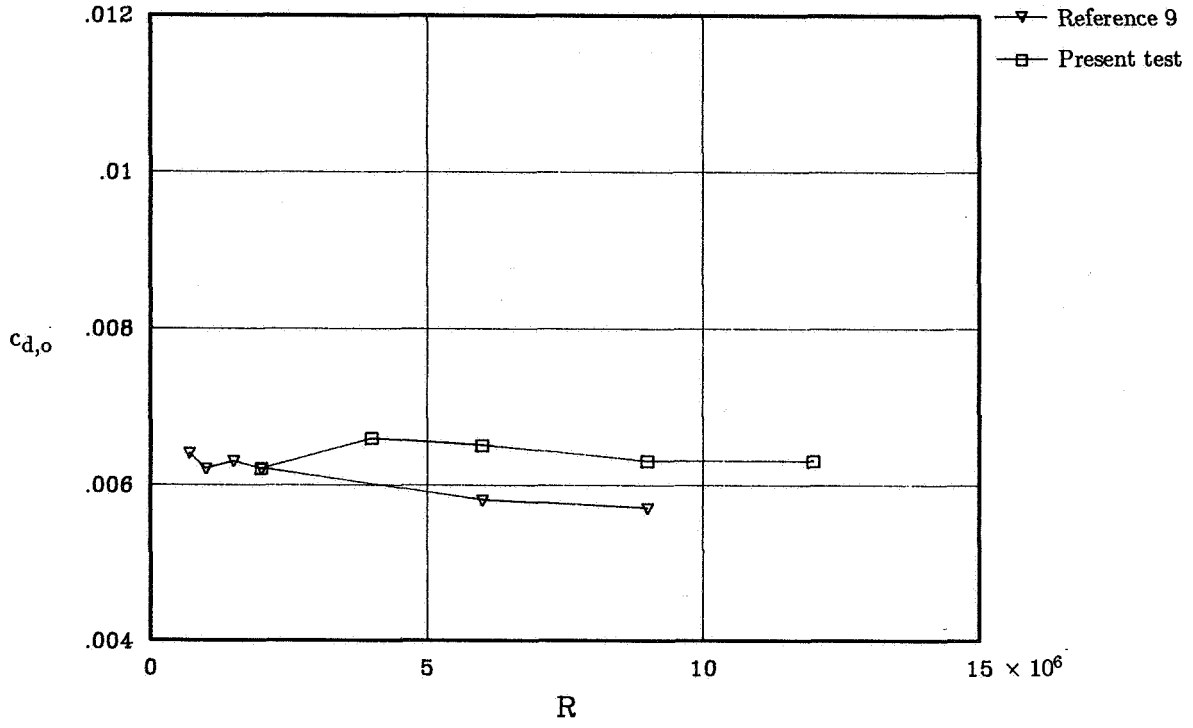

(a) Free transition.

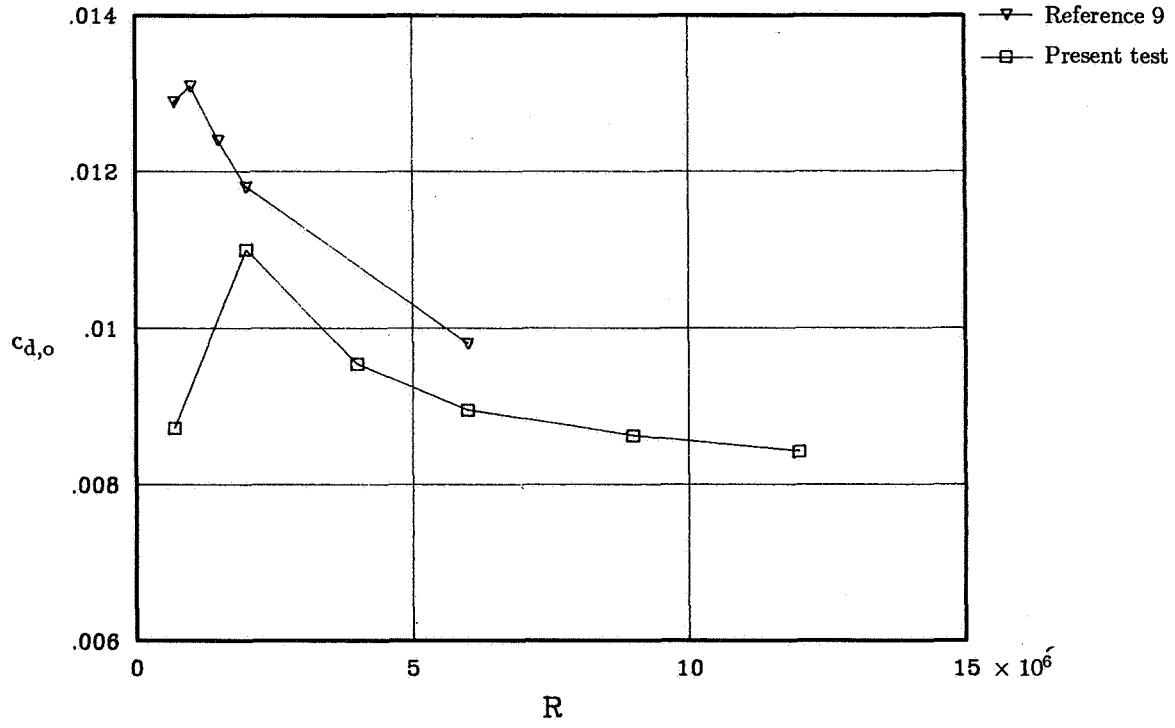

(b) Fixed transition (No. 60-W).

Figure 31. Comparison of drag coefficient at zero lift with previously published data (ref. 9) from same facility as function of Reynolds number for $M \leq 0.15$.

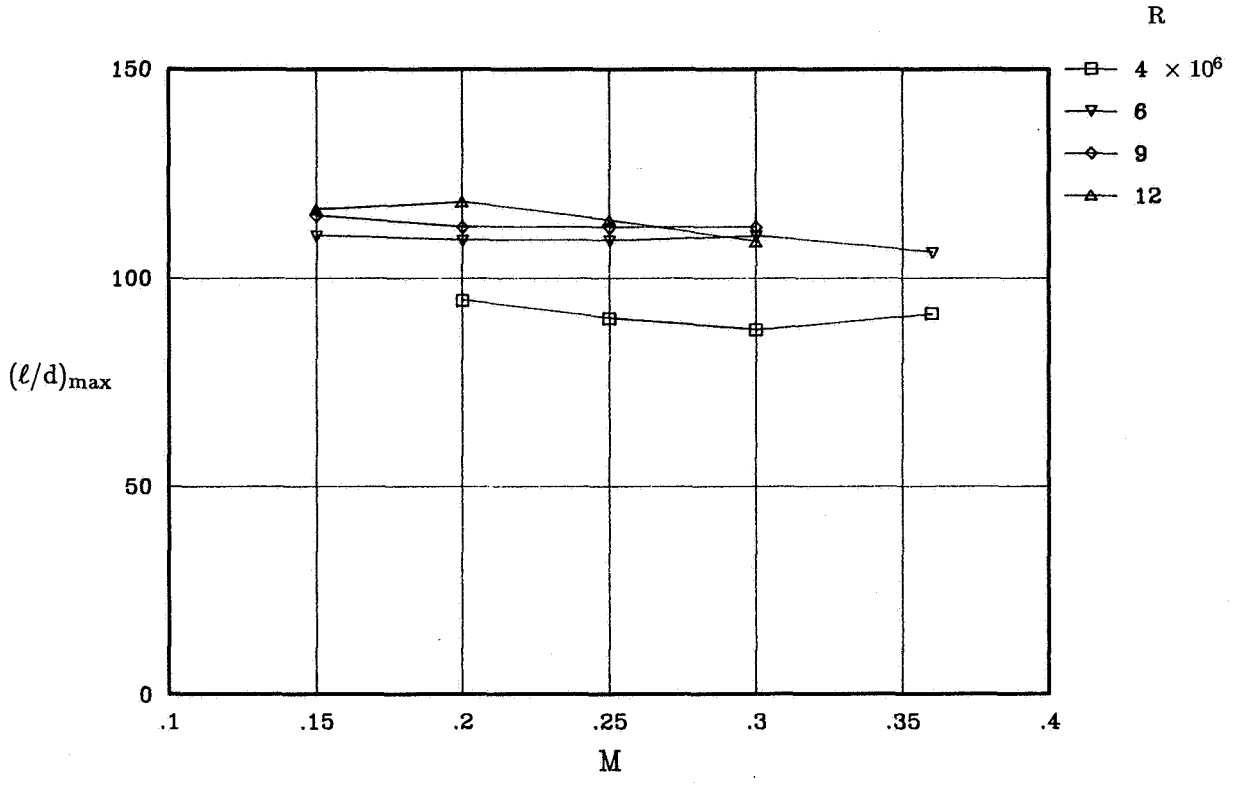

(a) Variation with Mach number.

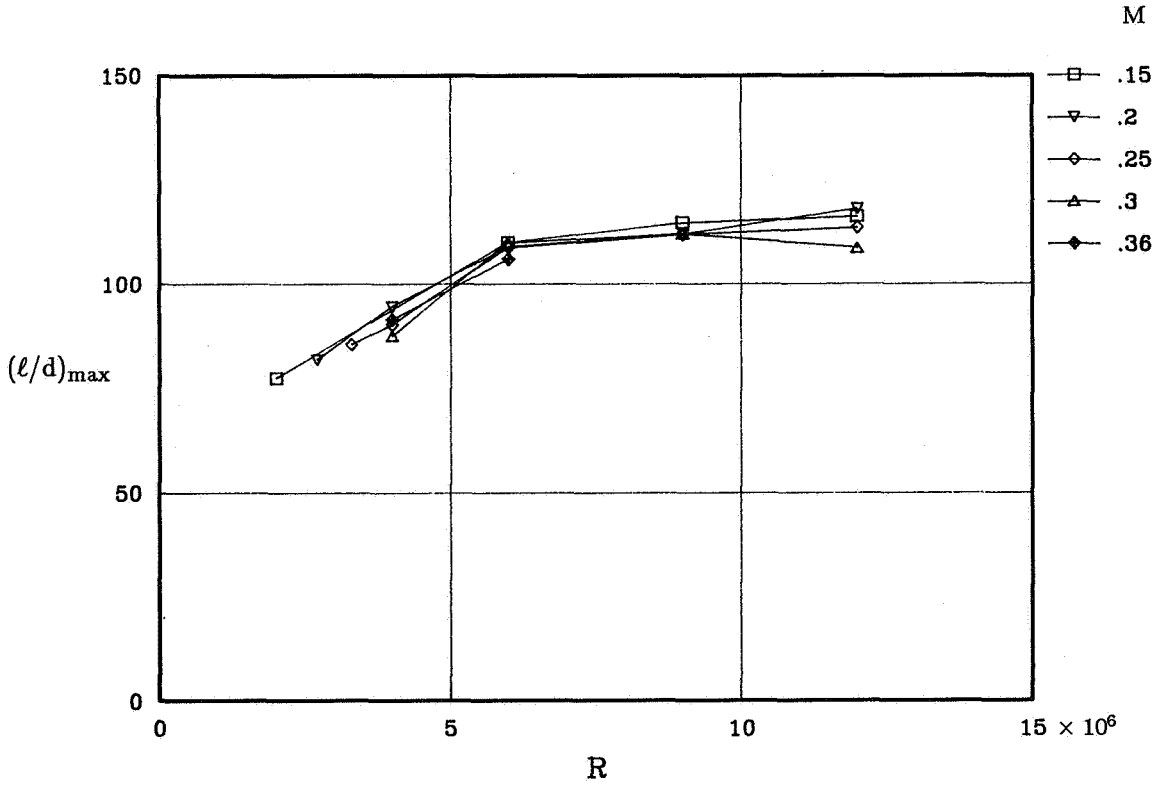

(b) Variation with Reynolds number.

Figure 32. Variation of maximum lift-drag ratio with Mach number and Reynolds number for free-transition case.

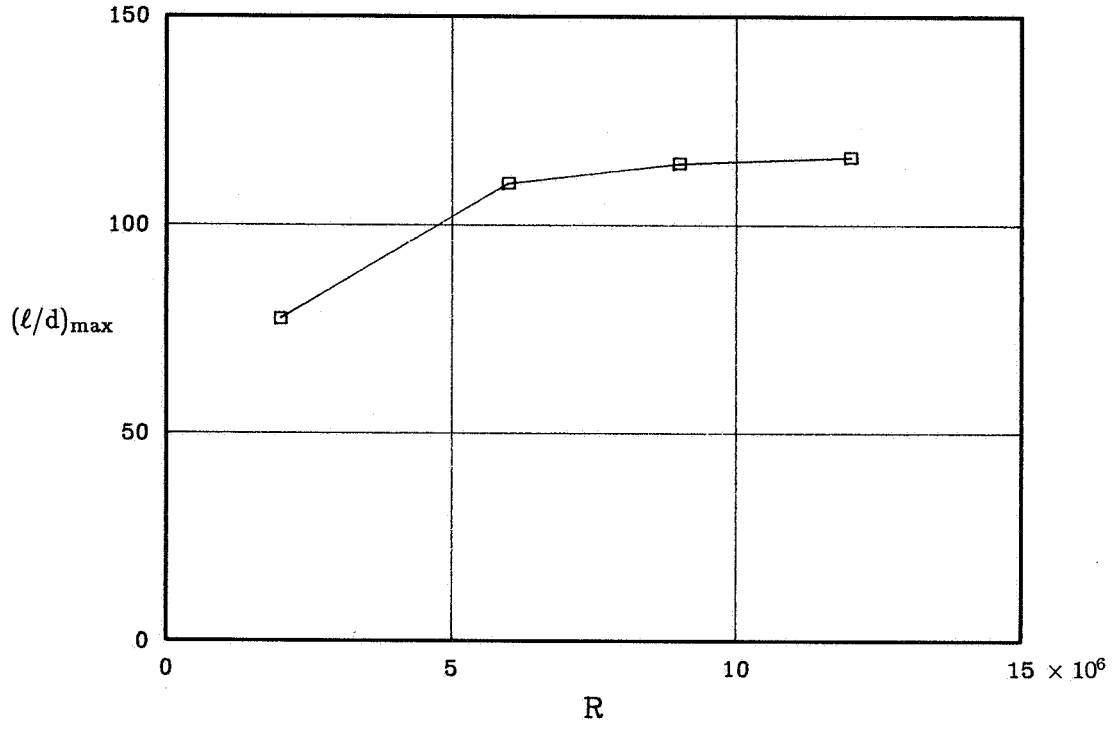

(a) Free transition.

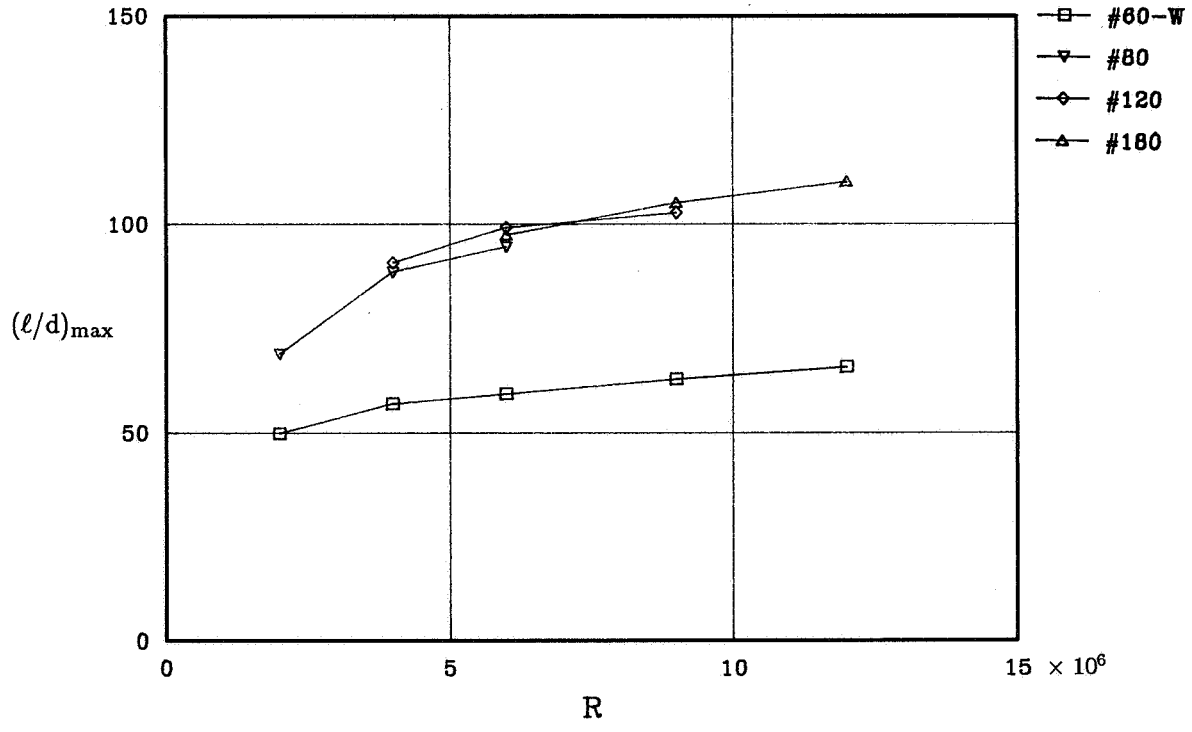

(b) Fixed transition.

Figure 33. Variation of maximum lift-drag ratio with Reynolds number for free and fixed transition at $M = 0.15$.

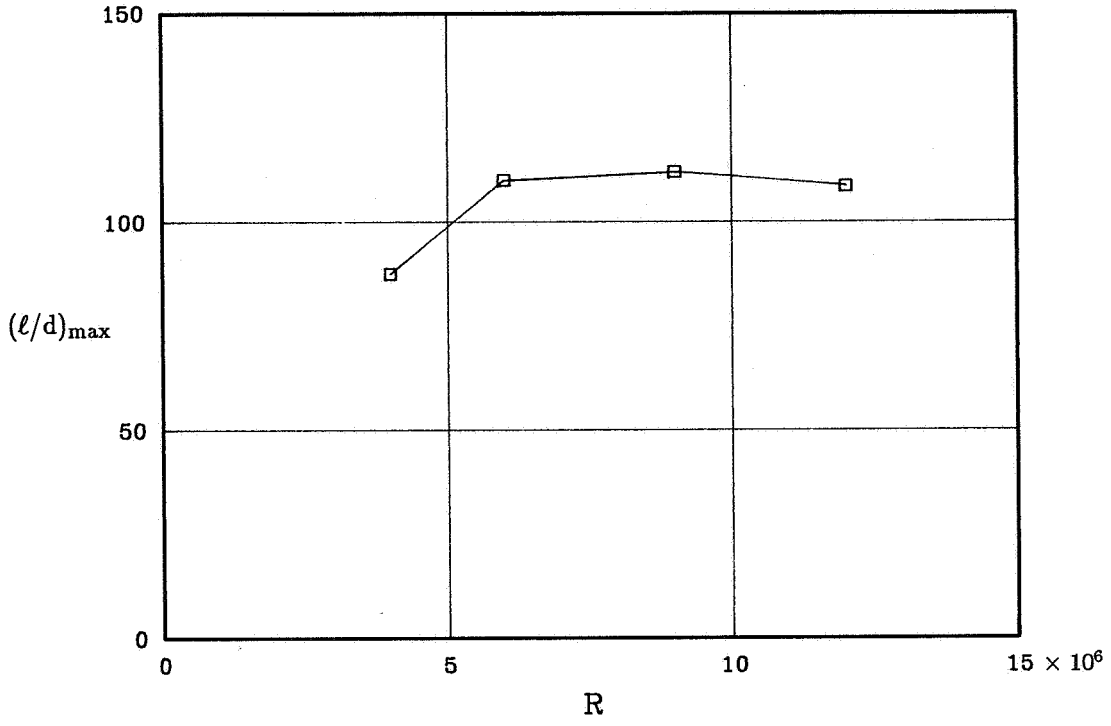

(a) Free transition.

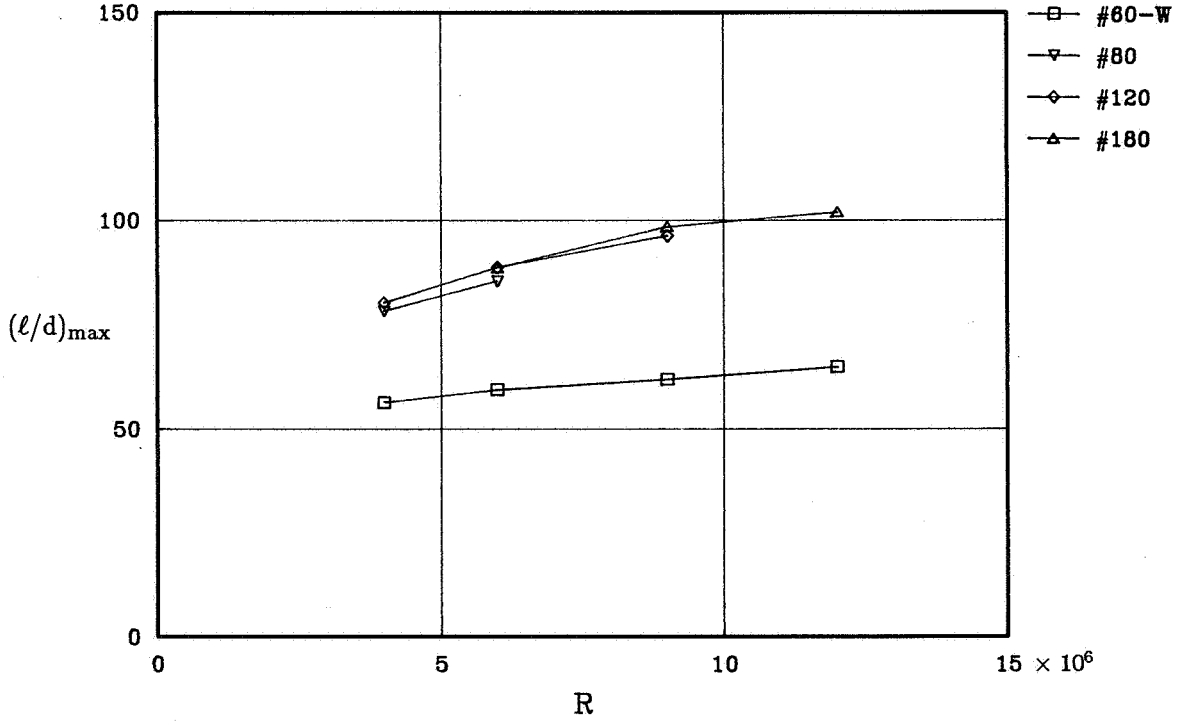

(b) Fixed transition.

Figure 34. Variation of maximum lift-drag ratio with Reynolds number for free and fixed transition at $M = 0.30$.

NASA
National Aeronautics and Space Administration

Report Documentation Page

1. Report No.	2. Government Accession No.	3. Recipient's Catalog No.
NASA TM-4074		

4. Title and Subtitle	5. Report Date
Effects of Independent Variation of Mach and Reynolds Numbers on the Low-Speed Aerodynamic Characteristics of the NACA 0012 Airfoil Section	October 1988
	6. Performing Organization Code
7. Author(s)	8. Performing Organization Report No.
Charles L. Ladson	L-16472
9. Performing Organization Name and Address	10. Work Unit No.
NASA Langley Research Center Hampton, VA 23665-5225	505-61-01-02
	11. Contract or Grant No.
12. Sponsoring Agency Name and Address	13. Type of Report and Period Covered
National Aeronautics and Space Administration Washington, DC 20546-0001	Technical Memorandum
	14. Sponsoring Agency Code

15. Supplementary Notes

16. Abstract

This report contains a comprehensive data base on the low-speed aerodynamic characteristics of the NACA 0012 airfoil section. The Langley Low-Turbulence Pressure Tunnel was used to obtain the data. Included in the report are the effects of Mach number, Reynolds number, and transition fixing on the aerodynamic characteristics. Also presented are comparisons of some of the results with previously published data and with theoretical estimates. The Mach number varied from 0.05 to 0.36. The Reynolds number based on model chord varied from about 2 to 12 $\times 10^6$.

END

DATE

NOV. 8, 1988

17. Key Words (Suggested by Authors(s))	18. Distribution Statement
Low-speed airfoil data Reynolds number effects Experimental-theoretical comparisons	Unclassified—Unlimited Subject Category 01

19. Security Classif.(of this report)	20. Security Classif.(of this page)	21. No. of Pages	22. Price
Unclassified	Unclassified	95	A05

For sale by the National Technical Information Service, Springfield, Virginia 22161-2171